



POLITECNICO DI TORINO

Department of Mechanical and Aerospace Engineering

Master's degree in
Automotive Engineering

UNICARagil – Structural analysis of carbon fiber
components for autonomous driving mobility

Supervisor

Prof. Andrea Tonoli

Candidate

Giampiero Titone

Student ID 246081

A.Y. 2019/2020

Ringraziamenti

Ringrazio il Prof. Andrea Tonoli prima per la formazione che mi ha dato come studente e poi per il supporto durante la fase più importante del mio percorso formativo.

Ringrazio la Technische Universität München per avermi dato la possibilità di svolgere il mio lavoro di tesi in un luogo stimolante e interessante, che mi ha permesso di mettermi in gioco e fare un'esperienza che sarà preziosa per il mio futuro.

Un ringraziamento speciale alla mia famiglia per il sostegno e l'amore che mi hanno sempre dimostrato. Tramite i sacrifici affrontati in questi anni mi hanno dato la possibilità di portare avanti la mia passione per il mondo Automobilistico.

Infine, ringrazio i miei amici e compagni di studio per aver allietato le giornate di studio e reso il periodo universitario un'esperienza indimenticabile.

Table of contents

| | | |
|-------|-------------------------------------------------------------|----|
| 1. | Introduction | 1 |
| 1.1 | UNICARagil project | 3 |
| 1.1.1 | UNICARagil prototypes | 6 |
| 1.2 | Objective of the thesis..... | 7 |
| 1.2.1 | Procedure and structure of the work | 7 |
| 2 | State of Art | 10 |
| 2.1 | Design principles for doors | 10 |
| 2.1.1 | Swing doors | 10 |
| 2.1.2 | Swing sliding doors | 12 |
| 2.1.3 | Folding doors..... | 13 |
| 2.1.4 | Sliding doors | 13 |
| 2.1.5 | Gull swing doors | 14 |
| 2.2 | Door structures in current autonomous vehicle concepts..... | 15 |
| 2.2.1 | Volkswagen Sedric | 15 |
| 2.2.2 | Toyota e-Palette | 16 |
| 2.2.3 | Westfield POD | 17 |
| 2.2.4 | Olli | 19 |
| 2.2.5 | Common door features | 20 |
| 3 | Current status of doors and roof | 21 |
| 3.1 | Door design | 21 |
| 3.2 | Roof design..... | 22 |
| 3.3 | AUTOtaxi and AUTOelf doors and roof adopted solution..... | 26 |
| 3.3.1 | Doors | 28 |
| 3.3.2 | Roof | 31 |
| 3.4 | AUTOshuttle and AUTOcargo doors adopted solutions..... | 35 |
| 3.5 | Kinematics - Arms and sliding mechanism position..... | 37 |
| 3.6 | Latches position and soft-close mechanism | 42 |
| 4 | Methods..... | 45 |
| 4.1 | CAD models parameterization..... | 45 |
| 4.1.1 | Definition of parameters | 45 |
| 4.2 | CAD editing..... | 46 |

| | | |
|-------|-------------------------------------------------------|-----|
| 4.2.1 | Geometry for safety | 46 |
| 4.2.2 | Latches position..... | 47 |
| 4.2.3 | Sealing | 50 |
| 4.3 | Materials | 55 |
| 4.3.1 | Composite materials..... | 57 |
| 4.4 | Delivery test | 64 |
| 4.5 | Finite Element Analysis..... | 65 |
| 4.5.1 | Introduction to FEM | 65 |
| 4.5.2 | Pre-processing environment | 66 |
| 4.6 | Static Analysis..... | 83 |
| 4.6.1 | Sag test | 83 |
| 4.6.2 | Strength in side internal impact against people | 84 |
| 4.6.3 | Door bending..... | 87 |
| 4.6.4 | Strength of the interior panel against people..... | 89 |
| 5 | Post-processing and Results | 90 |
| 5.1 | AUTOshuttle | 90 |
| 5.1.1 | SAG test | 90 |
| 5.1.2 | Side Internal impact..... | 91 |
| 5.1.3 | Door bending..... | 92 |
| 5.1.4 | Interior panel..... | 94 |
| 5.2 | AUTOtaxi | 95 |
| 5.2.1 | SAG test | 95 |
| 5.2.2 | Side Internal impact..... | 96 |
| 5.2.3 | Door bending..... | 97 |
| 5.2.4 | Interior panel..... | 98 |
| 6 | Optimization..... | 100 |
| 6.1 | Structural Optimization | 100 |
| 6.2 | Composite Optimization..... | 101 |
| 6.2.1 | Free-Size Optimization..... | 102 |
| 6.2.2 | Size Optimization..... | 108 |
| 6.2.3 | Shuffle Optimization | 110 |
| 6.3 | Comparison between Optimization and Patch Adding..... | 113 |
| 7 | Conclusions | 114 |

Bibliography117

List of Figure120

List of Tables125

Table of Abbreviation

| | |
|--------|------------------------------------|
| - OEM | Original equipment manufacturer |
| - CAD | Computer Aided Design |
| - CFRP | Carbon Fiber Reinforcement Polymer |
| - HMI | Human machine Interface |
| - ABS | Acrylonitrile butadiene styrene |
| - UD | Unidirectional |

1. Introduction

Autonomous driving has attracted the interest of researchers for many decades. In fact, we are on the brink of the next mobile revolution. The benefits are doubtlessly appealing: safer and more efficient driving, with the “Vision Zero” that no fatal accidents occur [1]. Autonomous vehicles will become an element of road traffic. For this reason, a standard for levels of driving automation has been required to interface with rules and clarify among consumers.

Although fully autonomous cars are not commercially available to common consumers at this stage, partially automated vehicles, which are defined as level 2 and level 3 autonomous vehicles by SAE (Society of Automotive Engineers) J3016 standard, are widely tested by automakers and researchers [2].

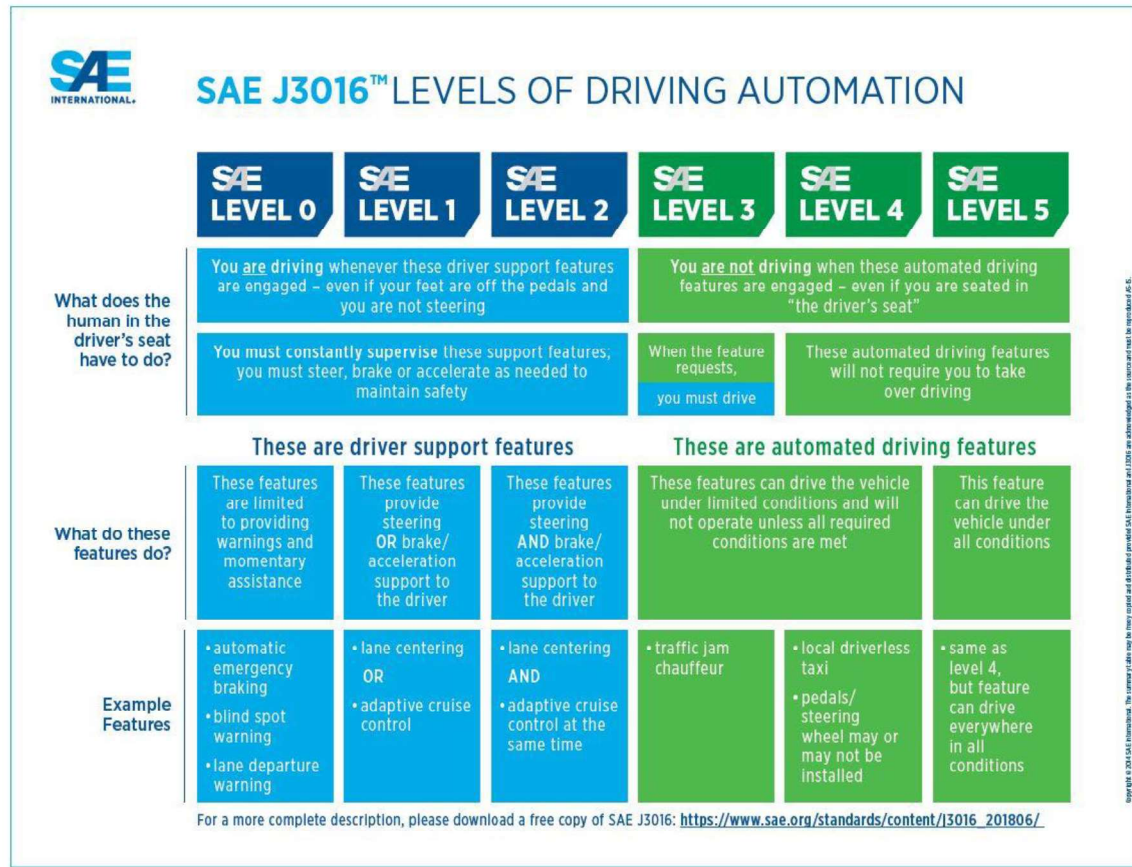


FIGURE 1-1 LEVELS OF DRIVING AUTOMATION [2]

Over the last years, the automobile industry has invested huge capital in the development of autonomous vehicles. However, the data needed are many and additional sensors, compared to the automated driving system that are currently used in cars, e.g., Adaptive Cruise Control (ACC) to control the velocity of the car automatically, or Lane Keeping Assist (LKA) to support the driver staying on the current lane provided by cameras and sensors, has to be implemented [3].

These vehicles permanently share information with the transport infrastructure and with one another. An area that will probably become more and more of interest in the future is exactly that of connected vehicles.

However, the technological aspect of autonomous driving is only one of the many. Autonomous vehicles will also have a direct impact on our society. Initially, moral inquiries will override all others. Just when autonomous vehicles have effectively been furnished with a sort of morals in dynamic will driving mechanical technology have the option to stand up for itself by and by [4]. This is particularly valid for the so-called dilemma situations, in which it has to be weighed up, in the case of an unavoidable collision, what behaviour will cause the least amount of harm to the persons involved both inside and outside the vehicle [4]. A further key inquiry to clear up is the thing that legislative outcomes could result here (e.g., traffic guidelines).

A further issue concerns the presentation of machine observation. This faces different cut-off points: Sensors, cameras, or components decline and undergo in their reliability on server time. At the state of art, it is possible to evaluate state vulnerabilities, and from this to check machine-discernment execution. At any rate, in the community doubts about the real possibility of predicting failures and of ensuring automotive machine's safe state under every possible situation, are present. This issue can be summarized much more unmistakably in one keyword: robotification. Accordingly, autonomous driving can open new chances, but additionally carry with its negative eventual outcomes

.

All large vehicle manufacturers are making substantial investments in connected and autonomous vehicle technology. Nevertheless, most automotive OEMs expect fully autonomous technology to become available after 2025 [5].

To anticipate and shape future scenarios of mobility, the German team UNICAR*agil* has decided to develop completely driverless electric vehicles, laying the foundations for the improvement of our mobility system and paving new ways

for the development of agile automated and electrified urban vehicles [6]. In UNICAR*agil* vehicles, occupants will be only passengers, never being involved in driving.

1.1 UNICAR*agil* project

UNICAR*agil* brings together a consortium of seven universities and six industrial partners. Under the leadership of the RWTH Aachen University, the universities TU Braunschweig, TU Darmstadt, Karlsruhe Institute of Technology, TU München, University of Stuttgart and Ulm University work together with the industrial partners Atlatec GmbH, flyXdrive GmbH, iMAR Navigation GmbH, IPG Automotive GmbH, Schaeffler Technologies AG & Co. KG and Vires Simulationstechnologie GmbH (Figure 1-3) [6].

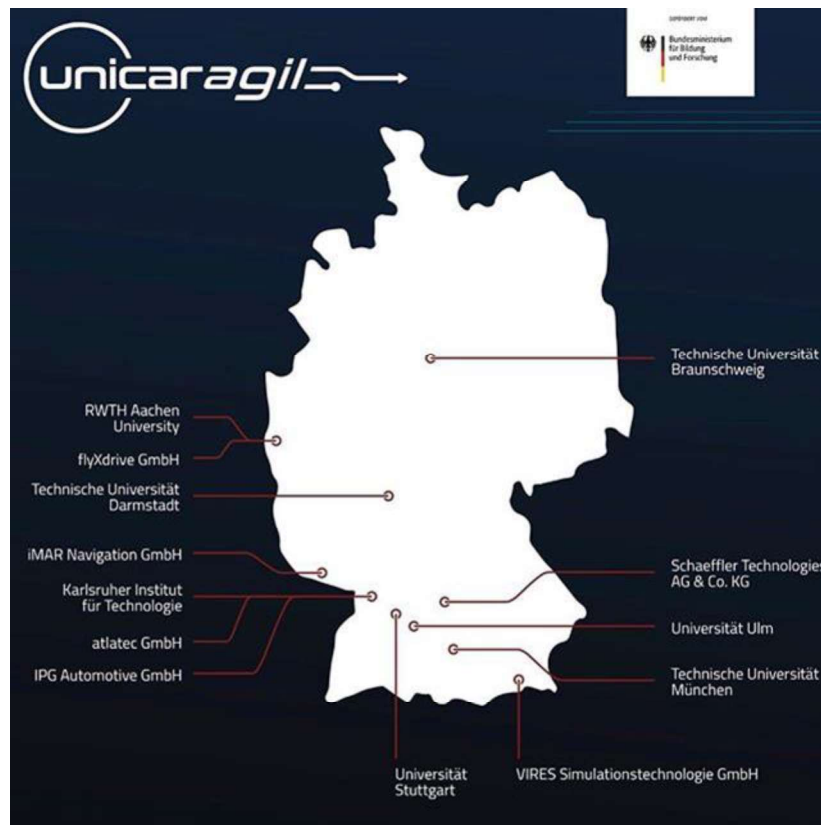


FIGURE 1-2 UNICARAGIL PROJECT PARTNERS [7]

UNICAR*agil* is designed to flexibly manage use cases such as logistics and passenger transport with a modular and scalable vehicle concept. The vehicles with utility and drive unit are driverless and emission-free [6]. They should mainly drive autonomously and only be controlled by a driver in an emergency or critical

situation. The Chair of Vehicle Technology at the Technical University of Munich is responsible for teleoperated driving by means of a control centre and for the design of the entrance doors and flaps of the various vehicle models AUTOfaxi, AUTOelfe, AUTOshuttle and AUTOfargo.

UNICAR*agil* vehicles are based on an innovative concept, whose schematic overview is shown in (Figure 1-4)

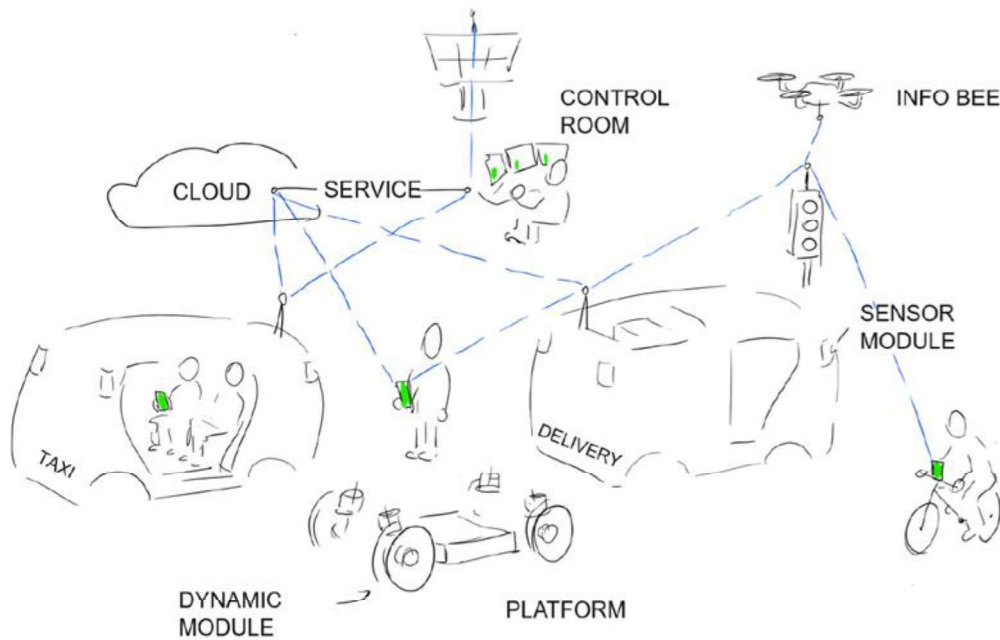


FIGURE 1-3 SCHEMATIC OVERVIEW OF THE OVERALL UNICARAGIL CONCEPT [6]

At its centre, a scalable platform provides the basis for various new vehicle concepts. It is equipped with four dynamic modules that are responsible for steering, accelerating and braking the vehicle. Each module has wheel hub motor and can reach steering angles of up to 90 degrees. New agile manoeuvres become possible, since each module is independently steerable.

The platform can be equipped with various add-on modules and thus be used for different purposes. The goal is to develop fully automated and driverless vehicles. The interior design is deliberately conceptualized in consideration of a driverless operation. The sensors required for environment perception are integrated into the vehicles in the form of disruptive sensor modules that combine various sensor technologies, with safety-relevant redundancies in mind [6].

Communication between vehicles and cloud services are used to share and evaluate data, which helps planning a safer and more efficient behaviour. A control room allows remote human intervention in case of exceptional conditions such as an inability of the platform to manoeuvre safely. In such situations, the vehicle will slow down and eventually stop. Afterwards, the control room can take over driving via teleoperation [6].

Moreover, electric vehicles offer new vehicle design options due to the reduced footprint for the power unit, compared to the internal combustion engine. In combination with the loss of a driver and a driver's seat, new possibilities are created in the electric and autonomous vehicle for the occupants of the vehicle as well as for the design of the vehicle interior and the entire vehicle. Comfort, especially in the entrance area, is becoming more and more important.

Entry comfort means taking into account the ergonomic requirements of humans. In order to use a door concept in the various vehicle variants of UNICARagil, the system must also ensure the functions of the automatic package system in the autoCARGO. The entrance doors and their functioning should be modular and scalable to the resulting geometric requirements to apply to all vehicle models.

In order to develop an optimal concept, existing door concepts and roof opening concepts were used in this work in terms of their suitability for autonomous operation, as well as in terms of their modularity and adaptation to the geometric requirements and ergonomic requirements are analysed and compared. Based on the requirements, the first space planning and concepts were designed under knowledge of the legal framework.

One challenge here has always been to adapt to the circumstances regarding the current state of the platform and the current design concept of the vehicle and to set requirements for the platform and design to ensure a functioning door. Ever changing requirements influence the methodology for developing a door or assembly concept and run through the whole project.

With the knowledge of the necessary safety guidelines, stability concepts were designed, simulated and adapted to the circumstances. In this way, a stable door can be constructed, and the safety of the passenger can be guaranteed.

The work as part of the vehicle door assembly in the large project UNICARagil gives a good insight into the coordination and challenges of a large-scale project to develop several complete vehicles. To meet the need to reduce costs of such a

project, the vehicles are modular, and whenever possible, parts should be used as part of an equal parts strategy with the same concepts.

1.1.1 UNICARagil prototypes

The aim of the project is to implement the four driverless vehicles, based on the same modular platform, in a proto-typical manner by February 2022.

The UNICARagil vehicle structure is divided into a driving platform and an add-on transport module. The former is scalable in its length and the latter in its length and height. A maximum amount of carry-over parts is targeted, and scalable interfaces are defined to ensure the maximum amount of flexibility. The number of different parts shall remain small [6].

The four UNICARagil vehicle prototypes are the following (Figure 1-5):

1. AUTOfaxi – driverless taxi: A fully automated and driverless taxi that is called by a smartphone and comfortably transports passengers to the desired destination
2. AUTOfelfe – autonomous family vehicle: This automated vehicle is privately owned and is considered part of a family to do shopping or to take the children to school
3. AUTOfargo – autonomous delivery vehicle for parcels: A "mobile packing station" with efficient and intelligent conveyor technology that can pick up and deliver parcels independently
4. AUTOfhuttle – vehicle for local public transport: Passengers can travel as if on a train, as several electronically coupled vehicles behave like one rail vehicle. The AUTOfhuttle transports small groups and is used in local public transport [6].



FIGURE 1-4 UNICARAGIL PROTOTYPES [8]

Due to their modular design, the four vehicles are very similar in appearance. However, the interiors are developed independently of each other with the aim of making the vehicles as user oriented as possible [6].

The four vehicles can be grouped into two categories: AUTOelf and AUTOtaxi, characterized by short wheelbase and low height, and AUTOshuttle and AUTOcargo, having long wheelbase and higher height. The vehicles of the first category have two doors on both sides and a lifting roof, while the ones of the second category have only two doors on one side.

1.2 Objective of the thesis

The Institute of Automotive Technology (FTM) at the TU Munich is responsible for the design of the entrance doors and roof of the four UNICARagil vehicles.

The aim of this work is to analyse and optimize the structural integrity. This analysis should explain the current status and at the end of the work these data should lead to an improvement of the door's stiffness and a mass reduction of them.

1.2.1 Procedure and structure of the work

This work focuses on the analysis of current doors concepts in relation to the UNICARagil project. This work is based on manufacturer specifications. In order to achieve the above objectives, the following structured approach will be followed (Figure 1-6).

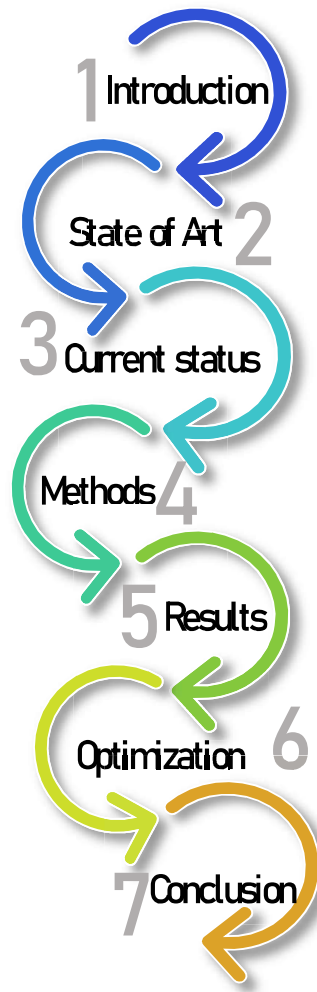


FIGURE 1-5 STRUCTURE OF THE THESIS

The thesis starts with an introduction in chapter 1 about autonomous driving vehicle and the opportunities that lie behind their applications. Follow the description of UNICARagil project and the placement in this environment.

In Chapter 2, the state of the art is presented, with today's doors and roof concepts presented and divided into various groups: swing doors, sliding doors, swing sliding doors gull wings doors.

Chapter 3 deals with the exposition of the design status of the doors and roof adopted so far.

Chapter 4 refers to the methods to which the analyses have been developed.: parametrization of the CAD components, material definition, pre-processing computation and type of analysis take into considerations.

The results of the analysis and the discussions take place in Chapter 5.

Chapter 6 summarizes the most important phases of the optimization. This aspect of the work serves as a decision-making aid of the doors and prepare them for the production.

The last chapter presents a short overview of the insights gained, as well as a brief outlook

2 State of Art

The possible solutions for opening and closing doors and roof, coming from the major car manufactures, are shown. Along this, a brief presentation of the main decisions regarding the current state of component design is made.

2.1 Design principles for doors

Among the past decades several types of opening mechanisms were developed by car manufactures. Each type of mechanisms performs a different function that may is requested, such as accessibility in the passenger compartment or lateral encumbrance.

2.1.1 Swing doors

For swing doors, the longitudinal edge of the door represents the axis of rotation. Depending on the hinge arrangement it is a right or left turn. The main advantages of this type of door are its universal use, flexible mountability and a space-saving concept. The illustrations shown below show the principle of a single-leaf swing door and illustrate with an example the use of this type of door in two different ways in a conventional vehicle from Fiat (FCA). On one side the representation of the Fiat 500 with a large door on each side of the vehicle (Figure 2-1), which not only provides access to the front seats but to the rear seats as well. On the other side a Volkswagen Up (Figure 2-2), which is equipped with separate doors for the front and rear rows of seats.



FIGURE 2-1 SINGLE-LEAF SWING DOOR - CONSTRUCTION PRINCIPLE AND FIAT 500 [9]



FIGURE 2-2 DOUBLE LEAF SWING DOOR - CONSTRUCTION PRINCIPLE AND VOLKSWAGEN UP [9]

If a second one supplements the single-leaf swing door, it is a double-leaf Swing door. This can be constructed in the same or opposite direction.

Compared to the double-leaf swing door shown in Figure 2-2, the co-rotating double-leaf swing door offers the advantage of getting in and out in more comfortable way. For access to the rear row of seats, the open door is not an obstacle. However, during the journey an unintentional rear door opening due to the wind can lead to the tearing off the door. For safety reasons, constructive measures or electrical interlocks are provided to prevent accidental opening during to counteract the journey. A design principle for the co-rotating double-leaf swing door is the Opel Meriva as an example vehicle (with B-pillar) with the Doors shown in Figure 2-3.

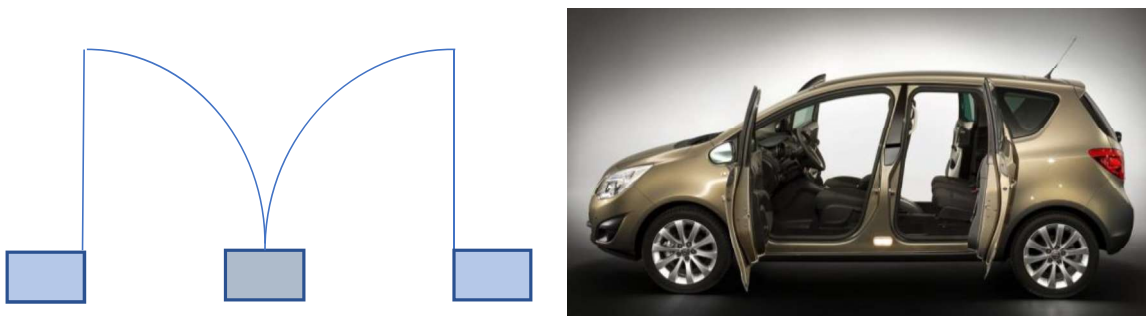


FIGURE 2-3 CO-ROTATING DOUBLE-LEAF SWING DOOR WITH B-PILLAR - CONSTRUCTION PRINCIPLE AND OPEL MERIVA [9]

Another example of the co-rotating double-leaf swing door is the i3 from BMW. In comparison to Figure 2-3, a missing B-pillar characterizes this vehicle in entrance area, which is integrated into the rear door. Figure 2-4 illustrates A design principle and a representation of the vehicle.

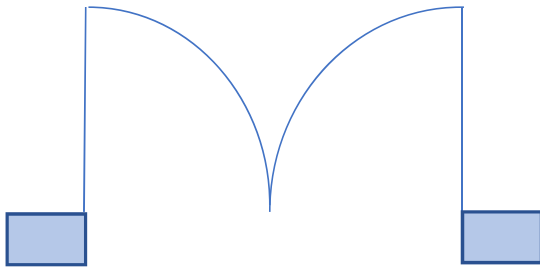


FIGURE 2-4 CO-ROTATING DOUBLE-LEAF SWING DOOR WITHOUT B-PILLAR - CONSTRUCTION PRINCIPLE AND BMW i3 [9]

The door concept of the BMW i3 looks elegant due to the omission of the B-pillar in the entrance area and massive at the same time. If the front door is opened, a lever to get in the back seat can open the rear door.

2.1.2 Swing sliding doors

Sliding doors are narrowly designed doors and allow for a lateral displacement the opening or closing of cockpit. In comparison with swing doors they do not require a turning space when opening. With a fully automatic door drive, they are used when fast and precise opening and closing is essential. A minimum distance to posts, walls, kerbs or similar must be maintained because otherwise a collision when opening the door is unavoidable. Furthermore, a sliding door provides a lot of space in the interior and is ideal for children. Figure 2-5 shows the design principle and a Ford B-Max as an example vehicle.

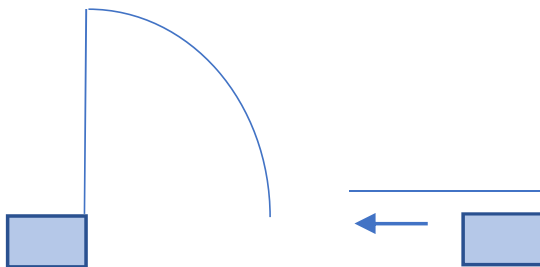


FIGURE 2-5 SLIDING DOOR - CONSTRUCTION PRINCIPLE AND FORD B-MAX

2.1.3 Folding doors

The structure of folding doors is divided into at least two door leaves, which are attached to the longitudinal edges of the door rotatably linked as well as at the top of the drive, with or without guide in the bottom. Opening and closing is possible by means of a lateral displacement. The doors open and close thanks to the use of a cylinder. The advantages of this door system are that it has a compact structure perfect performance and long service life, as well as additional safety protection against being clamped.

In vehicles, this door principle is used, for example, in buses. Figure 2-6 shows the design principle and an example of the vehicle, Scania Citywide.

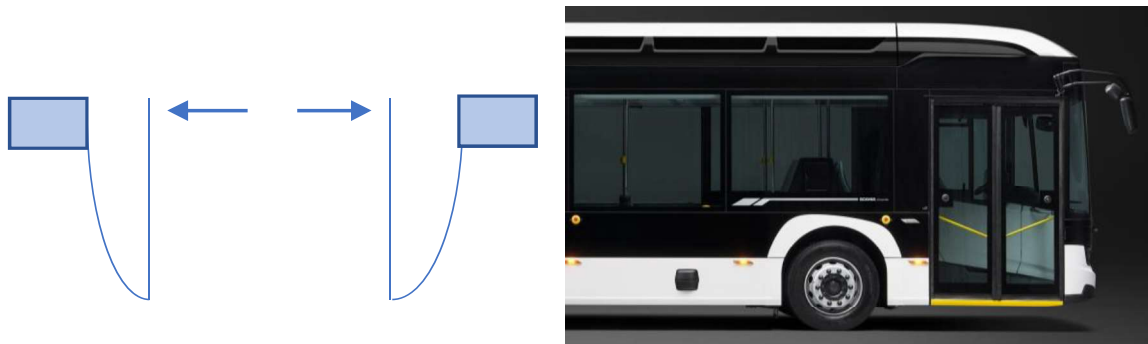


FIGURE 2-6 FOLDING DOOR - CONSTRUCTION PRINCIPLE AND SCANIA CITYWIDE

2.1.4 Sliding doors

A sliding door can increase the functionality of the space. A hinged door requires many more square feet of space than a sliding door. There is nothing impeding the door, since the sliding door operates on a track. It usually adopted for public transport such as buses and metro because of its versatility and safety aspects. Figure2-7 shows the design principle and an example of the vehicle, DB bus.

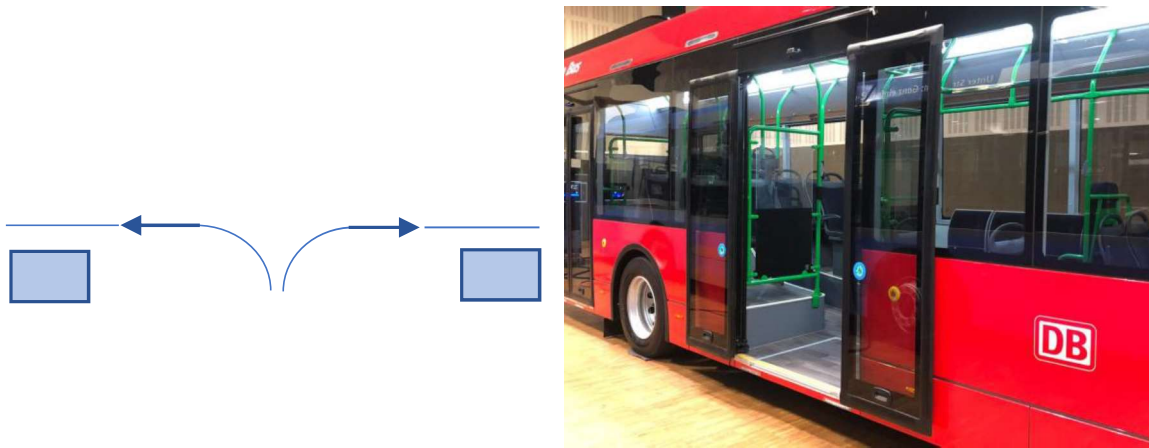


FIGURE 2-7 SWING- ARM DOOR – CONSTRUCTION PRINCIPLE AND DB BUS

2.1.5 Gull swing doors

In comparison with vertical hinge doors which they are attached at the front-facing edge of the door to the vehicle's pillars, gull-wing doors are hinged at the roof enabling the passenger to egress and ingress into the vehicle far easier. This is due to the increased area created by the upward motion of the door. By using the gull-wing doors, the need for extra space between parallel-parked cars also decreases. The door hinges act as a means of pivoting a door from an open and closed position but must also withstand sufficient loads to protect passenger against injury during collision [10]. In Figure 2-8 is illustrated the construction principle and the adopted design by Tesla with the so-called Falcon wing.



FIGURE 2-8 GULL-WING - CONSTRUCTION PRINCIPLE AND TESLA MODEL X

2.2 Door structures in current autonomous vehicle concepts

The concept cars are created as prefigures for new models or to show design solutions or advanced technologies that will be adopted in the future production of the manufacturer. The exhibition of these prototypes in the salons, allows the manufacturer to evaluate the popularity, through the reactions of the public and the specialized press. In the following sections an evaluation of the current status for electrified mobility vehicles from different car company is made.

2.2.1 Volkswagen Sedric

Sedric is the first autonomous concept car in the Volkswagen Group and is also the first car in the group with level 5 of autonomous driving, which means that a driver is not required. Sedric is designed for driving the children to school and then taking their parents to the office. It is also able to look independently for a parking space as well as picking up a visitor from the station. Sedric do all of that at the touch of a button, with voice control or with a smartphone app – fully automatically, reliably and safely [11]. The lounge atmosphere in the interior without a steering wheel and pedals provides all the occupants with enjoyable mobility and an unrestricted view through large window areas and a varied infotainment programme [12].



FIGURE 2-9. VOLKSWAGEN SEDRIC [13]

As can be taking a gander at Figure 2-9 the two sliding door create an opening from the sill to the roof that permits passengers to get in and out from the vehicle comfortably and effortlessly. The two parts of the swing door are made up of a CFRP structure and an external polycarbonate panel that occupies the entire surface.

The swing-arm doors, when closed, adopt a five latches system for the locking mechanism with the help of as many soft close motors. Four latches are installed in the vehicle structure, and only one is placed in the door that closes as second. This allows an optimization of the door packaging, enhance the cable management and avoiding an overload of the door structures.

In correspondence of the belt line there are two horizontal reinforcement of the structure in order to maximize the resistance to side impacts. The door kinematics is located at the lower and upper end of the door.

To ensure the sealing between doors a flange with gasket is present. Led strips are mounted in the area between the central bars working as an external HMI.

2.2.2 Toyota e-Palette

The e-Palette is a fully automated battery electric vehicle, designed to be scalable and customizable. In fact, there are three sizes of e-Palette concept, with different lengths, depending on the purpose-built specification. Thanks to a flat and extensive barrier free interior space layout designed with a low floor, equipment can be installed in accordance with the user's needs, such as ride sharing specifications, pizza delivery specifications and retail shopping specifications [14] (Figure 2-10).



FIGURE 2-10. POSSIBLE USES OF E-PALETTE CONCEPT [15]

This prototype has two doors positioned in the middle of the side panel with swing-arm opening. A perimetral metal frame and a glass window play an important role in the stiffness of the door. The structure is fixed at the top and bottom to the kinematics.

Unfortunately, no examples of e-Palette doors have ever been produced, except for a simplified version intended for the 2020 Tokyo Olympics (Figure 2-11). I



FIGURE 2-11. TOYOTA E-PALETTE FOR 2020 TOKYO OLYMPICS [16].

2.2.3 Westfield POD

This vehicle is a perfect example of the use of autonomous driving for public transport. It is the only autonomous transport system in which is commercially proven. It has been operational at Heathrow Terminal 5 since 2011 [17]. Two versions are currently in use:

- The version at Heathrow is fully autonomous but uses guideways with sensors to wirelessly tell the pod where it is and give it instructions to speed up, slow down, turn and stop. The information is relayed to the sensors from a central control room [17]

- The version demonstrated in Greenwich in 2017 dispenses with the external sensors. The vehicle has its own sensors and a highly detailed 3D map of the area. It decides for itself on the route to take, and how to interact with other road users - it can safely share a road or path with pedestrians, cyclists and animals, knowing when it is safe to move, and when it has to stop [17] (Figure 2-12)



FIGURE 2-12. WESTFIELD POD – OPENING OF THE DOORS [17]

The Westfield POD has an aluminum ladder chassis onto which the vehicle propulsion and guidance equipment is installed. Floor is designed with a structural aluminum honeycomb to lighten the structure. Body panels made of ABS or carbon fiber are bonded to the vehicle structure

The upper frame is made up of a welded steel tubular structure. In order to manage the vehicle's weight, slide doors are made of CFRP. Two shells can be recognized, inner and outer, both with structural function. In addition, a transparent polycarbonate glass is bounded to the external shell for the entire size of the door (Figure 2-13).



FIGURE 2-13. WESTFIELD POD INSIDE VIEW [17]

2.2.4 Olli

The transportation companies in Italy are trying to convert the public mobility with electric self-driving vehicles. It is possible to find an example in Turin. The concept is the result of an international synergic work carried out in collaboration between the City of Turin, ITCILO, Reale Mutua and Local Motors. Olli is an autonomously driven electric minibus created by assembled 3D printed parts: a product for sustainable urban mobility, innovative from a technological point of view, designed with particular attention to the characteristics of accessibility and respect for the environment. The shuttle will carry out transport services within the ITCILO campus (Figure 2-14).



FIGURE 2-14 OLLI-3D PRINTED MODEL [18]

2.2.5 Common door features

There are some common characteristics between the doors of the three self-driving vehicles described in the previous paragraphs. The three concepts have two side doors that open at the same time to provide a larger entrance area for passengers and goods.

Another common feature, which derives from the type of doors used, is the absence of the B-pillar. This solution causes a vulnerability of the doors in case of side impact and a structural deficiency of the frame, hence an increase in weight due to the need to reinforce the side of the two doors in correspondence with the interface between them.

An HMI is integrated in all the vehicles and it can be of different types, from a touch screen display to LED strips or simple buttons that allow other vehicles and road users to interact with the vehicle. Generally, for reasons of ergonomics, these devices are placed close to the vehicle's belt line.

Moreover, the upper part of the doors, and in some cases also the lower part, has a transparent outer panel made of polycarbonate to reduce weight.

3 Current status of doors and roof

The guideline followed during the design phase provides the adoption of a layout that can be scalable in the different UNICARagil prototypes, in the face of minor changes in parameters such as door height and width. Figure 3-1 shows the first concept of scaling the two platforms and vehicle structure.

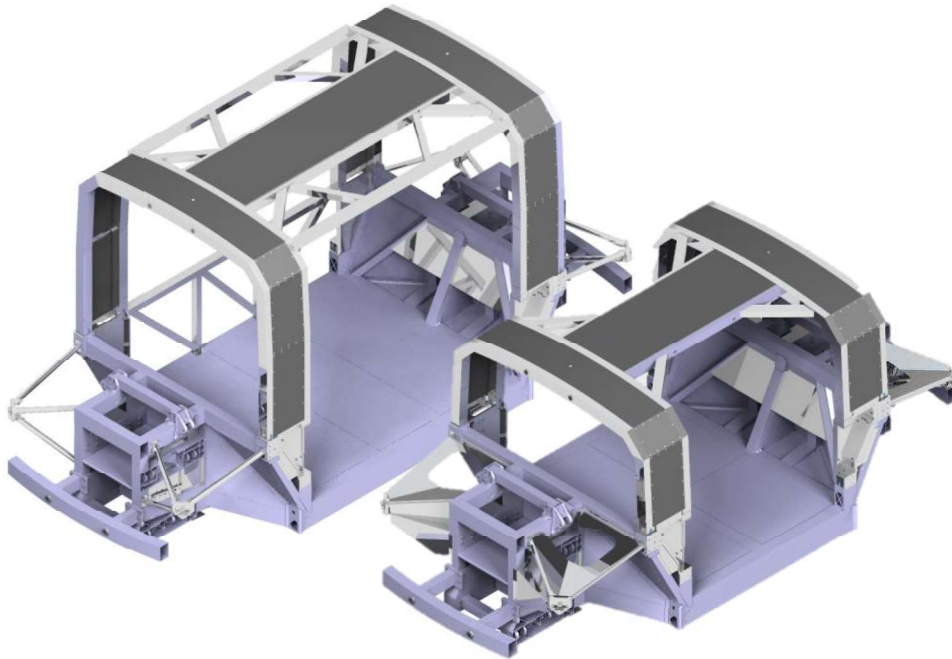


FIGURE 3-1. PLATFORM AND VEHICLE STRUCTURE: LARGER VEHICLES VS. SMALLER VEHICLES [19]

From Figure 3-1, it is possible to notice how different the dimensions of the structures are for the two categories of vehicles. Design started from the small one, the AUTOfaxi, and to obtain the AUTOfuttle the wheelbase and height of the hut was increased.

3.1 Door design

About the design of the doors, the aspects that most affects the design is the type of kinematics that is implemented. In relation to kinematics, various types of doors are adopted on current vehicles. Four main solutions – sliding doors, swing doors, swing arm doors, swing & slide doors have been evaluated and analysed by the team. The four UNICARagil vehicles have swing & slide doors.

There are many reasons for this choice, done mainly to solve some packaging problems. An example is the AUTOshuttle, the autonomous delivery vehicle for parcels, it has an internal arm with which it is possible to carry inside the passenger compartment parcels placed outside the vehicle. Parcels are positioned at 400 mm from the platform of the vehicle and the doors, during their opening, must not impact against those parcels.

3.2 Roof design

AUTOtaxi and AUTOelf, the smaller vehicles of UNICARagil, requires a roof opening to allow easy access to the interior of the vehicle, otherwise the sill height will prevent this. A roof hatch opens to avoid that the boarding person climbs a step and bends down at the same time, as in conventional vehicles. So, an opening in the roof solves the conflict of objectives that arises between comfortable access and low vehicle height(Figure 3-2).

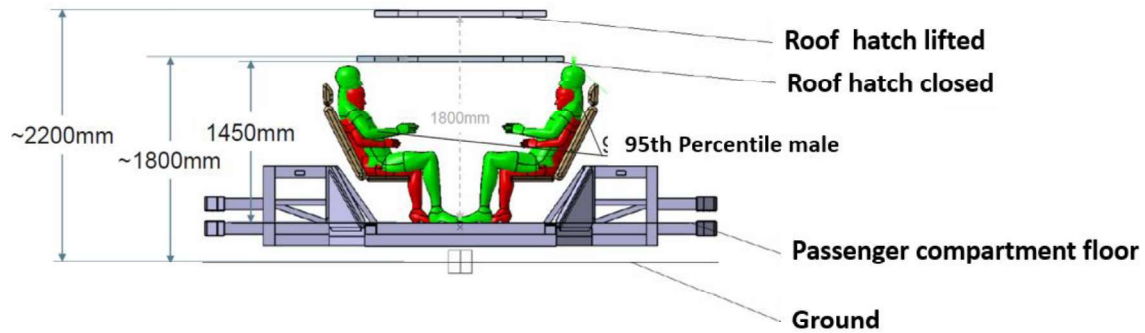


FIGURE 3-2 HEIGHT IN AUTOTAXI AND AUTOELF [20]

The shape of the hatch is determined by the fact that a person needs a certain amount of space to move and seat inside the vehicle. The basic requirements for the dimensions of the roof hatch are formulated by the TUM Chair of Ergonomics. From these requirements, it results the specification of two symmetrical but not parallel sides of the roof shape.

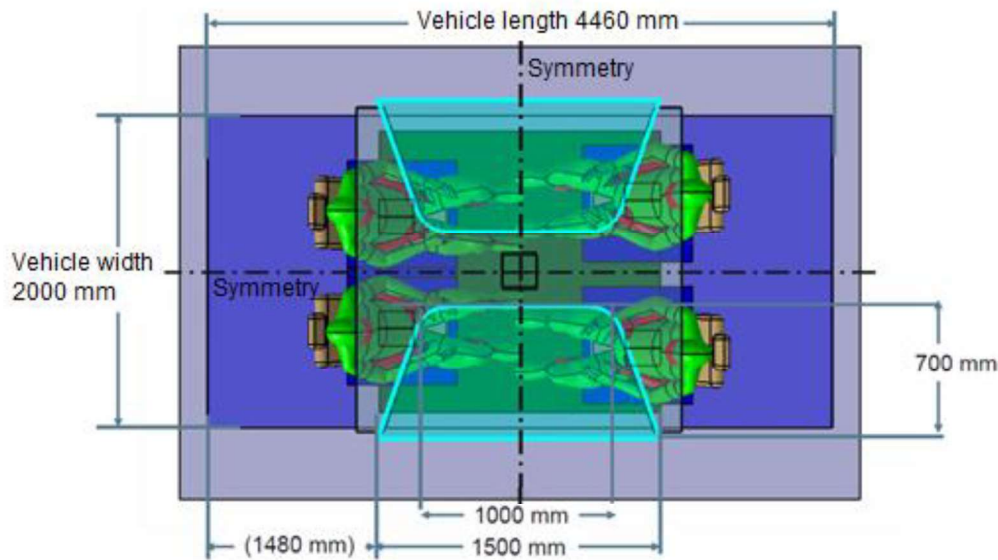


FIGURE 3-3 DIMENSIONAL REQUIREMENTS FOR THE ROOF HATCH DUE TO ERGONOMICS [20]

So, the symmetrical, non-parallel sides of the hatch require the kinematic mechanisms to be placed at an angle to each other. In addition to this, the roof kinematics must be arranged in such a way as not to restrict the space created by the opening of the roof door, so as not to reduce the space available for people to enter the vehicle.

The roof hatch has, a 3-link mechanism. Analysing the different options for the lifting mechanism, the team recognized four possible solutions: sliding mechanism, swing arms, X mechanism, 3-link mechanism [21]. By considering pros and cons of each mechanism such as the encumbrance of the roof once opened or the height the opened roof can reach with the different solutions. Among these mechanisms the design choice fell on the swing arm doors.

Similar to swing arm doors, a roof with a similar four-joint mechanism can be developed. The roof hatch would rise above the roof structure and would only require space on the sides of the roof opening for the mechanism and drive (Figure 3-4). Nevertheless, a mechanism such that need a lot of effort to implement rain protection because the roof hatch moves towards the center of the vehicle [22]. Moreover, this kind of solution can create instability problems.

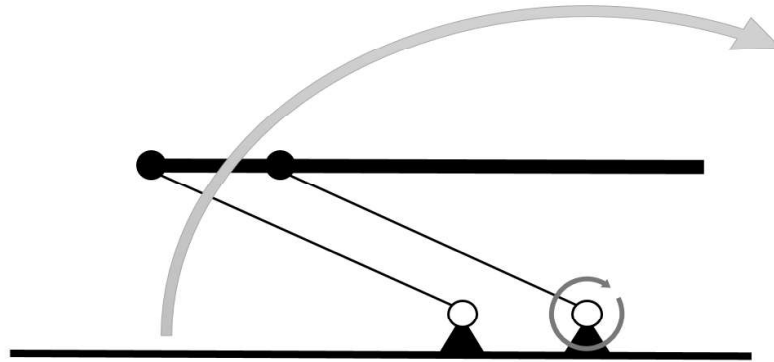


FIGURE 3-4. SWING ARM ROOF [22]

A 3-link mechanism, with two links placed on the roof hatch sides and one link positioned on the rear part of the roof hatch, ensures the same advantages given by a four-joint mechanism. Even if the problem of rain protection is not solved, this mechanism allows solving the automation problem. In fact, in this case, it is possible to use only one motor in correspondence of the link placed on the rear part of the roof. [23]

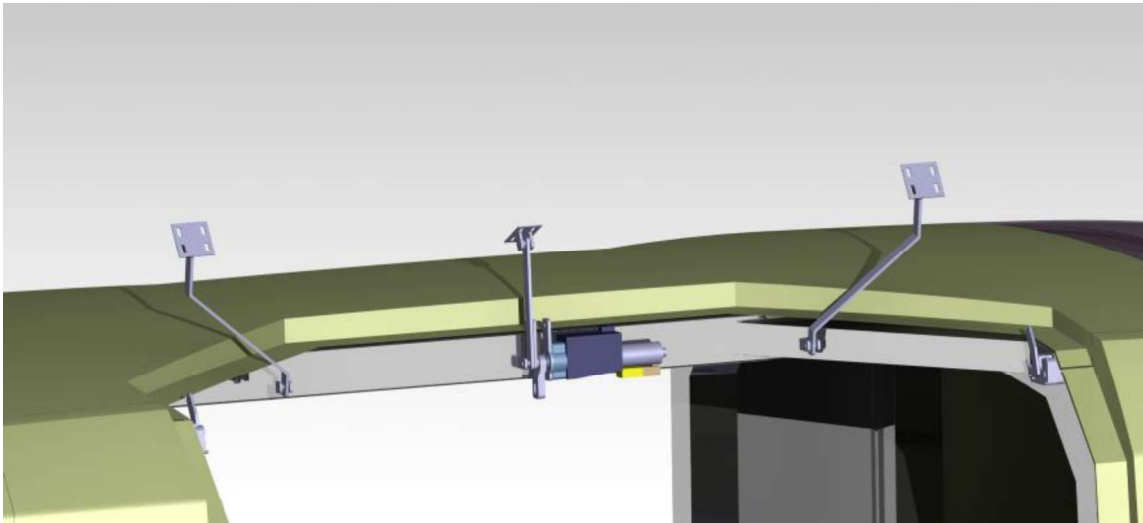


FIGURE 3-5. 3-LINK MECHANISM [24]

Furthermore, in order to keep the roof closed when it is in the closed state, a proper locking system must be adopted.

In AUTOfaxi and AUTOfelf, the door opening has to be combined with a roof opening. This creates an interruption in the transmission of forces between front and rear part of the vehicle in case of an accident. To solve this problem, a beam located in the roof hatch is able to connect to the vehicle structure when closed and absorb all forces and, if necessary, moments in the spatial directions. A locking

mechanism has been developed in order to perform the connection between the beam in the roof hatch and the vehicle structure.

The basic mechanism consists of a striker pin fixed to the roof bar and a support with a rotating hook fixed to the upper body ((Figure 3-6)).

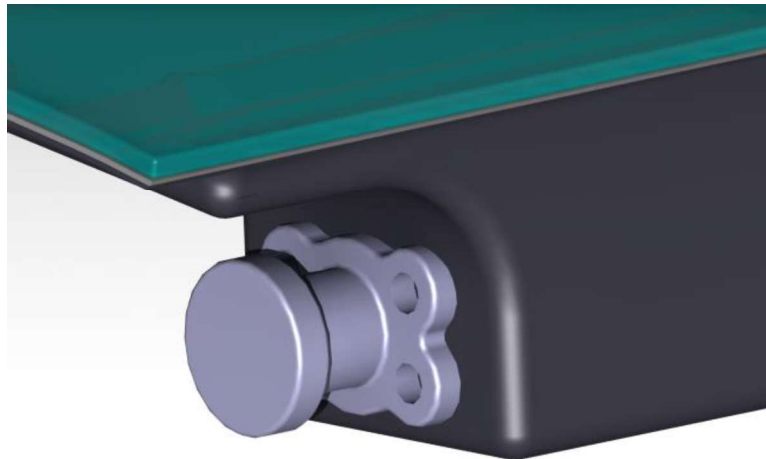


FIGURE 3-6. BLOCKING - STRIKER FIXED TO THE ROOF BAR AND SUPPORT WITH A ROTATING HOOK FIXED TO THE UPPER BODY [24]

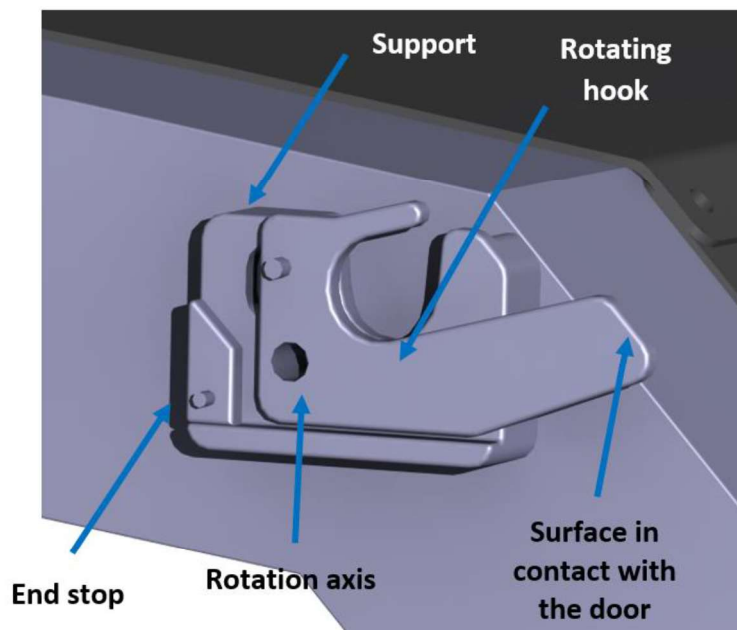


FIGURE 3-7 SUPPORT WITH A ROTATING HOOK FIXED TO THE UPPER BODY [24]

In the UNICAR*agil* project, a solution such that is undoubtedly a good compromise between the needs of a lifting roof and a rigid frame. The support is fixed to the main roof frame with the opening upwards and the striker pin is fixed on the side of the beam placed in the roof hatch so that it enters the support when it is closed. Additional mechanisms or drives are not required for this blocking.

3.3 AUTOtaxi and AUTOelf doors and roof adopted solution

Designers of the external shape of the vehicles choose the separation planes of the external shape, except the line of cuts between the doors and the roof as regards AUTOtaxi and AUTOelf that was a matter for the roof designers. Therefore, this cut has been defined considering the already mentioned scalability of vehicles and the structural feasibility of the chosen cut line

Keeping in mind the first aspect, all the vehicles followed the same cutting plane for the doors. Starting for the external shape of the bodywork cutting planes were defined by fixing specific measures for both the four prototypes. The measures taken in consideration were the following plane distances:

- Definition of the yz middle plane of the vehicle
- Definition of the xz middle plane of the vehicle
- Distance of a horizontal plane with respect to the ground for the definition of the sill cutting line
- Distance of a horizontal plane with respect to the ground for the definition of the belt cutting line
- Distance of a yz plane with respect to the front wheel arc
- Distance of a yz plane with respect to the rear wheel arc
- Distance of a xz plane with respect to the middle plane for the definition of the roof cutting line

Under these considerations the principal cutting lines were defined as shown in Figure 3-

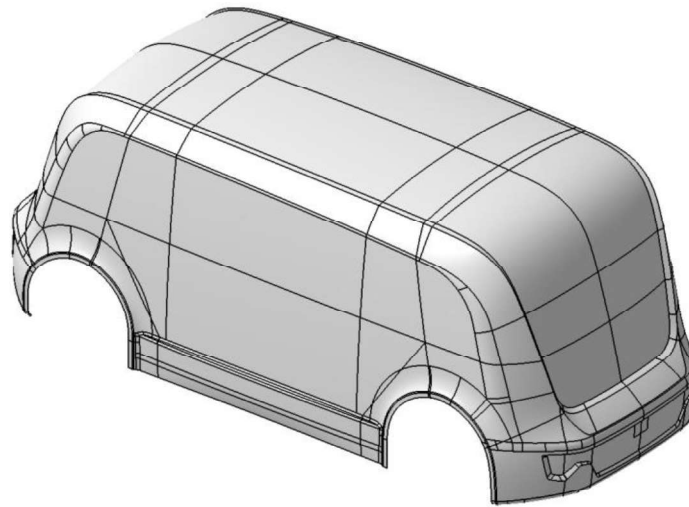


FIGURE 3-8. AUTOSHUTTLE AND AUTOCARGO EXTERNAL SHAPE AND ROOF CUT LINE [25]

[B12]

From the lines drawn by the intersection of planes and bodywork, the external shape of the door has been outlined.

The reason why for the AUTOtaxi and AUTOelf the line of cuts between the doors and the roof was different from the one of the AUTOshuttle and AUTOcargo is explained in Figure 3-9. Since the material chosen for the roof was CFRP similar to the doors, the roof have two shells. It consists of one internal and one external shell, which are connected along the perimeter by a flange of 20 mm. Due to the presence of this flange, if the same cutting as the AUTOshuttle was chosen, the main beam of the roof would be too much shifted inward.

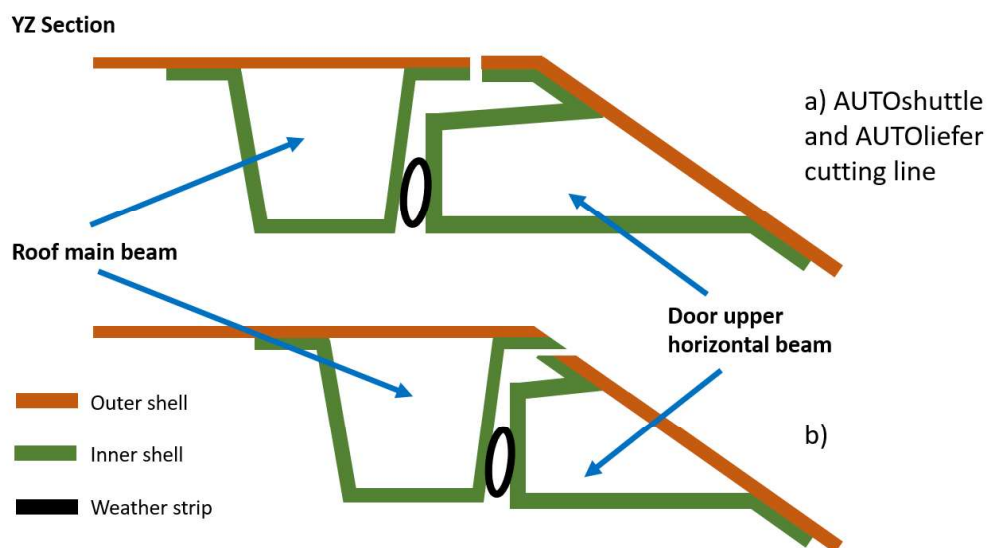


FIGURE 3-9. SECTION OF THE DOOR TO ROOF INTERFACE WITH TWO DIFFERENT CUTTING LINES [23]

This would cause the upper part of the door very protruding inwards, creating a shift of the center of gravity towards the inside of the vehicle, compromising the functioning of the kinematics. In addition, the roof bar will no longer be in an optimal position to design a locking mechanism that secures the roof to the upper body when closed.

3.3.1 Doors

In the design of the door structures was necessary to study an optimal arrangement for the structural elements and accessories to be installed on the door. In fact, AUTOfaxi and AUTOelf doors have an additional element with respect to AUTOfhuttle and AUTOfargo doors, the HMI matrices, but also less space available due to their smaller size.

Therefore, it has bars along the perimeter and two horizontal bars, one at the height of the locks and one supporting the kinematics. The kinematics bar is 230 mm high.

The vertical bars and those at the upper and lower ends, which make up the perimeter of the door, have a section of 50x50 mm, mostly obtained in the inner shell. The bar at the height of the belt line, which connects the central lock to the side lock, has the same section as the perimeter bars. All the bars are realized by outer and inner shells bonded together.

One of the main features of this version was the integration, in the inner shell, of a cover to host the latch. This solution allows the lock between the doors to be mounted directly on the door structure, without the need for additional components. The latch is fixed on the inner shell of the rear door, while the striker pin on the outer shell of the front door (Figure 3-10).



FIGURE 3-10. INTEGRATED COVER FOR THE LATCH HOUSING [26]

From Figure 3-10, it is possible to notice that no flange is present between the kinematic bar and the belt line bar. In fact, in this area, the inner shell is directly attached to the outer shell.

The outer shell also acts as an external panel. The transparent top panel is made of 5mm thick polycarbonate. This material has been selected after having compared the weight of the transparent panel in case of laminated glass and polycarbonate. The results of this comparison are reported in Table 3-1. By using polycarbonate, the advantage in terms of weight is quite relevant.

TABLE 3-1 TRANSPARENT PANEL: COMPARISON BETWEEN GLASS AND PC [23]

| | Panel density | Panel mass | Percentage variation |
|-------|------------------------|------------|----------------------|
| Glass | 2,5 g/cm ³ | 6,015 kg | |
| PC | 1,22 g/cm ³ | 2,935 kg | - 51,2 % |

CFRP Front Door –
Transparent Panel

| | Panel density | Panel mass | Percentage variation |
|-------|------------------------|------------|----------------------|
| Glass | 2,5 g/cm ³ | 6,38 kg | |
| PC | 1,22 g/cm ³ | 3,113 kg | - 51,2 % |

CFRP Rear Door –
Transparent Panel

An exploded view of the door is reported in Figure 3-8.

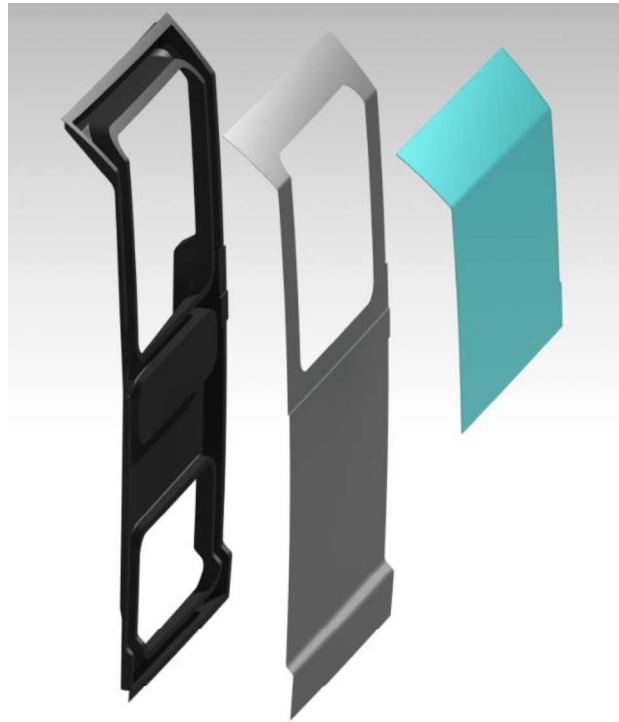


FIGURE 3-8. EXPLODED VIEW OF THE AUTOTAXI AND AUTOELF DOOR [26]

In Figure 3-9, it is possible to see the assembly made by the front and rear doors together from the inside and outside view. Between the doors there is a constant gap of 5mm.

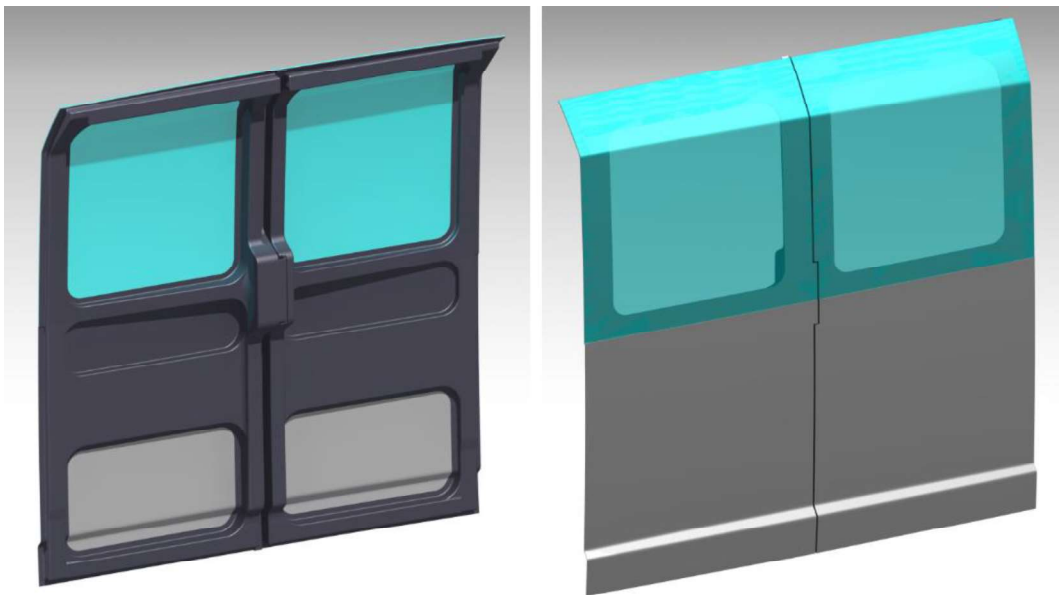


FIGURE 3-9. CFRP DOORS - VIEW FROM THE INSIDE AND THE OUTSIDE [26]

3.3.2 Roof

The inner shell of roof hatch (Figure 3-10) has a main beam in the front and a perimeter structure with constant section that is also used for the sealing. The front bar, with constant section 70x70mm, has the structural function of transferring the forces in the x direction in case of frontal impact and withstanding forces acting along the z axis in case of roll-over of the vehicle.

Since a 3-link mechanism has been chosen to open and close the roof hatch, it has also a central bar in correspondence with the link located in the middle of the roof hatch. This beam is also used to connect the front latch in the main roof bar to the rear one placed in the upper body. In this way, the deformation of the roof during the test is reduced, avoiding damages to the transparent panel.



FIGURE 3-10. INNER SHELL OF THE ROOF HATCH [23]

Three different versions of the roof have been proposed:

- 1) Without transparent parts (Figure 3-11). The roof consists of an inner shell, with structural function, and an outer shell that covers the entire surface of the roof.



FIGURE 3-11. ROOF SOLUTION WITHOUT TRANSPARENT PARTS [23]

- 2) With transparent parts (Figure 3-12). An outer shell and an inner shell create a structure on which a transparent part is installed. The transparent part is placed in a shallow created with flanges. In this way, there is no discontinuity in the external surface of the roof.

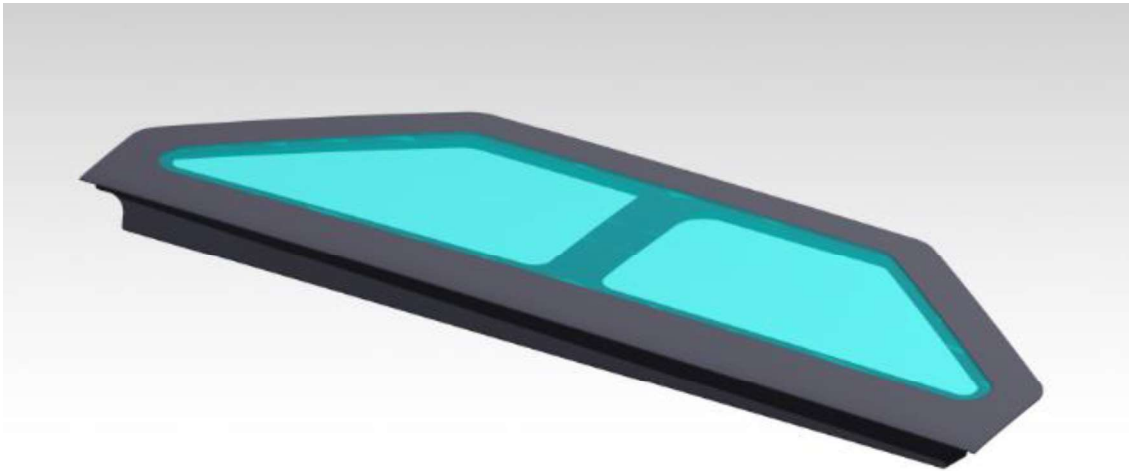


FIGURE 3-12. ROOF SOLUTION WITH TRANSPARENT PARTS [B6]

- 3) Transparent total coverage (Figure 3-13). Similar solution to the previous one, but in this case the transparent part covers the whole external surface.

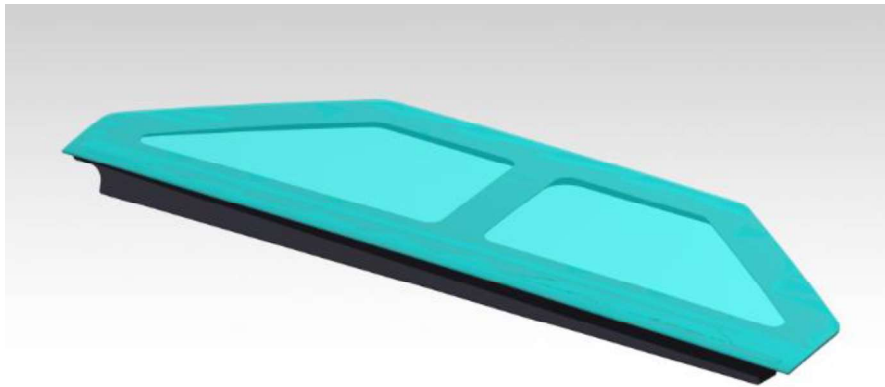


FIGURE 3-13 ROOF SOLUTION WITH TRANSPARENT TOTAL COVERAGE [23]

Even if, from the weight point of view, the first solution is the most convenient, for ergonomic and aesthetic reasons, the last one has been chosen. In fact, the total transparent coverage allows a better illumination of the internal space and create continuity with the upper part of the doors that have a transparent part starting from the belt line.

Roof and doors are shown together in the assemblies reported in Figure 3-14

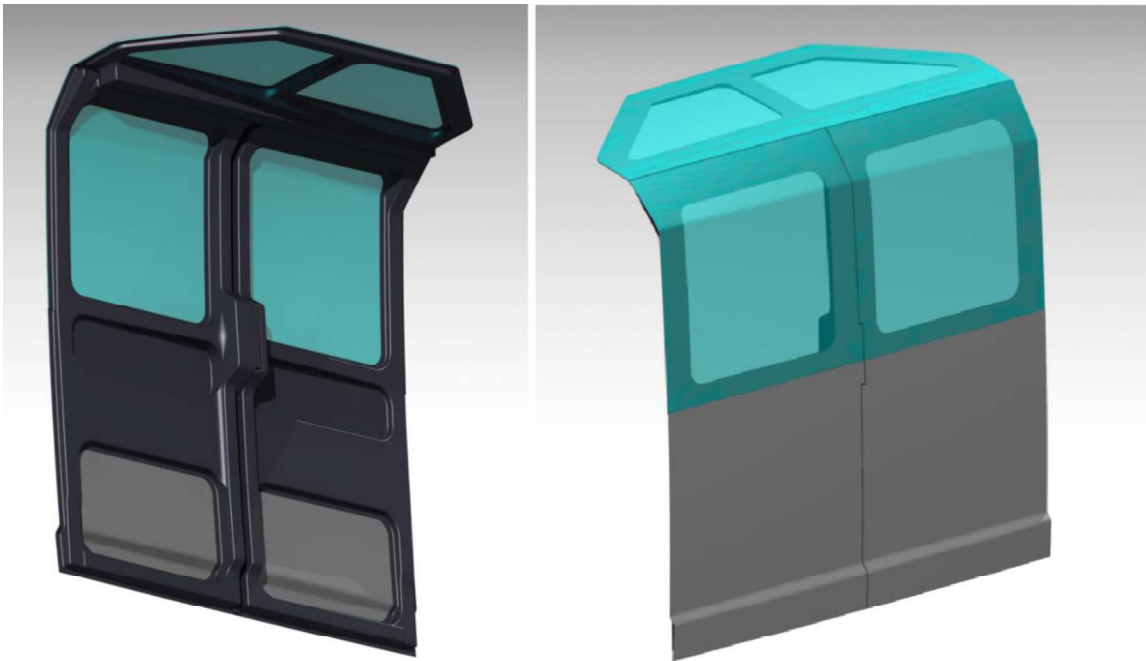


FIGURE 3-14. ROOF AND DOORS ASSEMBLY – VIEW FROM THE OUTSIDE [27]

Figure 3-15 shows the roof hatch installed on the 3-link mechanism constituting the roof kinematics. Two are connected to the sides of the roof and to the upper body (Figure 3-16), while the central one is connected to the center of the roof bar and to an electric motor fixed on the upper body. The same Bosch motor used for the doors is used also for the roof automation. The two lateral links are shaped in order to optimize the space inside the vehicle cabin when the roof is closed. They follow the roof frame created by the upper body. The links are produced from a steel profile that is bent and drilled.

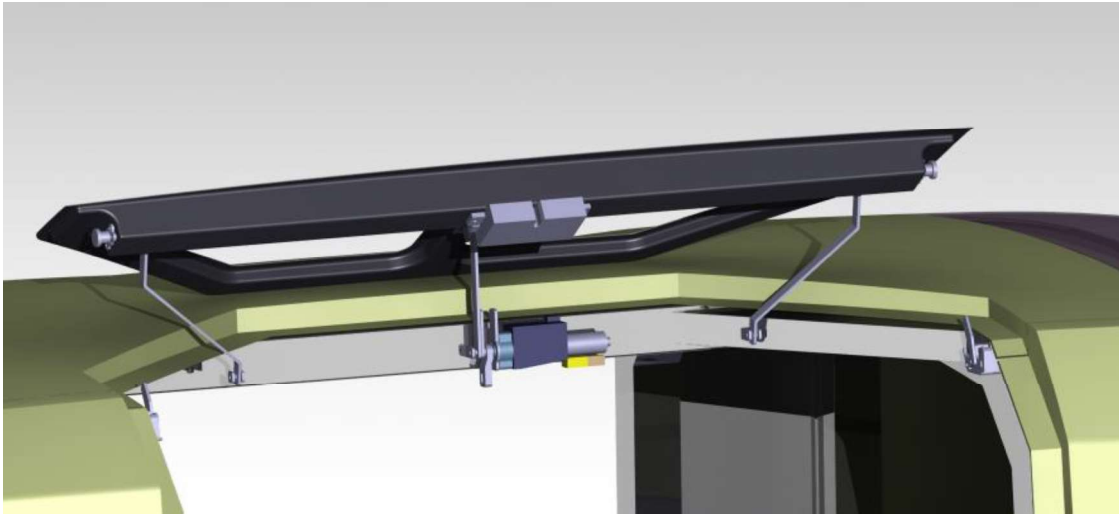


FIGURE 3-15. ROOF HATCH INSTALLED ON THE ROOF KINEMATICS [24]

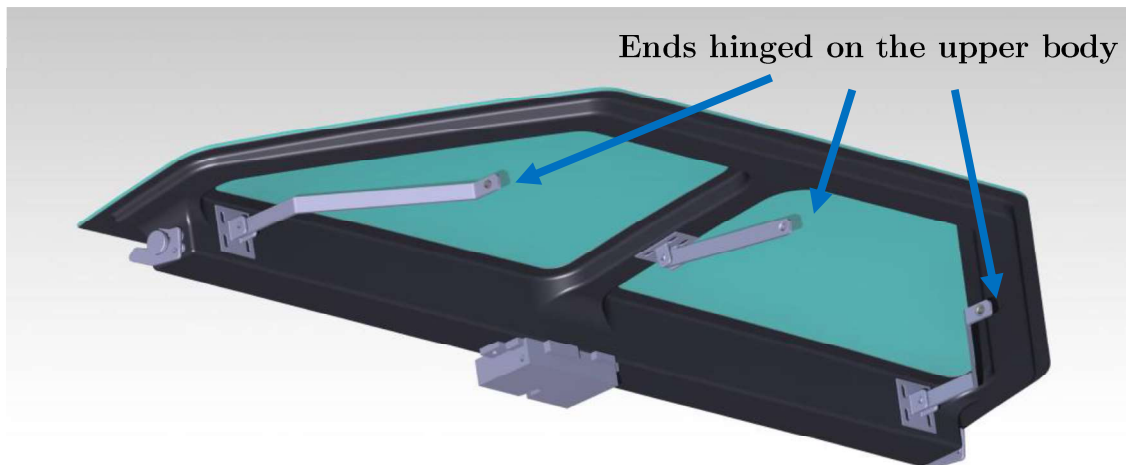


FIGURE 3-16. DETAILS OF THE 3-LINK MECHANISM [24]

3.4 AUTOshuttle and AUTOCargo doors adopted solutions

About the AUTOshuttle and AUTOCargo design of the doors, a critical point is not the packaging but the stiffness of the structure. Even if a scalable concept was followed, the difference in height and width could turn in a lower structural stiffness. For this reason, the box structure size created by the inner and outer shell has been increased from 50 mm x 50 mm to 60 mm x 60 mm.

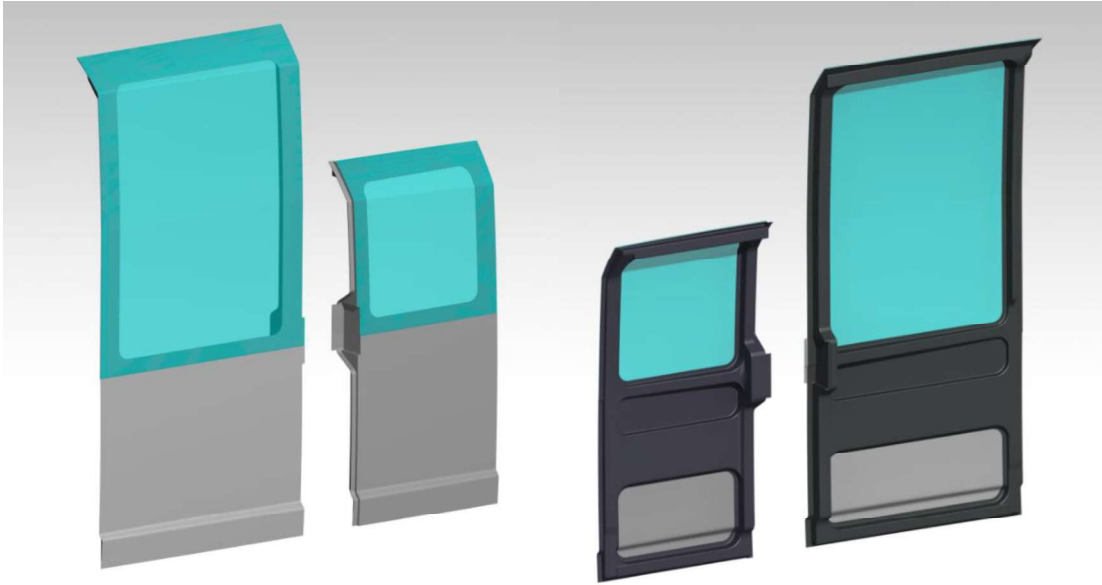


FIGURE 3-17. AUTOSHUTTLE AND AUTOCARGO VS. AUTOTAXI AND AUTOELF DOORS (INSIDE-OUTSIDE) [26][B6]

The dimensions of the two doors are reported in Table 3-2

TABLE 3-2 DIMENSIONS OF LARGER AND SMALLER DOORS

| | Height [mm] | Width [mm] |
|-------------------------------------------|----------------|---------------|
| AUTOshuttle and AUTOCargo door | 2243 | 1060 |
| AUTOfaxi and AUTOelf door | 1582 | 785 |

CURRENT STATUS OF DOORS AND ROOF

For the external transparent panel, a 5 mm thick polycarbonate panel is used, as in AUTOshuttle and AUTOcargo doors, for the same considerations done for AUTOfaxi and AUTOelf doors.

Last modification made on the doors concern the need of cover the kinematic mechanism. The solution chosen by the team was to add a trapezoidal panel on the side of the doors. In this way, when the doors close, they cover also the space where swing arms and motor are placed. This panel, integrated into the two door shells, must be design so that the sealing of the doors can be guaranteed. In order to have a stiff panel, a 50 mm wide perimeter frame was created in the inner shell and is also used as a sealing surface.

In addition, AUTOfaxi and AUTOelf doors are further modified in order to install HMI matrices. In the central part of the door, flanges in the shells were created between the two central bars and a 3 mm thick polycarbonate panel is fitted inside. The size and thickness of this panel that takes care of the HMI matrices of the vehicles were defined by the team.

Figure 3-18 and -Figure 3-19 illustrate the final AUTOfaxi and AUTOelf doors and their details.

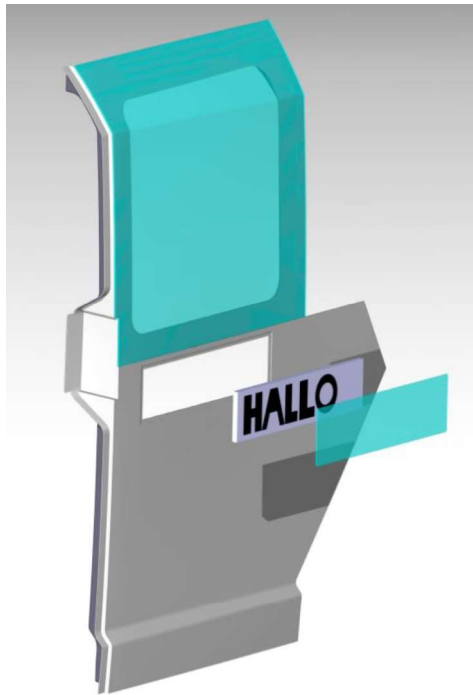


FIGURE 3-18, AUTOfAXI AND AUTOELF DOOR WITH TRAPEZOIDAL PANEL AND HMI MATRIX [27]

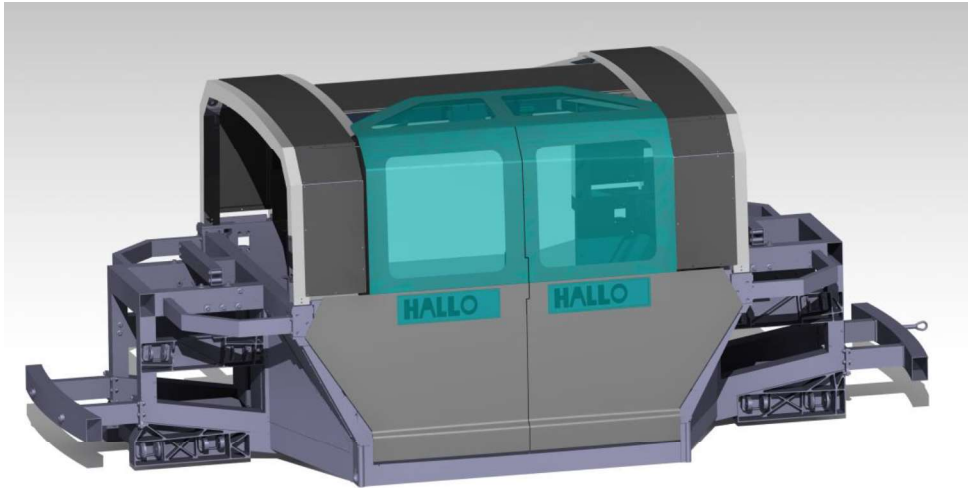


FIGURE 3-19. AUTOTAXI AND AUTOELF DOORS ASSEMBLED ON THE VEHICLE STRUCTURE [19]

3.5 Kinematics - Arms and sliding mechanism position

The door concept of UNICARagil, as said in the first sentences of this chapter, should be applicable to all four vehicle derivatives, i.e. AUTOtaxi, AUTOelf, AUTOshuttle and AUTOcargo and scalable accordingly. The challenge is to design the kinematic mechanism so stable that it can hold the heavier door of the large vehicles on the one side and fit into the low-available space of the smaller vehicles on the other hand.

Taking into account all the kinematic and ergonomic requirements mentioned, door opening looks like Figure 3-20 for the AUTOtaxi, where reaching positions depend on the door mechanism.

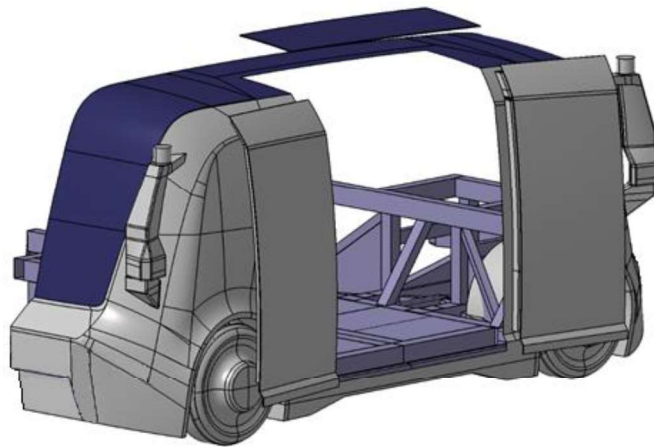


FIGURE 3-20. POSSIBLE DOOR OPENING CONCEPT OF THE AUTOTAXI [25]

CURRENT STATUS OF DOORS AND ROOF

As far as the swing & slide mechanism is concerned, the only space available for the installation of the arms and the motor used to automatize the opening of the doors is the one highlighted in red in Figure 3-21:

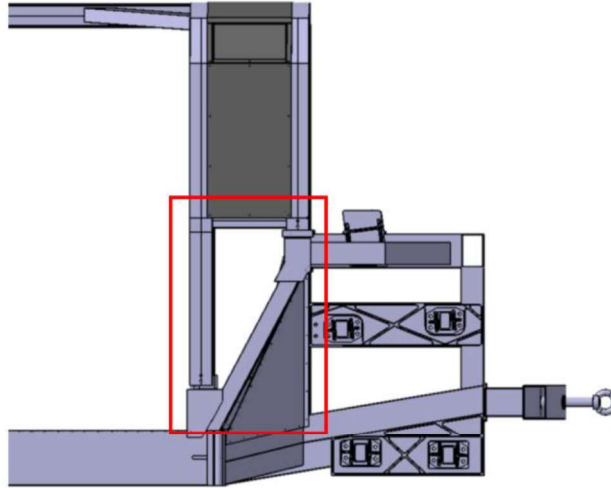


FIGURE 3-21. SPACE AVAILABLE FOR THE INSTALLATION OF THE ARMS ON THE VEHICLE STRUCTURE

The door kinematics was based on a single-rail mechanism, in the current version a double-rail mechanism is adopted and the distance between the rails is 180 mm. Figure 3-22 shows the new version of the kinematics, based on two separate rails, each of which has two runner blocks.



FIGURE 3-22. RAILS AND RUNNER BLOCKS USED FOR DOORS AUTOMATION [28]

This mechanism is provided by Bosch Rexroth, who is working with the kinematics team to find the right parameters to minimize the reaction forces and moments on the arms and therefore on the frame. The characteristic parameters of this system are the distance between the rails and the distance between the two runner blocks of each rail. In the definition of position and distance between the rails of the linear mechanism, possible interferences with upper body and doors components – latches arrangement, HMI matrices, sensors, structural elements (longitudinal and vertical bars) were taken into account.

In this version, shown in Figure 3-23, there is an adapter plate (in light blue) used to connect the arms to the four runner blocks of the linear mechanism. On this plate there are 6 slotted holes for each runner block that can be used to adjust the position of the sliding mechanism in the z direction. The two parts in violet and blue are used to connect the upper arm to the adapter plate.

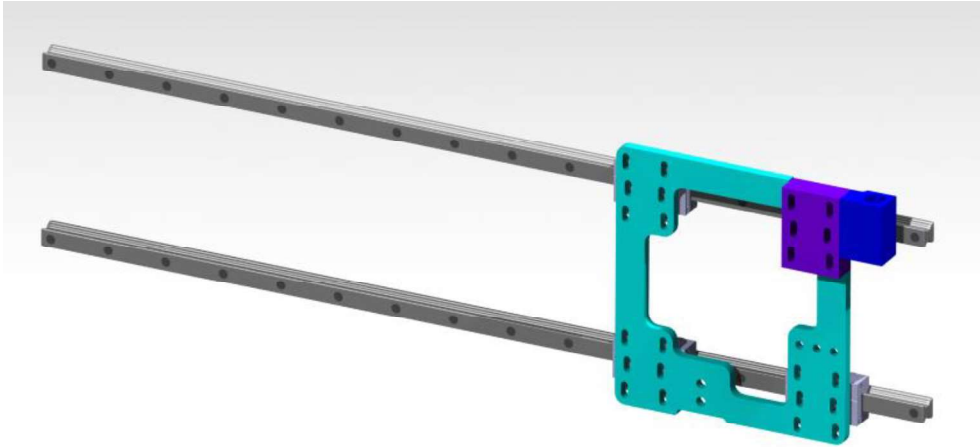


FIGURE 3-23. AUTOSHUTTLE AND AUTOCARGO DOOR KINEMATICS [29]

For each door there are two motors, one used for the automation of the swing arms and one for the linear mechanism. The first motor, connected to the lower arm, is a 12V motor produced by Bosch, commonly used for the rear door of the Audi Q7 4M (Figure 3-24) equipped with its own gearbox and two Hall Effect angular sensors (Figure 3-25). When the doors are completely open, the arms are rotated by 121.5° with respect to the closed position.

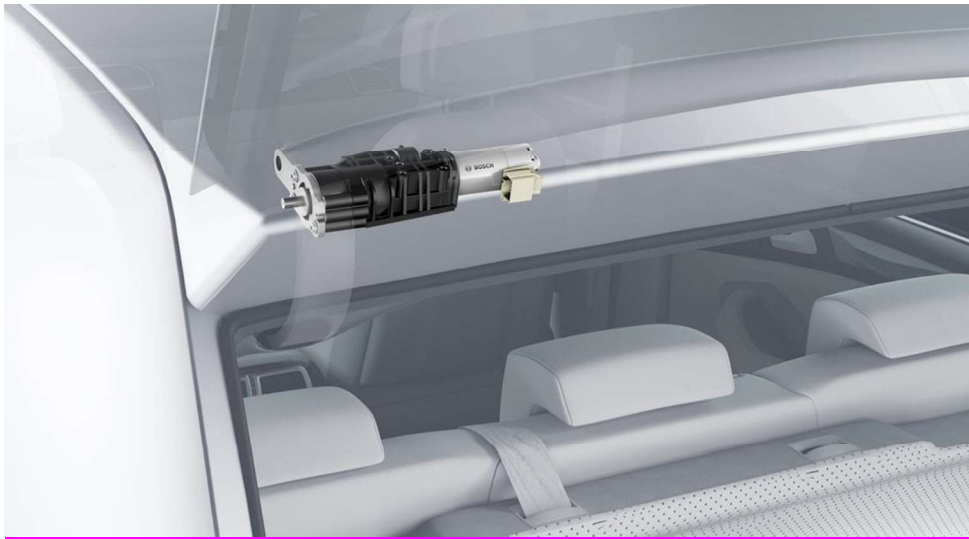


FIGURE 3-24. BOSCH MOTOR MOUNTED IN THE AUDI Q7 4M [30]

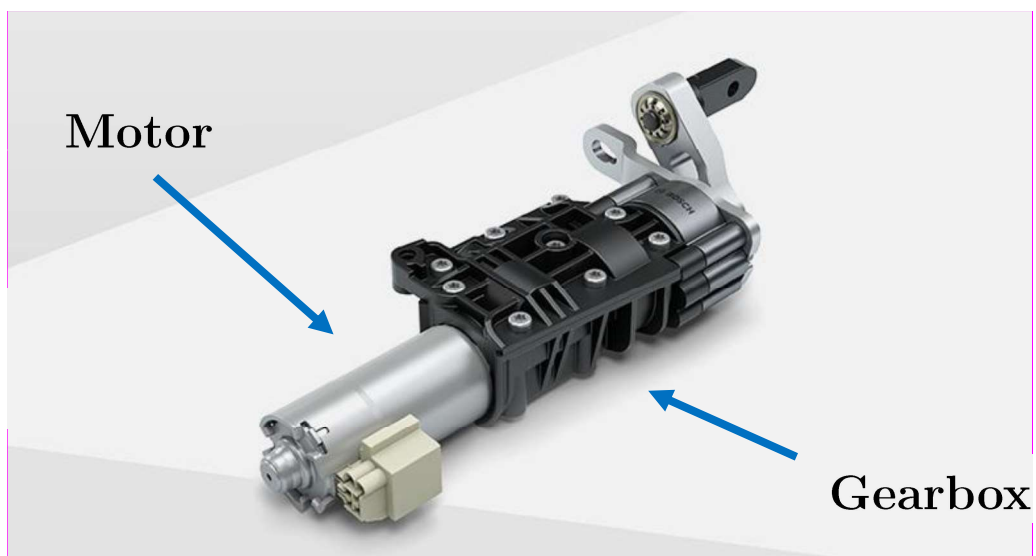


FIGURE 3-25. BOSCH MOTOR WITH GEARBOX [30]

For the automation of the linear mechanism, a 12V/24V motor produced by Mädler (Figure 3-26) is used, connected to a cable drive mechanism. The cable drive mechanism consists of a drum or pulley and a cable. The cable is wound around the drum and has the two ends connected respectively to the ends of the rails. The problems associated with this mechanism are the possibility of having a relative slip between the cable and the pulley and the possibility of having a deformation of the cable. Both problems cause an error in the position of the door with respect

CURRENT STATUS OF DOORS AND ROOF

to the one determined by the motor. The first problem is solved by increasing the number of cable windings on the rotating drum, while the second by choosing a cable characterized by low stretching.



FIGURE 3-26. MAEDLER MOTOR USED FOR THE SLIDING MECHANISM AUTOMATION [31]

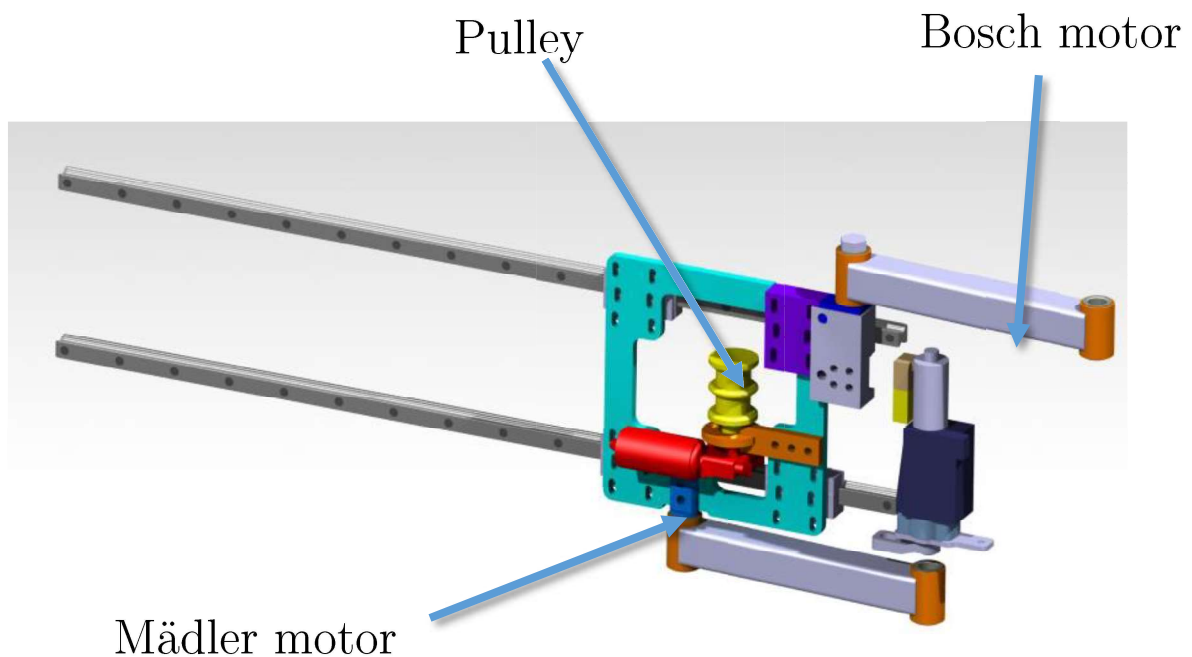


FIGURE 3-27. NEW KINEMATICS, USED IN THE FINAL SOLUTION [29]

3.6 Latches position and soft-close mechanism

The positioning of the locks should ensure the force flow from the door structure into the vehicle structure and at the same time fix the door in all directions. The positioning of the locks in UNICAR*agil* follows the positioning of the locks in the VW Sedric (Figure 3-28), which represents an already implemented benchmark. The locks should transmit the forces as far as possible at the nodes of the door structure in order to introduce non-additional levers. One of the vehicle doors should therefore be closed laterally to the body, at the bottom to the sill and at the top to the roof. The second door then closes sideways to the body and to the other vehicle door [22].



FIGURE 3-28. LOCK POSITIONS IN VW SEDRIC, RIGHT DOOR CLOSES FIRST [22]

In UNICARagil vehicles (Figure 3-29), as in VW Sedric, the front door closes before the rear one.

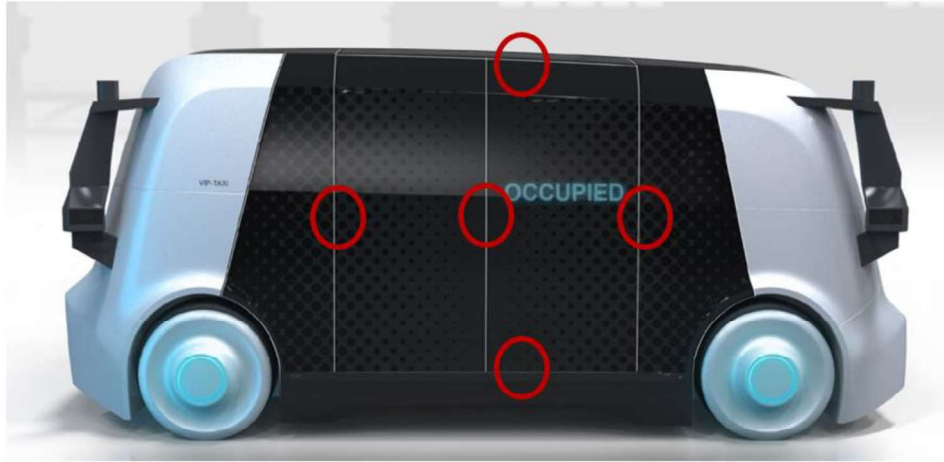


FIGURE 3-29. LOCKS POSITION IN UNICARAGIL VEHICLES [32]

The hold of the door in a case of a force acting to the outside of the vehicle is mainly guaranteed by the locks. The locks therefore were connected to the respective structure both on the door side and on the vehicle side, keeping in mind that, in order to reduce the weight of the doors and to avoid a complex cable management due to the soft-close mechanism, latches were placed in the vehicle structure side. The only exception was the lock between the doors, for obvious reasons.

Soft-close mechanisms are used as locks. This mechanism is adopted in order to help the engine in closing the doors, as this is made difficult especially by the presence of seals. The mechanism adopted in UNICARagil is the same used in the tailgate of BMW 5 (Figure 3-30). If the vehicle is equipped with a Soft-Close automatic tailgate drive, the tailgate only has to be pressed lightly into the tailgate lock to close it. This starts the drive and closes the tailgate completely. The tailgate lock can also be electrically unlocked and then opened via the control points (e.g. identification transmitter, external tailgate button, internal tailgate button). In the same way, thanks to this technology, UNICARagil doors can be closed lightly and the system will automatically take it over. The sensor detects the attempt to close the door and once the latch (Figure 3-31) catches the striker pin, an electric motor is turned on (each latch has an electric motor). The electric motor has the sole task to pull the door firmly, with a noise that can be barely noticed [23].

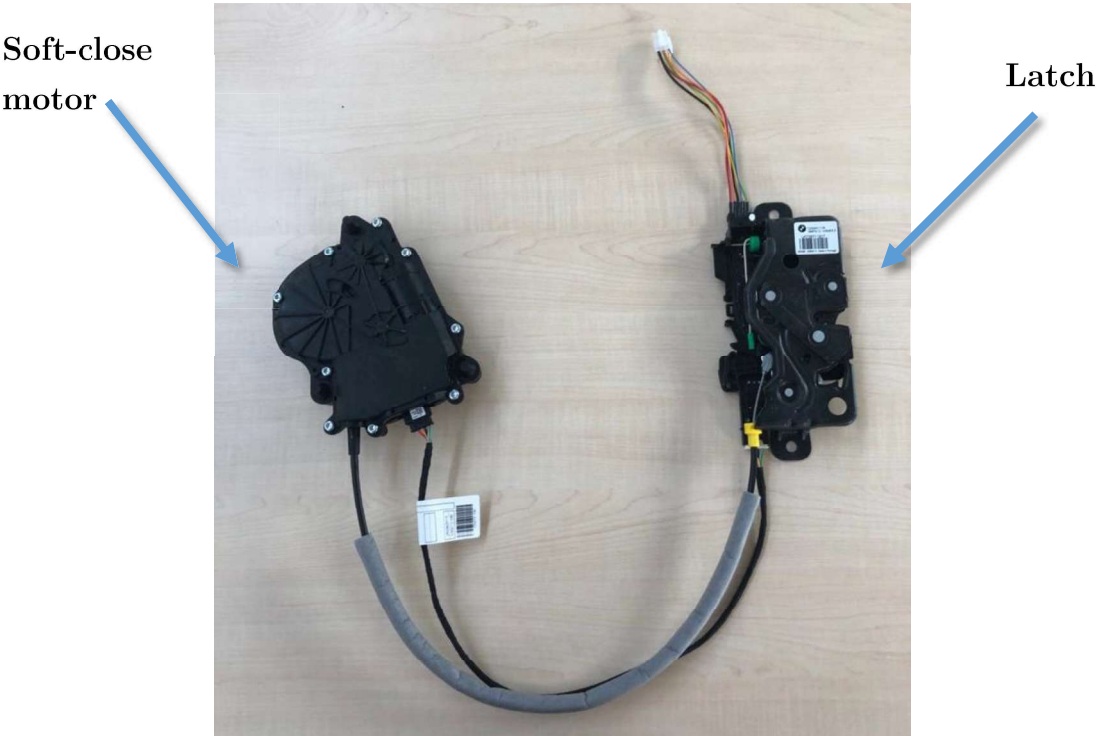


FIGURE 3-30. SOFT-CLOSE MECHANISM

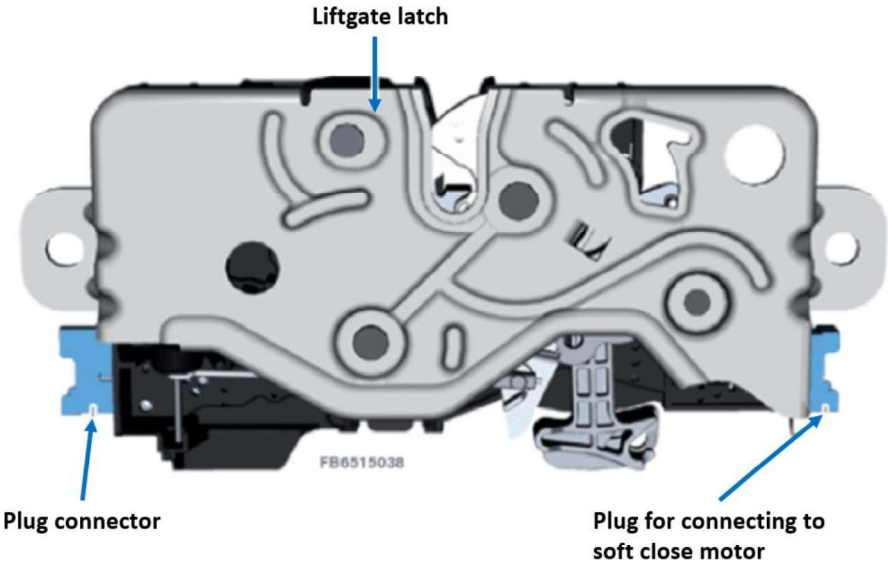


FIGURE 3-31. LATCH OF THE SOFT-CLOSE MECHANISM [2]

4 Methods

In this chapter, the methodology used for the design of the doors and the roof will be illustrated. Requirements and targets to be met with the design will be shown. The proposed solutions will be explained in detail and motivated, in terms of materials and construction.

4.1 CAD models parameterization

In shape design optimization, the purpose of design parameterization is to characterize the changes in dimensions and movements of geometric control points that govern the shape of the structural boundary. These design variables are allowed to vary in the design process in order to improve structural performance. With the recent development of dimension-driven CAD tools, the design engineer can more easily capture design intent in the CAD model. The design engineer first concentrates on the shape of the part leaving certain dimensions as variables which may be adjusted later in the design process [33].

4.1.1 Definition of parameters

The CAD models provided by the team for future structural analysis were modelled with parametric software, Catia V5. In the mind grip of the various models, the logical steps behind the component construction were complex and sometimes not completely clear.

Considering the future changes required to complete the components, after careful evaluation, the team came up with the decision of re-designing the components using reference dimensions and surfaces, as well as connections between components. The initial changes were made keeping the previous geometries as guidelines.

Design started with a logical tree organization equal for all components with a subdivision of the various properties:

- Main structure
 - Sketches
 - Points and lines
 - Surfaces
- Inserts
 - Sketches

- Points and lines
- Surfaces
- Wiring holes
 - Sketches
 - Points and lines
 - Surfaces
- Sensors
 - Sketches
 - Points and lines
 - Surfaces
- External references
 - Sketches
 - Points and lines
 - Surfaces

Doors compose part of the external bodywork and made with two shells. During the design phase, given the surface constraints imposed on the components, a father-son dependence was chosen between the outer and inner shells respectively. In this way, the correspondence between the two shells has been ensured even in case of future modifications of the external surfaces.

4.2 CAD editing

Before starting with the structural analyzes on the components, changes were made at the functional level, such as the introduction of passenger safety geometries, the position of the latches and the identification of a path to seal the doors.

4.2.1 Geometry for safety

Passenger safety aspects must be taken into consideration during the design phase. The term geometry for safety refers to all those design measures that contribute to ensuring greater protection against accidental collisions that may occur during the use for which the components were designed.

By applying this concept to the design of the surfaces in question, a study on passenger safety during the opening and closing phases of the doors was necessary. To identify any risk areas, the first step was to carry out an analysis of the kinematics of the doors. By analyzing the movements of the doors during the

opening and closing phases, it was possible to identify some areas where an unwanted collision with the passengers' limbs could have led to their crushing.

In this sense, by simplifying the geometries in these areas, a safe distance between door structure and vehicle frame is insured. Figure 4-1 shows the changes made.

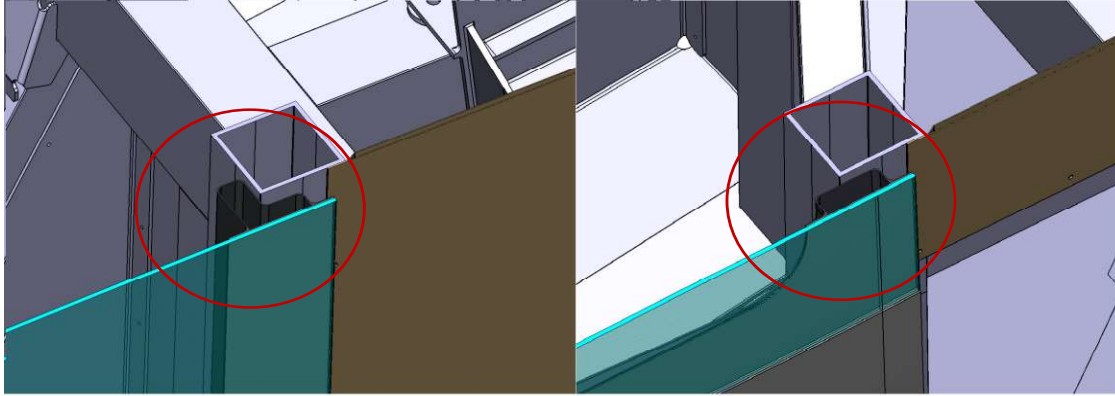


FIGURE 4-1 LATERAL BEAM BEFORE(LEFT) AND AFTER(RIGHT) EDITING

Anti-crushing devices which, from an electronic point of view, consists in the introduction of sensors to detect anomalous current peaks inside the motors used for door opening and closing operations. A current peak during one of these phases indicates an anomalous overload on the motor that could be due, for example, to a limb stuck between the two doors that prevents them from closing. Such a system can prevent damage to passengers by removing power from the motors or by reversing the movement.

4.2.2 Latches position

The latches are fixed on the frame and on the movable parts following the configuration described below. Figure 4-2 illustrates that the two lateral latches are fixed on the upper body and the lower latch on the platform. While the upper latch is placed on the roof structure and the central one is placed on one of the two doors.

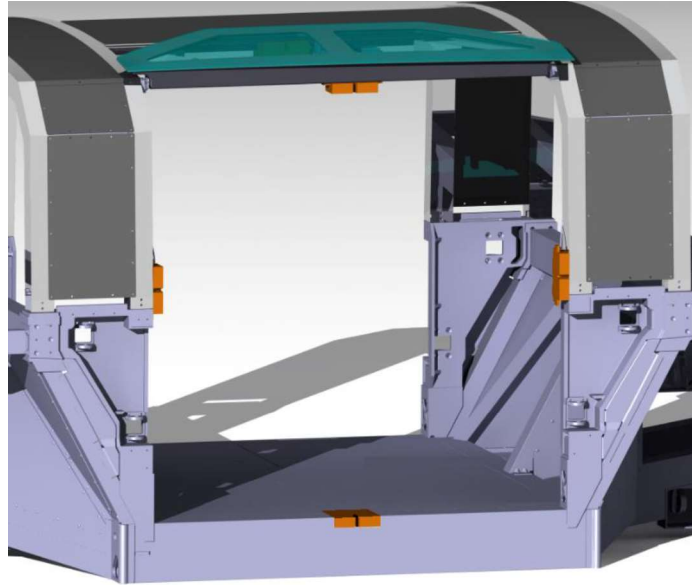


FIGURE 4-2 LATCHES IN AUTOTAXI AND AUTOELF [19]

Initially, a layout was preferred in favour of a greater seal. This arrangement involves anchoring the strikers and their latches on the door that closes last. In this way, the front door would be pushed towards the closing by the rear door which could count on three anchorage points. This configuration ensures greater sealing and stability of the moving parts.

A second analysis revealed some critical points brought by a solution of this type. In particular, it was necessary to position the latches to facilitate the manual opening of one of the two doors in case of emergency. An arrangement like the one just described involved the use of four latches on the rear door. Considering that the opening sequence of the doors requires the rear door to open first, it was therefore decided to position the upper and lower latches not on the rear door but on the front door, in order to deal just with the opening of two latches during an emergency phase.

The configuration of the central latch has been completely revised. In the previous configuration the weather strip on the central latch passed behind the latch leaving it exposed to the weather. The new case requires the front door to have a continuous flange from the upper latch to the lower latch. This allows the central latch to be sealed as well. In addition, the weather strip's path no longer has any pronounced curvature, thus ensuring better sealing.

The changes that have been made to the doors as a result of the above-mentioned features are as shown in Figure 4-3

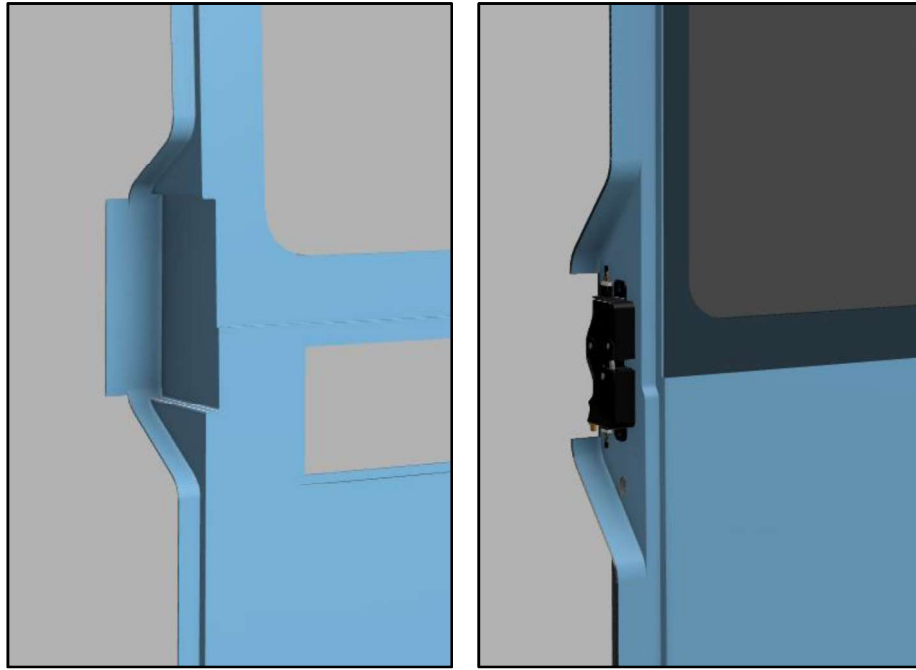


FIGURE 4-3 DETAIL OF THE LATCH CASE BEFORE(LEFT)AND AFTER (RIGHT) EDITING

In addition, in order to be able to place the latch on the roof, it has also been revised and a compartment for latch and soft-closing motor is added (Figure 4-4). The latch that locks the rear part of the roof is directly fixed on the upper body, close to the motor for the roof automation (Figure 4-5)



FIGURE 4-4 ROOF SOFT-CLOSING MOTOR CASE

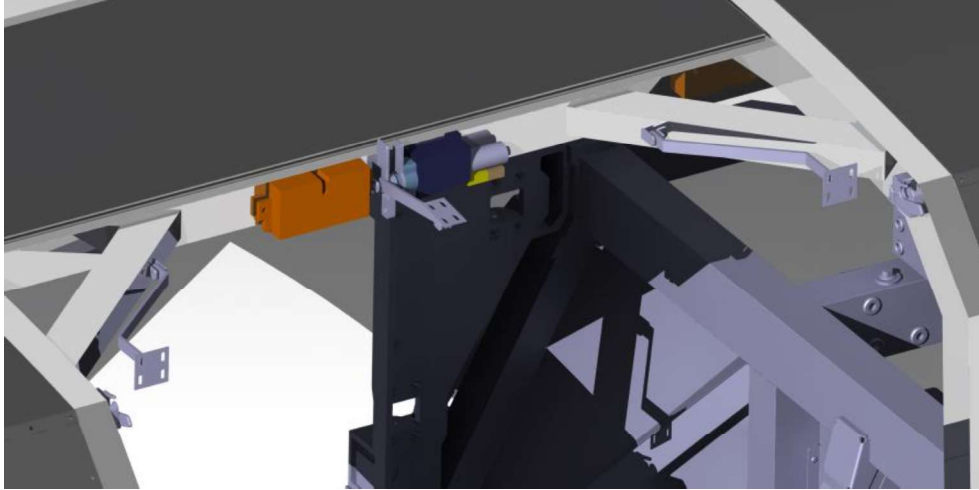


FIGURE 4-5 SECOND LATCH OF THE ROOF FIXED TO THE UPPER BODY [24]

4.2.3 Sealing

The main mission of the weather strips is to seal the passenger compartment and luggage from noise, air, water, snow, mud and powder. Body weather strips should comply with elastic deformations in the order of millimetres: allowed flexibility is only limited by the dynamic seal capability, i.e. the ability to match quickly and completely the surfaces to be sealed [34]

The seals operate within their own rigidity range. Values above the range lead to closing pressures that are not compatible with the rigidity of the structure. For values below the stiffness range, the seal pressure does not provide insulation against water and dust ingress.

The sealing properties must remain unchanged throughout the life of the vehicle, which means that the sealing strips have to withstand the aging promoted by environmental, physical and chemical agents, including solar radiation, humidity and temperature changes, contact with hydrocarbons and many types of gas, dust, sand, etc. This is achieved mainly through the appropriate choice of material, which was once natural rubber and today is mainly composed rubber, mainly EPDM (Ethylene Propylene Diene Monomer) and Santoprene (a mixture of thermosetting rubber and thermoplastic polymers) [34].

Sealing is one of the critical aspects of UNICAR*agil* project, especially in AUTOt*axi* and AUTOe*lf* that have two doors and a lifting roof. The aim is to have an effective sealing between the moving components and the vehicle structures and between the components themselves.

The primary seal could be mounted on the door frame or on the vehicle structure. The first solution would involve the use of two separate seal rings, one for each

door, and would lead to an ineffective seal at the interface between the doors. For this reason, in the UNICAR*agil* project, it has been decided to install the seal on the vehicle structure and not on the doors, as this solution allows to have a single continuous seal ring along the vehicle structure.

Between the two doors, a bulb weather strip is located. In particular, it is carried by the front door, which is the first to be closed. The problem of this configuration lies in the triple node, where both weather strips are overlapped. This causes a sharp thickness variation which leads to water leakage into the passenger compartment.

During the design phase, various sealing issues have been considered.

The curvature radius of the weather strip must never be less than the values reported in Figure 4-6. This rule is intended to preserve the seal from buckling defects and section reduction that causes loss of contact. The minimum recommended radius around an axis parallel to the sealing flange is 40 mm, while around an axis perpendicular to the sealing flange it should never be less than 150 mm [34].

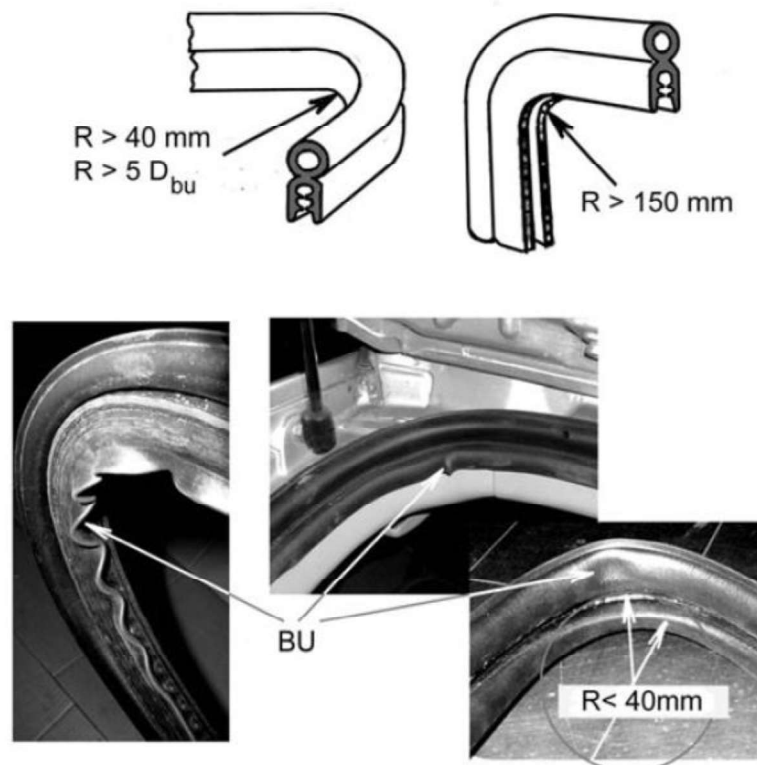


FIGURE 4-6. DESIGN RADIUS TO AVOID BUCKLING (BU) [34]

The seal used are always of the bulb type, the base of which is directly glued to the surfaces of the vehicle structure and the flange of the front door by means of a double-sided adhesive tape or a specific adhesive, making the seal effective.



FIGURE 4-7. BULB SEAL USED FOR UNICARAGIL VEHICLES [35]

The type of weather strip used as well as the dimensions and the bonding solution are the result of appropriate evaluations also with the members of the teams that deal with the chassis and the body of the vehicle. The lack of flanges in the bodywork made it impossible to use a snap seal.

During the design of the doors, a 10mm gap between this surface and the door frame has been left so that the seal could be positioned in that space (Figure 4-8).

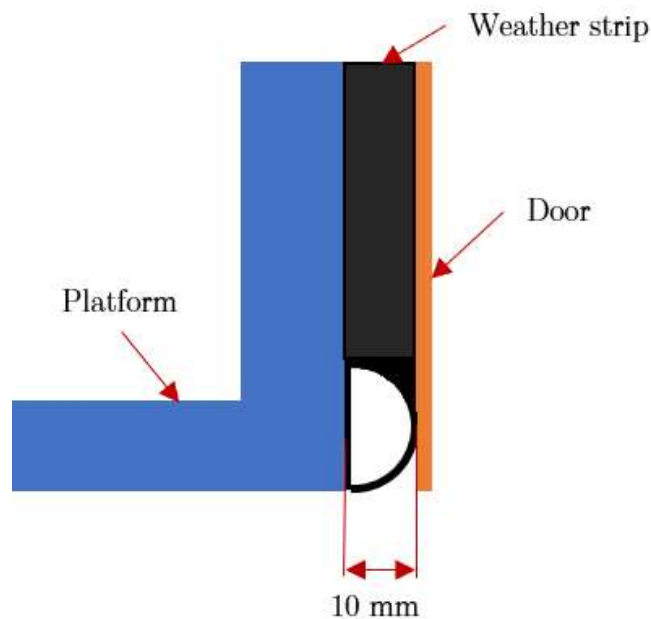


FIGURE 4-8. SEAL BETWEEN DOOR STRUCTURE AND PLATFORM

Although the seal ring has similarities between smaller and larger vehicles, they will be treated separately.

AUTOtaxi and AUTOelf are the vehicles with the highest number of critical points in terms of sealing. In fact, the presence of the movable roof makes it more complex to seal the passenger compartment.

The solution used on this vehicle is based on a single ring that partly surrounds the two doors and partly the roof. The weather strip is installed directly on the upper body, as shown in Figure 4-9. In the upper part, the ring continues along the entire perimeter of the roof frame and in the lower part it surrounds the two areas where the arms are fixed.



FIGURE 4-9. SEAL RING OF AUTOTAXI AND AUTOELF [19]

Due to the presence of a roof hatch, it is necessary to place a gasket also on the roof main beam in order to ensure a perfect sealing between roof and doors (Figure 4-10).

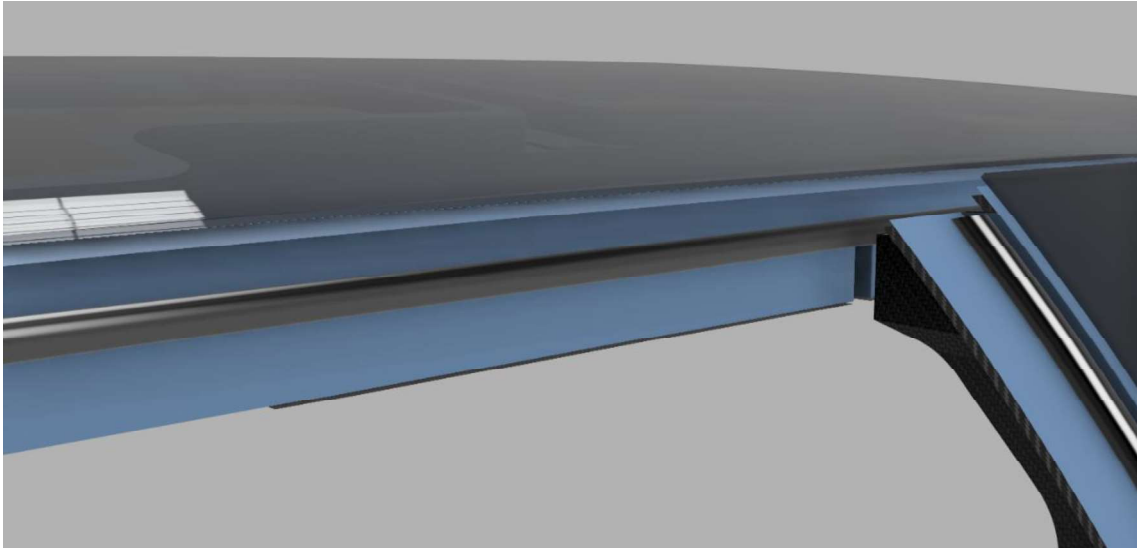


FIGURE 4-10 ROOF-DOOR SEALING

The last component of the AUTOfaxi sealing system is the weather strip between the two doors, Figure 4-11. Taking up the concept of the twin doors of commercial vehicles, it is positioned on the flange obtained in the door that closes first.

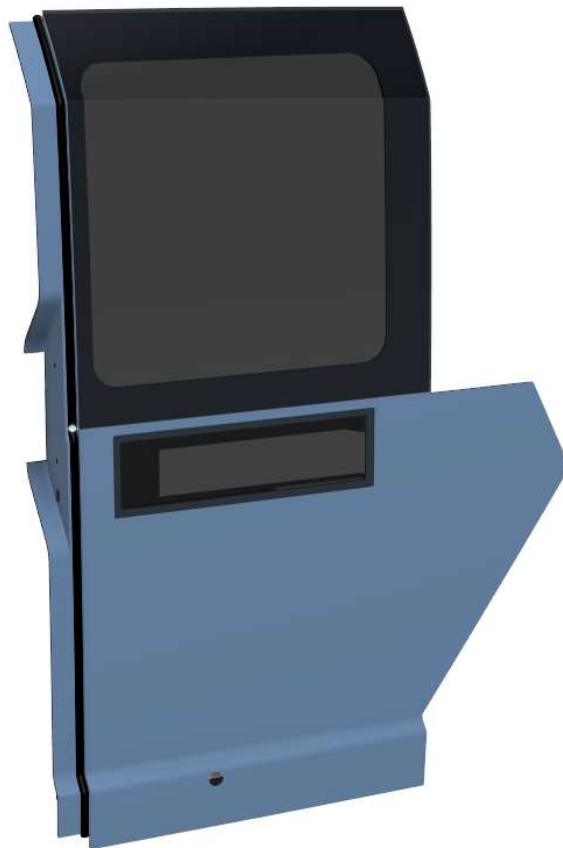


FIGURE 4-11. SEAL PLACED ALONG THE FRONT DOOR FLANGE

For the study of the seals of AUTOshuttle and AUTOcargo, the same concept illustrated for the smaller vehicle is used. However, that solution is adapted to the different characteristics of this vehicle.

The large vehicle does not have a movable roof. To create the seal ring, the roof bar integrated in the upper body is used to position the gasket, as shown in Figure 4-12.

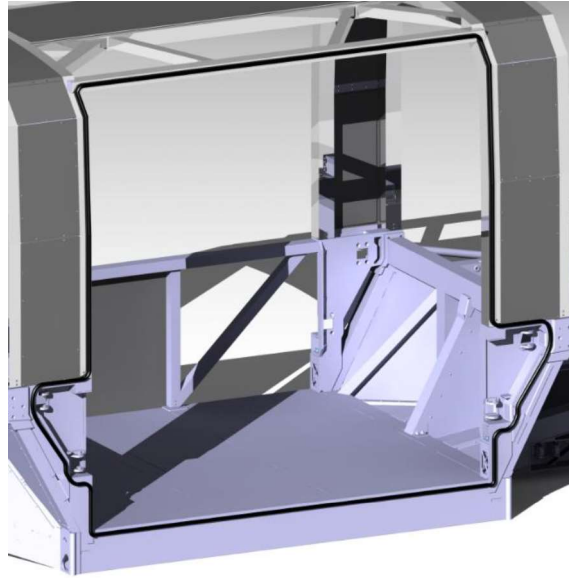


FIGURE 4-12. SEAL RING ON AUTOSHUTTLE AND AUTOCARGO [19]







4.3 Materials

The previous team carried out an in-depth study of the material to be used to produce these components. In their analysis, three different materials that are used in the automotive field were taken into consideration: aluminium. Magnesium and carbon fibre reinforced polymer.

The common factor that led to the choice of these materials was their low density. Weight management, when dealing with electric vehicles, is a very important variable in component design. Below are the main results of this study.

Table 4-1 shows the total mass values of the three models. As a conservative approach, in accordance with the team practices, it was decided to add 20% of the value obtained in CATIA, so as to ensure that the maximum limit established for each door is not exceeded. The last column shows whether or not the total mass, including 20 %, meets the maximum limit requirements. It should be noted that the masses for the front door and the rear door are different due to the lack of symmetry in the doors, determined by the design of the external shape [23].

TABLE 4-1 FRONT AND REAR DOOR MASSES FOR THE THREE DOOR SOLUTIONS [23]

| <i>REAR DOOR</i> | Structure mass [kg] | Transparent glass panel mass [kg] | External panel mass [kg] | Total mass [kg] | Total mass + 20 % [kg] | Threshold limit: 37,4 kg |
|-------------------|---------------------|-----------------------------------|-------------------------------|-----------------|------------------------|---------------------------------------------------------------------------------------|
| Aluminum alloy | 12,829 | 14,189 | 5,644 | 32,662 | 39,194 |  |
| Magnesium alloy | 12,526 | 15,954 | 4,465 | 32,945 | 39,534 |  |
| CFRP | 12,181 | 15,954 | Integrated in the outer shell | 28,135 | 33,762 |  |
| | | | | | | |
| <i>FRONT DOOR</i> | Structure mass [kg] | Transparent glass panel mass [kg] | External panel mass [kg] | Total mass [kg] | Total mass + 20 % [kg] | Threshold limit: 37,4 kg |
| Aluminum alloy | 12,84 | 14,617 | 5,855 | 33,312 | 39,974 |  |
| Magnesium alloy | 12,812 | 15,316 | 5,409 | 33,537 | 40,244 |  |
| CFRP | 12,293 | 15,316 | Integrated in the outer shell | 27,639 | 33,167 |  |

As shown in the Table 4-1, the only door to satisfy the maximum limit of mass is the one realized of CFRP. The other two doors, which have a mass about 20 % higher than the CFRP one (Table 4-2), do not guarantee a maximum mass of 60 kg [23].

TABLE 4-2 PERCENTAGE VARIATION OF THE DOOR MASSE WITH RESPECT TO CFRP DOOR MASS [23]

| | <i>REAR DOOR</i> | | <i>FRONT DOOR</i> | |
|--------------------|---------------------------|--------------------------------|---------------------------|--------------------------------|
| | Total mass + 20 % [kg] | Percentage variation [%] | Total mass + 20 % [kg] | Percentage Variation [%] |
| CFRP | 33,762 | | 33,167 | |
| Aluminum alloy | 39,194 | +16,09 | 39,974 | +20,52 |
| Magnesium alloy | 39,534 | +17,10 | 40,244 | +21,34 |

Therefore, according to the selection method defined in [23], the door structures for the four UNICARagil vehicles will be made of CFRP

4.3.1 Composite materials

The composite materials of engineering interest are mainly composed of two components: matrix and reinforcement.

The continuous component, generally present in larger quantities, is called matrix. The properties of the matrix are improved by introducing a new component, the reinforcement, thus forming the composite. The role of the matrix is to transfer the load to the reinforcements, keeping them together. The matrix itself does not have high mechanical properties [36].

The second component of a composite material is the reinforcement, which has the function of increasing the mechanical properties of the matrix. It is the reinforcement that generally absorbs a large part of the stresses acting on the material and that gives it the required strength and stiffness. composite materials can be reinforced with continuous fibers (long fibers) with one or two preferential directions, called unidirectional or fabric, respectively. In the case of fiber-reinforced plastics (FRP) the matrix is made of a resin (mainly epoxy, polyester or phenolic), while the reinforcement is made of various types of fibers: carbon fiber (CFRP) as shown in Figure 4-13, glass fiber (GFRP), aramidic fibers (AFRP), etc.. [36]

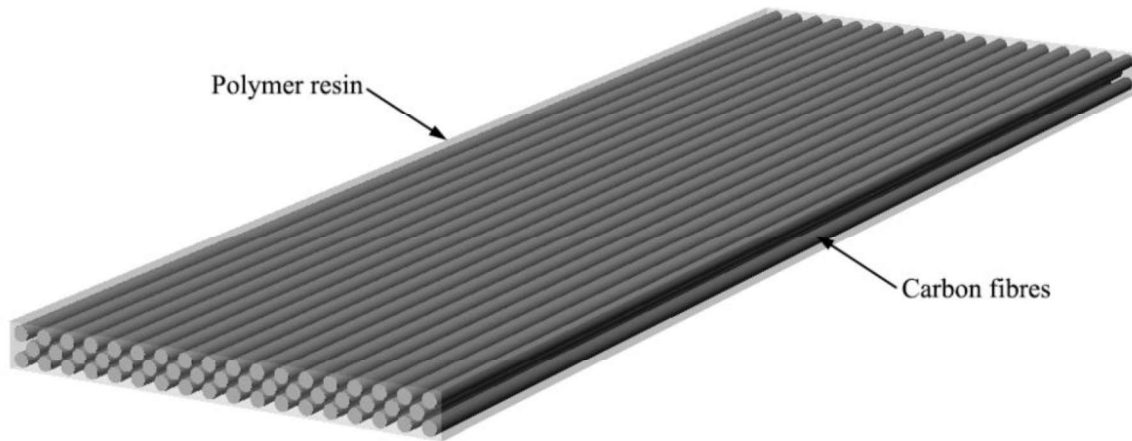


FIGURE 4-13. CFRP [37]

To produce a composite part, two decisions can be taken:

- Preimpregnate the fiber with resin, forming an intermediate product called prepreg. Composite part are then produced in a subsequent manufacturing process, known as dry process or prepreg based process, in which prepreg is used as the raw material.
- Combine fiber and liquid resin matrix while simultaneously producing the final composite part, in a process known as wet process or non-prepreg based process.

The use of prepreg reduces material variability but increases costs, while wet processes result in increased material variability but are relatively inexpensive [38]. Even if the cost is higher, the UNICAR*agil* team decided to use a prepreg based process in order to ensure a lower variability in the material.

So, prepreps are specially formulated resin matrix systems that are reinforced with carbon fibers. The thermoset resin cures at elevated temperature, undergoing a chemical reaction that transforms the prepreg into a solid structural material that is highly durable, temperature resistant, exceptionally stiff and extremely lightweight. This growth in the use of prepreg composites over metal has been driven by higher strength to weight performance, better fatigue strength and potential to offer greater freedom of design.

The position of prepreg technology in terms of performance and production volumes is compared below with other fabrication processes (Figure 4-14)

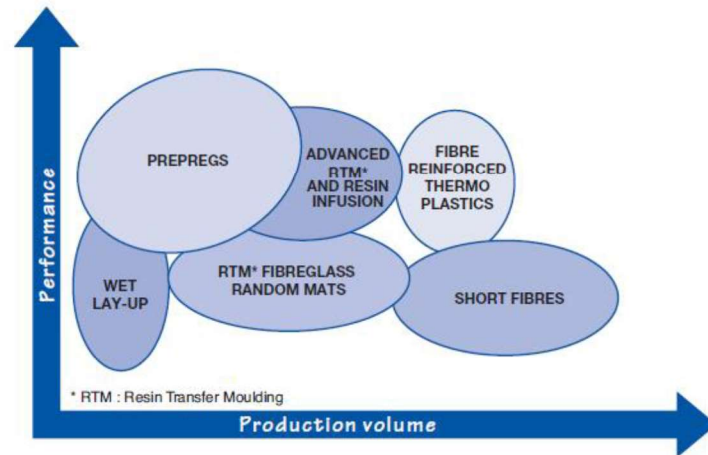


FIGURE 4-14. PRODUCTION VOLUME AND PERFORMANCE OF COMPOSITE TECHNOLOGIES [39]

Reinforcement materials provide composites with mechanical performance: excellent stiffness and strength, as well as good thermal, electrical and chemical properties, while offering significant weight savings over metals [39].

The matrix also determines environmental resistance and maximum service temperature of a prepreg [39]. Thermoset resins cure permanently by irreversible cross linking at elevated temperatures. This characteristic makes the thermoset resin composites very desirable for structural applications [40]. Traditionally, the resin adopted in the automotive industry is epoxy, because of its excellent mechanical performance, good environmental resistance, high toughness and easy processing [39].

A prepreg is available in unidirectional form and fabric form (Figure 4-15).

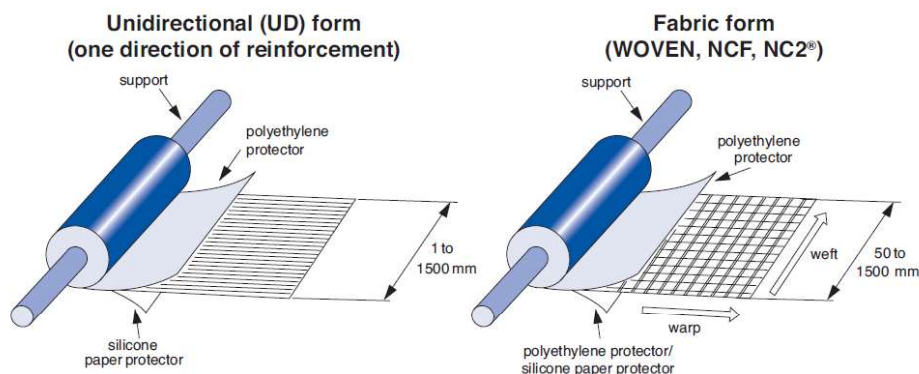


FIGURE 4-15. DIFFERENT PRODUCTION TECHNIQUES FOR PREPREG [39][B5]

Fabrics consist of at least two threads which are woven together: the warp and the weft. The weave style can be varied according to crimp and drapeability. Low crimp

gives better mechanical performance because straighter fibers carry greater loads; a drapeable fabric is easier to lay up over complex forms. There are three main weave styles: plain, satin and twill weave (Figure 4-16) [39].

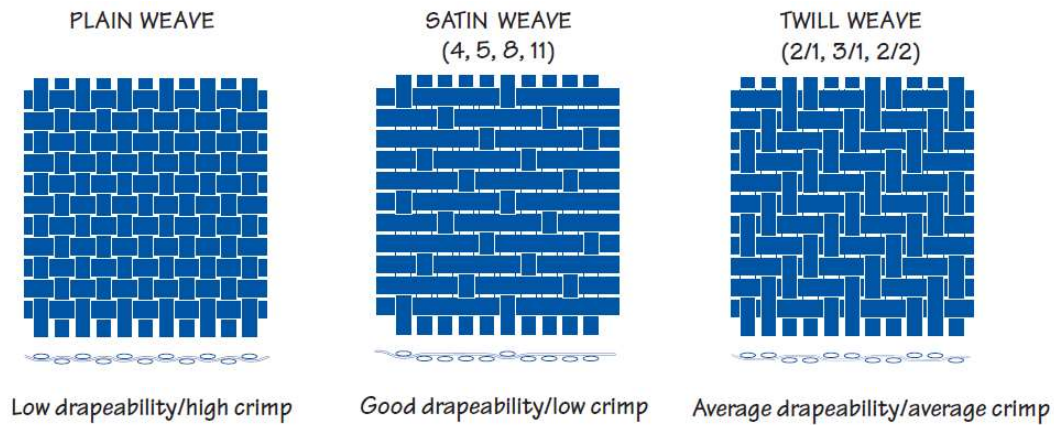


FIGURE 4-16. DIFFERENT WEAVE STYLES [39]

Unidirectional composites (UD) have predominant mechanical properties in one direction and are said to be anisotropic. Fabric instead have predominant mechanical properties in two directions. Isotropic materials (most metals) have equal properties in all directions. Components made from fiber-reinforced composites can be designed so that the fiber orientation produces optimum mechanical properties, but they can only approach the true isotropic nature of metals (Figure 4-17) [39].

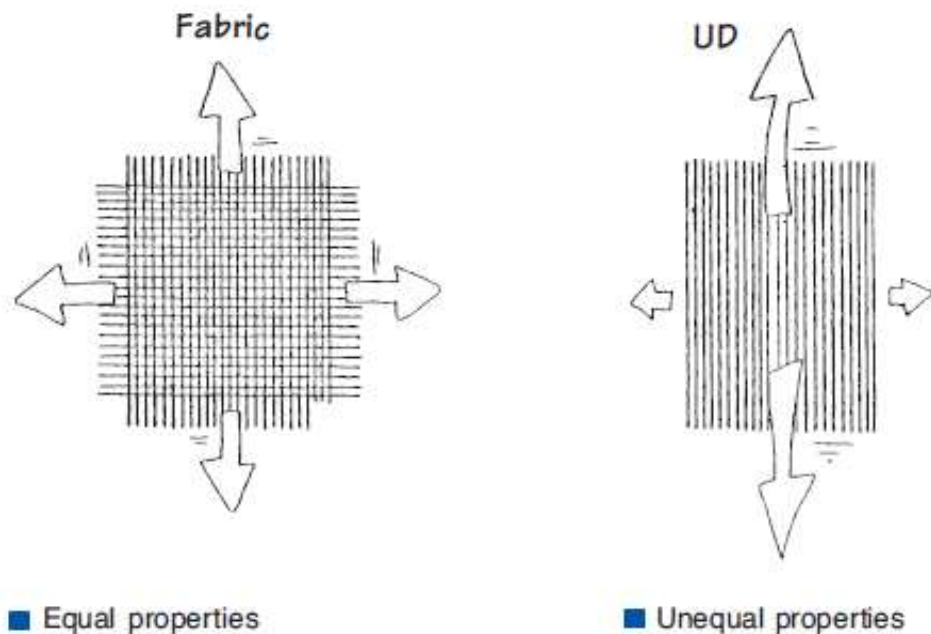


FIGURE 4-17. PROPERTIES OF FABRIC AND UNIDIRECTIONAL COMPOSITES [39]

The fibre directions can be arranged to meet specific mechanical performance requirements of the composite by varying the orientation [39]. Figure 4-18 shows two examples of fibres arrangement, using multiple unidirectional layers.

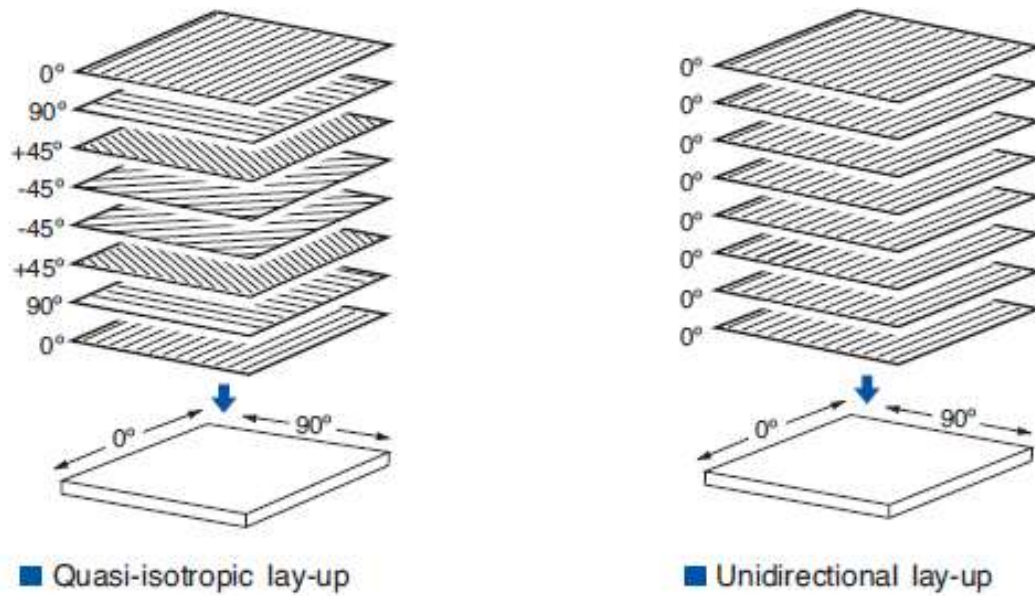


FIGURE 4-18. DIFFERENT WAYS TO ARRANGE THE FIBRE DIRECTIONS [39]

For the UNICAR*agil* doors, the team decided to use twill weave fabric because, thanks to its characteristics – average drapeability and average crimp – it is possible to both have good mechanical performance and realize the complex shape of the doors. Epoxy was chosen as resin.

Vacuum bag/oven and autoclave processing are the two main methods for the manufacture of components from prepreg. The processing method is determined by the quality, cost and type of component being manufactured (Table 4-3) [39]. [B5]

TABLE 4-3 COMPARISON AMONG DIFFERENT COMPOSITES PROCESSING METHODS [39]

| Processing method | Component | | Processing costs | |
|-----------------------|-------------------|-------------------|------------------|-------------------|
| | Quality | Section thickness | Equipment cost | Cure cycle energy |
| • Standard vacuum bag | Good - Excellent* | Thin to Thick | Moderate | Low |
| • Autoclave | Excellent | Thin to Thick | High | High |

*dependent on prepreg definition and application.

Vacuum bag processing is suited to monolithic components of varying thickness and large sandwich structures. The vacuum bag technique involves the placing and sealing of a flexible bag over a composite lay-up (Figure 4-19, left) and evacuating all the air from under the bag (Figure 4-19, right).



FIGURE 4-19. STEPS OF THE VACUUM BAG PROCESSING [39][B5]

The removal of air forces the bag down onto the lay-up with a consolidation pressure of up to 1 atmosphere (1 bar). The completed assembly, with vacuum still applied, is placed inside an oven or on a heated mold with good air circulation, and the composite is produced after a relatively short cure cycle. Some high performance prepreps can be cured using standard vacuum bag techniques and provide near autoclave quality components [39].

Autoclave processing is used for the manufacture of superior quality structural components containing high fiber volume and low void contents. The autoclave technique requires a similar vacuum bag but the oven is replaced by an autoclave (Figure 4-20). The autoclave is a pressure vessel which provides the curing conditions for the composite where the application of vacuum, pressure, heat up rate and cure temperature are controlled. High processing pressures allow the moulding of thicker sections of complex shapes. Honeycomb sandwich structures can also be made to a high standard, typically at lower pressures. Long cure cycles are required because the large autoclave mass takes a long time to heat up and cool down. Sometimes slow heat up rates are required to guarantee even temperature distribution on the tooling and composite components [39].

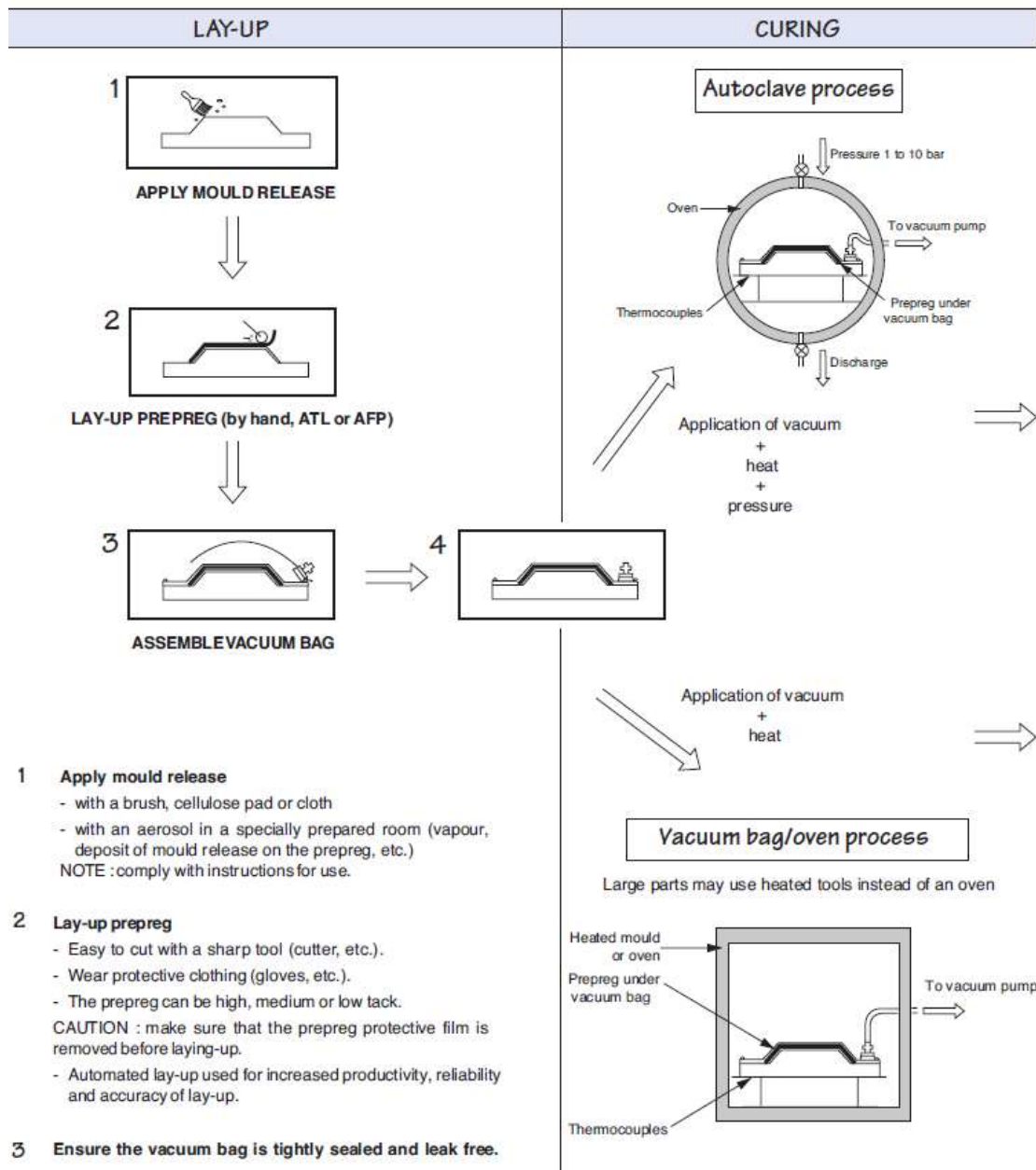


FIGURE 4-20. DIFFERENCE BETWEEN VACUUM BAG/OVEN AND AUTOCLAVE PROCESS [39]

UNICAR*agil* doors will be manufactured by means of an autoclave processing, in order to ensure high quality.

4.4 Delivery test

Every car manufacturer has their own list of delivery tests, in according to standard delivery test specifications.

Door delivery testing on standard vehicles, which is performed on simple assembled frames as well as on completely trimmed doors, can be summarized as follows:

- Sag test;
- Strength in side internal impact against people;
- Door bending;
- Strength in side impact against poles or other vehicles;
- Strength in side internal impact against people;
- Noise, water and powder seal effectiveness (with weather strips) [34]

The UNICAR*agil* project is a university project with the aim of producing four show cars, created specifically for public display rather than sale. For this reason, the strength in side impact against poles or other vehicles is not taken into account, as the vehicles will not be subjected to any side crash tests. For the same reason, the doors will not have any side impact protection beam, whose function is the absorption of the crash energy in the door area and the protection of the vehicle's occupants. In addition, the doors will not be subjected to any fatigue test, as the models will only be used during the IAA exhibition.

All the tests where the human interaction is considered, must be performed considering a 95th percentile male, whose anthropometric data are reported in Figure 4-21

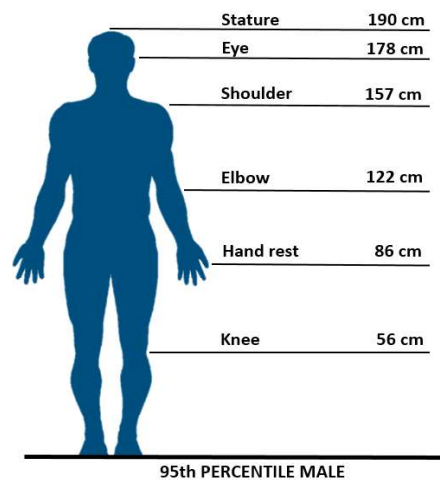


FIGURE 4-21 ANTHROPOMETRIC DATA OF 95TH PERCENTILE MALE [41]

Doors with their sealing solutions must provide protection in the event of rain. Therefore, the positioning of the seals was taken into account during the design.

4.5 Finite Element Analysis

4.5.1 Introduction to FEM

Mechanical components in the schematic form of beams can be analyzed rather easily with the traditional methods of calculation of mechanics, but the real components are rarely so simple, and for the designer it is necessary to use less invasive approximations, experimentation or numerical methods. There are many numerical methods used in engineering for which the use of a computer is very useful. Computer-aided Engineering (CAE) is often used in mechanical design, and one method of analysis that integrates very well with it is Finite Element Analysis (FEA). The mathematical theory behind this method is broad and has many applications, such as static and dynamic analysis, both linear and non-linear, of stresses and deformations, free and forced vibrations, elastic instability, heat transmission, fluid dynamics, acoustics, electrostatics and magnetism [42].

Restricting ourselves to the description in the structural field, a component is a structure continuous material with elastic properties. The EAG method divides (discreetly) the structure in small but finished elastic sub-structures (elements) as shown in Figure 4-22

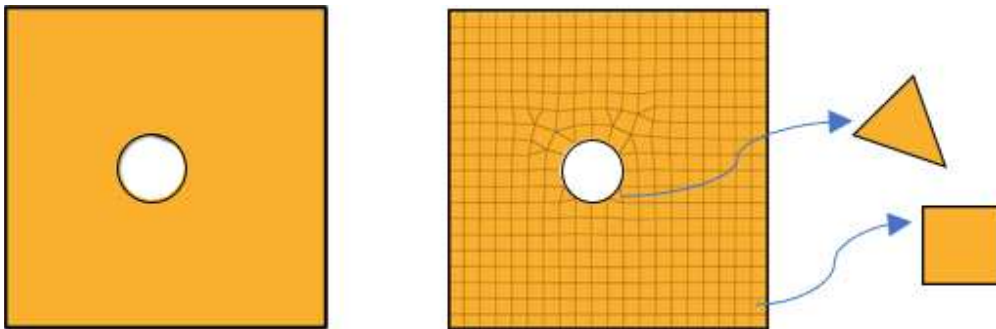


FIGURE 4-22 MESH DEFINITION

In a continuous problem of any dimension, i.e. in a body or region of space where a particular phenomenon, the field variable, such as pressure, displacement, temperature, speed or density, is function of each generic point in the definition domain. As a result, the problem has an infinite number of unknowns. The finite element discretization procedure reduces it to a problem with a finite number of unknowns, by dividing the domain into finite elements and expressing the unknown field in terms of approximate functions, defined as within each element [43].

The approximate functions, also called form functions, are identified through the values that the dependent variable assumes in specific points called nodes. The nodes are usually placed on the outline of the elements, in points common to two or more elements. In addition to the nodes on the outline, an element may have nodes inside it. The values that the field variable assumes on the nodes, univocally define the trend within the element. In the finite element representation of a problem, the nodal values of the field variable represent the new unknowns.

As mentioned above, the basic idea of approximation used in the finite element method is to approximate the true trend of the unknown function with that of some particular functions with a known trend: usually polynomial, but also trigonometric and exponential. A limited number of points are taken into account (also called nodes) internal to the integration domain, for which the values of the approximate function will be identical to the approximate function.

The working environment adopted is Altair HyperWorks™. The procedure is divided into three parts:

- Pre-processing
- Solution generation
- Post-processing

4.5.2 Pre-processing environment

The first part of the analysis consists in preparing the components with CatiaV5®. In order to be able to use shell elements, it is necessary to have surfaces, then proceed with the export, which is carried out in .iges files.

The Hyperwork software allows you to execute complex commands in a simple and intuitive way. The first operation performed with this program is to check the continuity of the various contact surfaces

Geometry

Even though the surfaces have been created and merged correctly once the file is imported into HyperMesh, it may result that the surfaces are not continuous.

The surfaces are checked in *geom> edge edit*. Figure 4-23 illustrates the surface joining lines, in areas where there are green-reddish lines and surfaces are not connected.

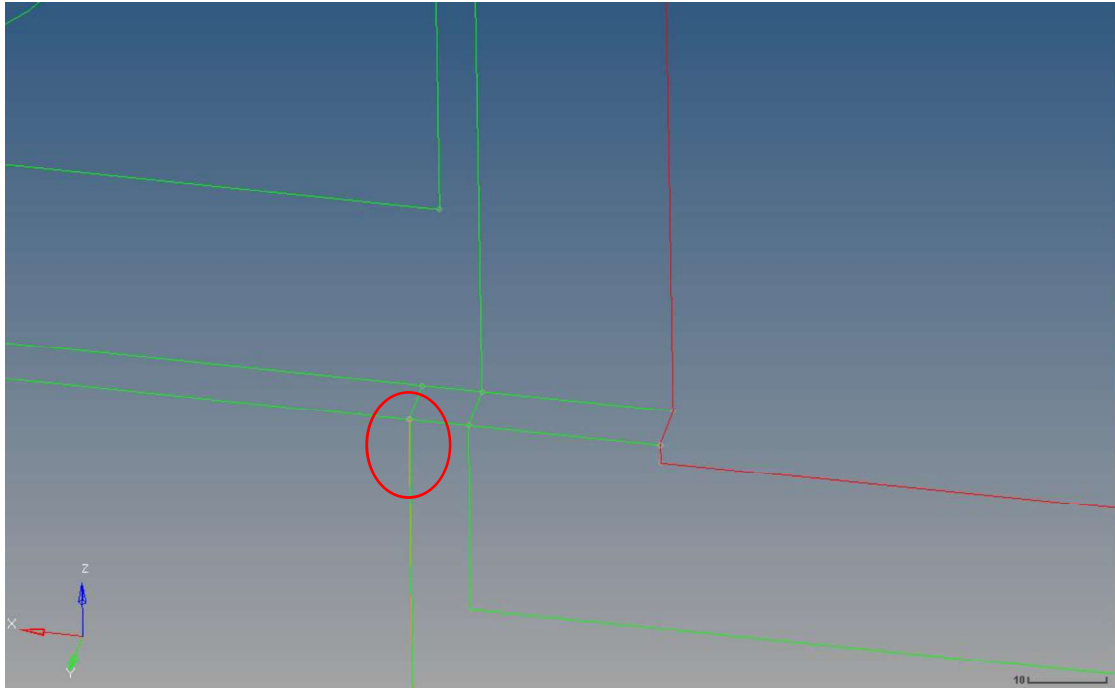


FIGURE 4-23 CONJUNCTION LINES OF SURFACES NOT MATCHED

By clicking with the mouse on these lines, it will be possible to modify them and bring them to a yellow color, which indicates the correct union between the surfaces Figure 4-24.

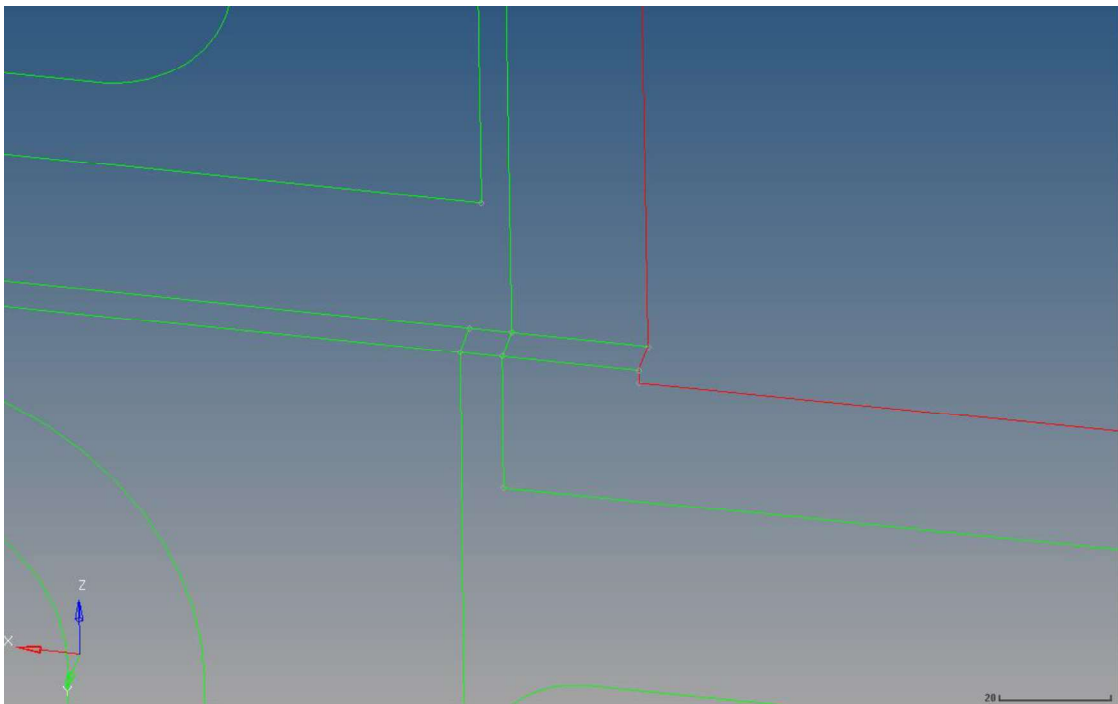


FIGURE 4-24 CONJUNCTION LINES OF SURFACES MATCHED

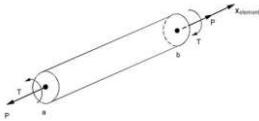
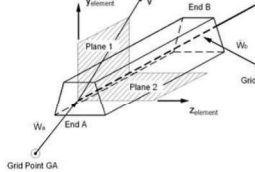
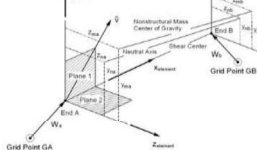
If by using this command the surfaces are not aligned, it must be executed the command reject, and in case, change the value of the clean-up tool from 0.2 to 0.5.

Mesh

There are several types of elements that can be used to create a finite element model. The choice between these depends on the characteristics of the problem that are being analysed and the geometries that are being studied.

- Elements 1D: this is the mono-dimensional elements characterized by two nodes. They are particularly suitable to represent components in which one dimension is predominant with respect to the other two [44].

TABLE 4-4 1D TYPE OF MESH

| Types | Rod/Truss | Bar | Beam |
|--------------|-----------------------------------------------------------------------------------------------------------------------------------------|---------------------------------------------------------------------------------------------------------------------------------------|---------------------------------------------------------------------------------------|
| Application | Two force members in which only tensile/compressive behaviours are possible | Members in which bending behaviour is possible | |
| | | Symmetric cross-section (Example: \square , $+$, I) | Asymmetric cross-section (Example: L) |
| N° of Nodes | <p style="text-align: center;">2</p> <p style="text-align: center;">(connecting nodes at both ends with a straight line)</p> | | |
| Shape |  |  |  |
| DOF per Node | <p style="text-align: center;">4</p> <ul style="list-style-type: none"> - 3 translation - 1 rotation () | <p style="text-align: center;">6</p> <ul style="list-style-type: none"> - 3 translation - 3 rotation (| |

- 2-D elements are used when two of the dimensions are very large in comparison to the third dimension [44].

TABLE 4-5 2D TYPE OF MESH

| Types | Shell | Plate | Membrane |
|--------------|------------------------------------------------------------------|-------|----------|
| Applications | Sheet metal parts, plastic components like instrument panel etc. | | |

| | | | |
|--------------|------------------------------------------------------------------------------------------------------------------------------------------------------------------------------------------------------------------------------------------|-----------------------------------------------------------------------------------------------------------------------------------------|-----------------------------------------------------------------------------------------------------------------------------------------|
| N° of Nodes | <p style="text-align: center;">2-D element shapes</p> <div style="text-align: center;"> </div> <p style="text-align: center;">* L – Linear element * P – Parabolic element * () – Indicates number of nodes/element</p> | | |
| Shape | | | |
| DOF per Node | <p style="text-align: center;">6</p> <ul style="list-style-type: none"> - 3 translation - 3 rotation () | <p style="text-align: center;">3</p> <ul style="list-style-type: none"> - 1 translation - 2 rotation () | <p style="text-align: center;">3</p> <ul style="list-style-type: none"> - 2 translation - 1 rotation () |

- **3D Elements:** these are solid elements, which are much more computationally demanding, and therefore should only be used when the other types of elements are not sufficient to approximate the system under study in an acceptable way [44].

TABLE 4-6 3D TYPE OF MESH

| Types | Tetrahedron | Pentahedron | Hexahedron |
|--------------|------------------------------------------------------------------------------------------------------------------------------------------|--------------------------------------------------------------------------------------------------------------------|--------------------------------------------------------------------------------------------------------------------|
| Applications | Gear box, engine block, crankshaft, etc | | |
| N° of Nodes | <ul style="list-style-type: none"> - 4 (lower-order elements) - 10 (higher-order elements) | <ul style="list-style-type: none"> - 6 (lower-order elements) - 15 (higher-order elements) | <ul style="list-style-type: none"> - 8 (lower-order elements) - 20 (higher-order elements) |
| Shape | | | |
| DOF per Node | <p style="text-align: center;">3</p> <ul style="list-style-type: none"> - 3 translation - No rotation DOF | | |

- Rigid Body Elements: these are elements that have the task of connecting a node (called reference nodes) with other nodes (called dependent nodes) so that the relative displacement between them and the reference node is zero, as if the RBE had infinite rigidity. These elements must be used with caution, because if positioned incorrectly they can lead to unreliable results [44].

As mentioned in the above, the analysis is performed through surfaces, so shell elements are used during mesh creation.

To mesh the surfaces, proceed with *2D> automesh>size and bias>mesh*; to better approximate the shape of the components the mesh type is set to “mixed”.

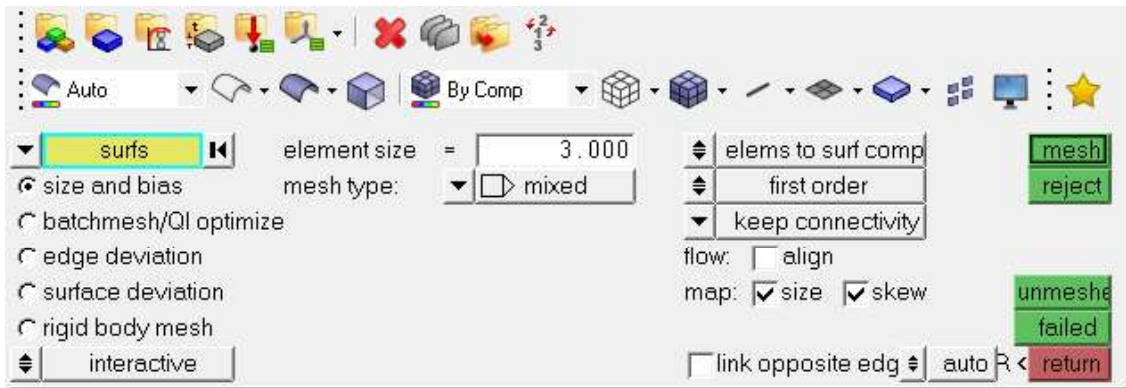


FIGURE 4-25 MESH CREATION PANEL

First order elements are used and an element size of 3 mm is set. Size and number of nodes affect the results of the analysis.

Mesh density depend on:

- type of analysis. Linear static analysis could be easily carried out quickly with many nodes and elements, but optimization, crash, nonlinear, CFD, or dynamic analysis takes a lot of time. Keeping control on the number of nodes and elements is necessary.
- Hardware configuration and graphics card capacity of the available computer. An experienced CAE Engineer knows the limit of the nodes that can be satisfactorily handled with the given hardware configuration.
- Timing. Available time is a major determinant in a decision concerning mesh density. A compromise is usually reached between the amounts of time dedicated to human time and that devoted to computer time [44].

Considering the number of components that are under examination, the type of analysis to be executed, linear static analysis and free size optimization, 3 mm, first

order elements is identified as a good compromise. For critical area where higher stress can occur, could be remeshed with a smaller element length in the second run.

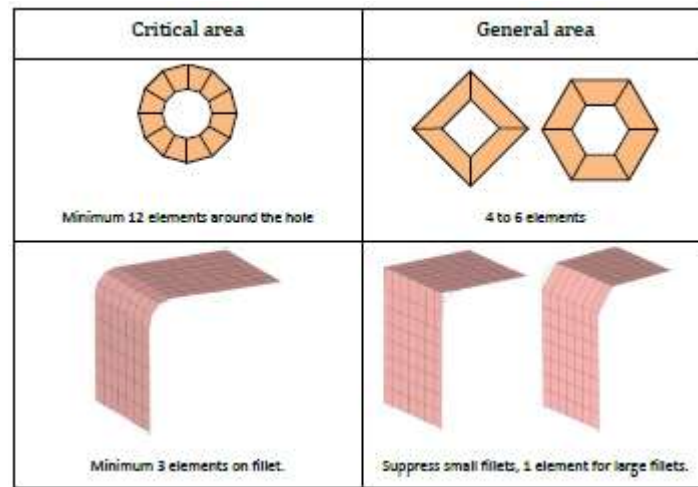


FIGURE 4-26 CRITICAL AREA MESHING [44]

The quality of the mesh is then checked. With the *2D> quality index* command, you display elements with incorrect or failed shapes, which are marked with yellow or red. Going to the *cleanup tool> node optimize* or *element optimize* part, with simple clicks on the element, it will be possible to modify it and bring it to a correct shape. Figure 4-27 shows correct (blue) and incorrect (yellow) elements.

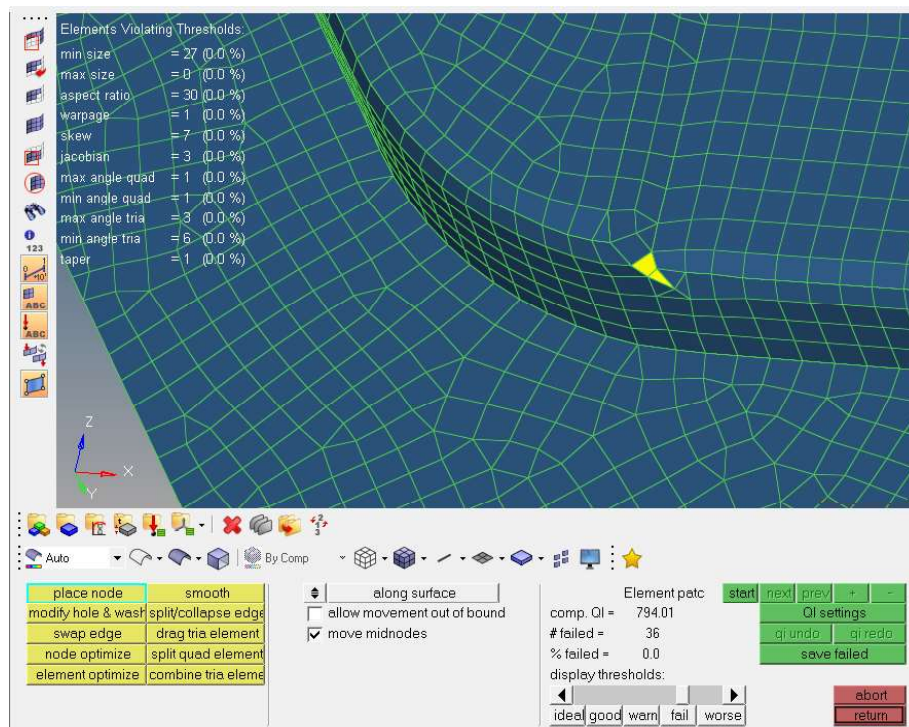


FIGURE 4-27 DAMAGED ELEMENTS CONTROL

It may happen, that after meshing a component's element normals point to different directions. This check should be executed before every finite element analysis, but with composites it is essentially required. Hence it is influenced, whether the laminate is applied symmetrically or one-sided outwards or inwards from element level. This is done with *2D>composites>element normal*. Last operation consists of checking the orientation of the material. (Figure 4-28)

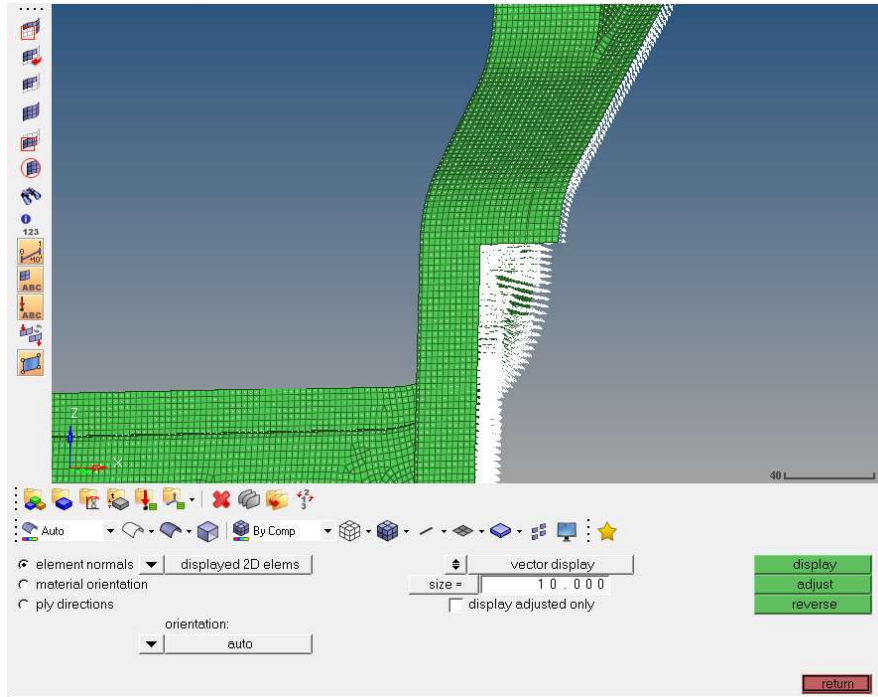


FIGURE 4-28 ELEMENTS NORMALS CHECK

The last operation consists of checking the material orientation. When setting up composite analyses the material orientation on the elements has to be checked and where necessary to be adapted, to be able to effectively compute the desired orientation of anisotropic materials. So in the present model the material orientation along the side-, upper- and under-surface of the components is aligned with the global x-axis, along the front- and rear-surface it was aligned with the global z-axis. Going to *2D>composites>material orientation*, it is possible to set it (Figure 4-29).

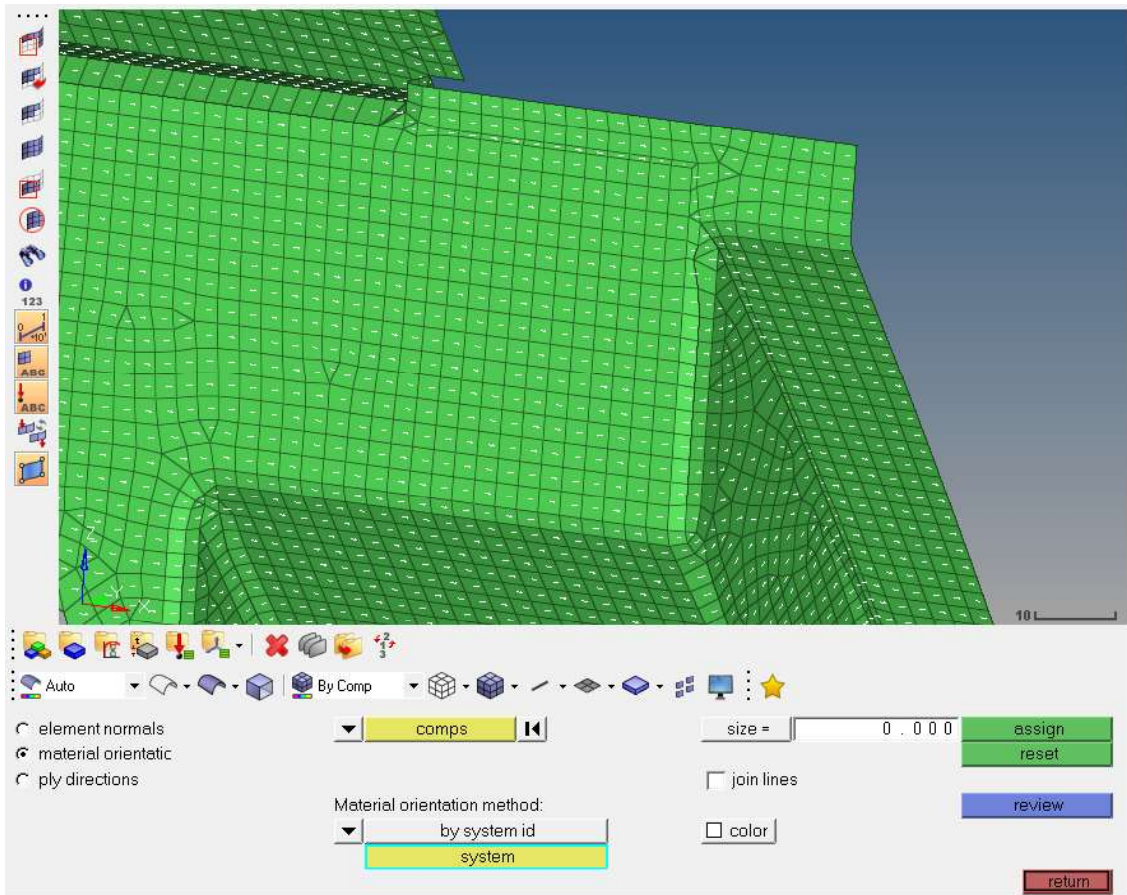


FIGURE 4-29 MATERIAL ORIENTATION

Laminate

In order to finely control the composite variables such as thickness orientation and direction of the plies the composite property PCOMPP (ply based) is adopted. Furthermore, in the optimization process, after the first step of the composite-cycle automatically the COMPP- property is used, regardless how the laminate was defined before.

First step for creating a laminate with PCOMPP-property is the creation of the material. UNICARagil team relies on an external company (Roding) to manufacture the CFRP components. For this reason, the type of pre-preg is not part of this study but pre-preg provided by the company is to be used. From the data provided by Roding, the material card in HyperMesh is fill in as shown in Figure 4-30.

| | MID | E1 | E2 | [NU12] | [G12] | [G1Z] | [G2Z] | [RHO] |
|-------|------|---------|---------|---------|---------|---------|---------|---------|
| MAT 8 | 2 | 6.0e+04 | 5.8e+04 | 0.330 | 2.0e+04 | | | 1.5e-06 |
| | [A1] | [A2] | [TREF] | [Xt] | [Xc] | [Yt] | [Yc] | [S] |
| | | | | 610.000 | 587.000 | 610.000 | 587.000 | |
| | [GE] | [F12] | [STRN] | | | | | |

User Comments

☐ MATT8
☐ MAT4
☐ MAT5
☐ MATF8
☐ MATX...

| | MID | E1 | E2 | [NU12] | [G12] | [G1Z] | [G2Z] | [RHO] |
|-------|------|---------|---------|---------|---------|---------|---------|---------|
| MAT 8 | 4 | 3.2e+04 | 3.1e+04 | 0.330 | 1.4e+04 | | | 1.5e-06 |
| | [A1] | [A2] | [TREF] | [Xt] | [Xc] | [Yt] | [Yc] | [S] |
| | | | | 678.000 | 621.000 | 678.000 | 621.000 | |
| | [GE] | [F12] | [STRN] | | | | | |

User Comments

☐ MATT8
☐ MAT4
☐ MAT5
☐ MATF8
☐ MATX...

FIGURE 4-30 TS245 (UP) - TS380 (DOWN)

In Figure 4-31 and Figure 4-32 are reported the datasheets of the pre-preg used.

GG245TSE(T300)-DT121H-38 (H 120 cm)

Caratteristiche del sistema resinoso/ *Features of the resin matrix: (*)*

| | |
|---------------------------------------------------------------------------------------------------------|-------------------------------------------------------------------------------------------------------------------|
| Natura del formulato/ <i>Chemical nature</i> | Epossidico termoidurente/ <i>Thermosetting epoxy</i> |
| Temperatura di cura/ <i>Cure temperature</i> | 80 ÷ 135°C |
| Gel time | 8 ÷ 13 min @ 120°C 3 ÷ 6 min @ 135°C |
| Tg [Ciclo di cura]/ <i>Tg [Cure cycle]</i> | Ref. to DT121H technical data sheet (1) |
| Viscosità/ <i>Viscosity</i> | Medio-bassa / <i>Low to medium</i> (2) |
| Trasparenza/ <i>Transparency</i> | Buona/ <i>Good</i> |
| Stabilità all'ingiallimento/ <i>UV stability</i> | Buona/ <i>Good</i> |
| Indicato per applicazioni dove siano richiesti: <i>Recommended for those applications requiring:</i> | -Buona finitura superficiale/ <i>Good laminate surface finish</i> -Buona trasparenza/ <i>Good transparency</i> |

(1) Minuta con DSC alla velocità di scansione di 20°C/min / *Measured by DSC @ 20°C/min*

(2) Viscosità complessiva misurata a 60°C compresa fra 300 e 500 Poise (frequenza 10 rad/sec) / *Complex viscosity measured @ 60°C between 300 and 500 Poise (frequency 10 rad/sec)*

Caratteristiche del tessuto impregnato/ *Features of the impregnated fabric:*

| | |
|---------------------------------------------------------------|--------------------------------------------------------------------------------------|
| Tipo di filato (Ordito; Trama)/ <i>Yarn type (Warp; Weft)</i> | Toray T300 3K |
| Stile di tessitura/ <i>Weaving style</i> | Twill 2x2 |
| Larghezza standard/ <i>Standard width</i> | 1200 ± 5 mm (esclusa cimosa/ <i>without selvage</i>) |
| Lunghezza standard/ <i>Standard length</i> | 50 ± 5 m |
| Ordito (fili/ cm)/ <i>Warp (ends/ cm)</i> | 6,00 ± 0,30 |
| Trama (fili/ cm)/ <i>Weft (picks/ cm)</i> | 6,00 ± 0,30 |
| Peso areale fibra secca/ <i>FAW</i> | 245 ± 10 g/m² |
| Contenuto di resina/ <i>Resin content</i> | 38 ± 3 % in peso/ <i>by weight</i> |
| Contenuto di volatili/ <i>Volatile content</i> | <1,0 % in peso/ <i>by weight</i> (3) |
| Spessore lamina/ <i>Laminate thickness</i> | 0,260 mm (4) |
| Conservazione/ <i>Shelf life</i> | 30 giorni @ 21°C/ <i>30 days @ 21°C</i> 12 mesi @ -18°C/ <i>12 months @ -18°C</i> |

FIGURE 4-31 GG245TSE PRE-PREG

GG380T(T700)-FR147F-42 (H 100 cm)Caratteristiche del sistema resinoso/ Features of the resin matrix: (*)**DELTA**preg

| | |
|-------------------------------------------------------------------------------------------------------|----------------------------------------------------------------------------------------------------|
| Natura del formulato/ <i>Chemical nature</i> | Epossidico termindurente flame retarded/ <i>Flame retarded thermosetting epoxy</i> |
| Temperatura di cura/ <i>Cure temperature</i> | 110 + 150 °C |
| Gel time | 8 + 14 min @ 120 °C 2 + 4 min @ 135 °C |
| Tg [Ciclo di cura]/ <i>Tg [Cure cycle]</i> | 140 + 145 °C [90 min @ 120 °C] 150 + 155 °C [40 min @ 135 °C] (1) |
| Viscosità/ <i>Viscosity</i> | Media/ <i>Medium</i> (2) |
| Trasparenza/ <i>Transparency</i> | Eccellente/ <i>Excellent</i> |
| Stabilità all'ingiallimento/ <i>UV stability</i> | Buona/ <i>Good</i> |
| Indicato per applicazioni dove siano richiesti:/ <i>Recommended for those applications requiring:</i> | Trasparenza e resistenza alla fiamma (UL94V-0)/ <i>Transparency and flame retardancy (UL94V-0)</i> |

(1) Misurata con DSC alla velocità di scansione di 20°C/min / *Measured by DSC @ 20°C/min*- (2) Viscosità complessa tra 300 e 500 Poise @ 60°C (10 rad/s)/ *Complex viscosity between 300 and 500 Poise @ 60°C (10 rad/s)*Caratteristiche del tessuto impregnato/ Features of the impregnated fabric:

| | |
|---------------------------------------------------------------|----------------------------------------------------------------------------------------|
| Tipo di filato (Ordito; Trama)/ <i>Yarn type (Warp; Weft)</i> | Toray T700 12K |
| Stile di tessitura/ <i>Weaving style</i> | Twill 2x2 |
| Larghezza standard/ <i>Standard width</i> | 1000 ± 5 mm (esclusa cimosa/ <i>without selvage</i>) |
| Lunghezza standard/ <i>Standard length</i> | 50 ± 5 m |
| Ordito (fili/ cm)/ <i>Warp (ends/ cm)</i> | 2,40 ± 0,20 |
| Trama (fili/ cm)/ <i>Weft (picks/ cm)</i> | 2,40 ± 0,20 |
| Peso areale fibra secca/ <i>F.A.W.</i> | 380 ± 15 g/m ² |
| Contenuto di resina/ <i>Resin content</i> | 42 ± 3 % in peso/ <i>by weight</i> |
| Contenuto di volatili/ <i>Volatile content</i> | < 2,0 % in peso/ <i>by weight</i> (3) |
| Spessore lamina/ <i>Laminate thickness</i> | 0,440 mm (4) |
| Conservazione/ <i>Shelf life</i> | 4 settimane @ 20°C/ <i>4 weeks @ 20°C</i> 12 mesi @ -18°C/ <i>12 months @ -18°C</i> |

FIGURE 4-32 TDS-GG380T PRE-PREG

For these materials, Roding has executed the standardized test to get their mechanical property of the woven laminates.

TABLE 4-7 WOVEN LAMINATE PROPERTIES

| PROPERTY | SYMBOL | UNIT | GG245TSE(T300)/ DT121H | GG380T(T700)/ FR147F | TEST STANDARD |
|------------------------|--------|------|---------------------------|-------------------------|---------------------------|
| Resin Content | | % | 38 | 42 | ASTM D3171 METHOD 8 |
| Cured Ply Thickness | | mm | 0.68 | 1.32 | ASTM D792 |

| | | | | | |
|--------------------------|-------|-----|-----|-----|----------------|
| 0° Tensile Strength | x_t | MPa | 610 | 678 | ISO 527-4 |
| 0° Tensile Modulus | E_1 | GPa | 60 | 32 | ISO527-4 |
| 90° Tensile Strength | y_t | MPa | 610 | 678 | ISO527-4 |
| 90° Tensile Modulus | E_2 | GPa | 58 | 31 | ISO527-4 |
| 0° Compressive Strength | x_c | MPa | 587 | 621 | SACMA SRM 1 54 |
| 90° Compressive Strength | y_c | MPa | 587 | 621 | SACMA SRM 1 54 |

It is possible to notice that in the two main orthogonal directions, 0° and 90°, the mechanical characteristics of GG245TSE and GG380T's plies are similar. This behaviour is to be attributed to the type of weaving used

After defined the material cards, plies are created. In this initial phase of the structural analysis, the stack it is going to be test is the one proposed by Roding.

With the creation of a ply-set, automatically, a corresponding element-set is generated

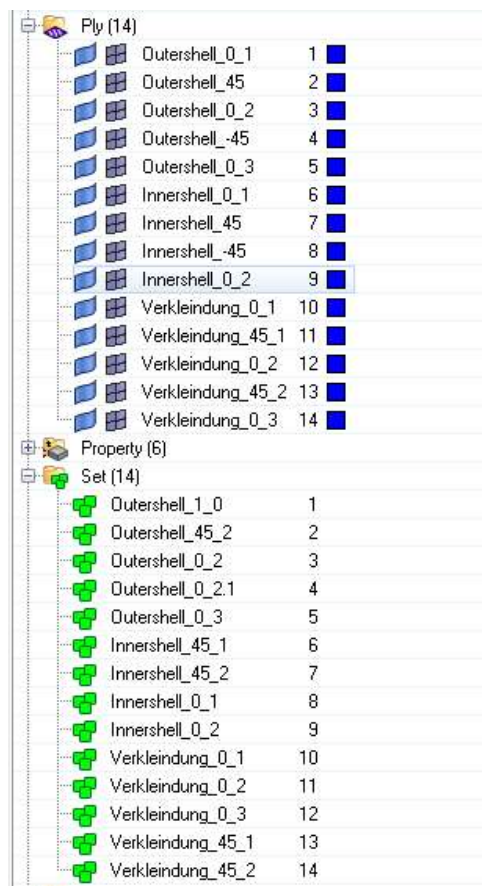


FIGURE 4-33 PLY-SETS; ELEMENT-SETS

Then, these laminates shall be generated as consecutively described.

Edit Laminate

Type: Ply laminate
 Name: Outershell
☐ Same as: Outershell
 Card image: STACK
☒ Update color: ■
 Laminate option: Total

Define laminate:

| Name | Id | Color | Material | Thickness | Orientation | IP | Result |
|-----------------|----|-------------------------------------|----------|-----------|-------------|----|--------|
| Rear_Outer_0_1 | 19 | ■ | GG245TSE | 0.26000 | 0.0 | 3 | yes |
| Rear_Outer_45_1 | 22 | ■ | GG380T | 0.44000 | 45.0 | 3 | yes |
| Rear_Outer_0_2 | 20 | ■ | GG380T | 0.44000 | 0.0 | 3 | yes |
| Rear_Outer_45_2 | 23 | ■ | GG380T | 0.44000 | 45.0 | 3 | yes |
| Rear_Outer_0_3 | 21 | ■ | GG245TSE | 0.26000 | 0.0 | 3 | yes |

FIGURE 4-34 LAMINATE OUTER SHELL

Edit Laminate

Type: Ply laminate
 Name: Innershell
☐ Same as: Innershell
 Card image: STACK
☒ Update color: ■
 Laminate option: Total

Define laminate:

| Name | Id | Color | Material | Thickness | Orientation | IP | Result |
|-----------------|----|-------------------------------------|----------|-----------|-------------|----|--------|
| Rear_Inner_0_1 | 24 | ■ | GG245TSE | 0.26000 | 0.0 | 3 | yes |
| Rear_Inner_45_1 | 27 | ■ | GG380T | 0.44000 | 45.0 | 3 | yes |
| Rear_Inner_45_2 | 28 | ■ | GG380T | 0.44000 | 45.0 | 3 | yes |
| Rear_Inner_0_2 | 26 | ■ | GG245TSE | 0.26000 | 0.0 | 3 | yes |

FIGURE 4-35 LAMINATE INNER SHELL

Edit Laminate

Type: Ply laminate
 Name: Verkleidung
☐ Same as: Verkleidung
 Card image: STACK
☒ Update color: ■
 Laminate option: Symmetric

Define laminate:

| Name | Id | Color | Material | Thickness | Orientation | IP | Result |
|----------------------|----|-------------------------------------|----------|-----------|-------------|----|--------|
| Rear_Verkleidung_0_1 | 29 | ■ | GG245TSE | 0.26000 | 0.0 | 3 | yes |
| Rear_Verkleidung_45 | 32 | ■ | GG380T | 0.44000 | 45.0 | 3 | yes |
| Rear_Verkleidung_45 | 33 | ■ | GG380T | 0.44000 | 45.0 | 3 | yes |

FIGURE 4-36 LAMINATE KINEMATIC INTERIOR COVER

These laminates are set up for all the components that are going to be analysed, either for AUTOshuttle or AUTOtaxis doors.

Contact

The phenomenon of contact occurs very frequently in mechanical design. In an assembly consisting of several parts, these interact with each other by exchanging forces on the interface surfaces.

Contact is an integral aspect of the analysis and optimization techniques that is utilized to understand, model, predict, and optimize the behavior of physical structures and processes. In OptiStruct, a variety of Contact capabilities are available to help model different scenarios.

The two main discretization options in OptiStruct that can be used to define Contact are Node-to-Surface (N2S) and Surface-to-Surface (S2S). Based on the interaction that is simulated between the master and slave, various types of contact are available.

Additionally, the gap stiffness values can change depending on the proximity of the master and slave surfaces, the type of analysis being performed, and the initial state of the contact interface [45].

The CONTACT and TIE Bulk Data Entries in conjunction with the PCONT Bulk Data Entry (if required) can be used to typically set up the majority of contact solutions in OptiStruct

Contact between the master and slave surfaces can be constructed through two main approaches. This process is called *discretization*, and it defines the basic structure of the contact elements that are constructed to handle the contact condition. They are as follows:

- *Node-to-Surface Discretization*

The Node-to-Surface Discretization approach involves the creation of contact elements linking the Master Surfaces to Slave Nodes. The contact interface is constructed by searching, for each slave node, a respective facet of the master surface, which contains the normal projection of the slave and is within the Search Distance (SRCHDIS field on the CONTACT entry), distance from the slave node [45].

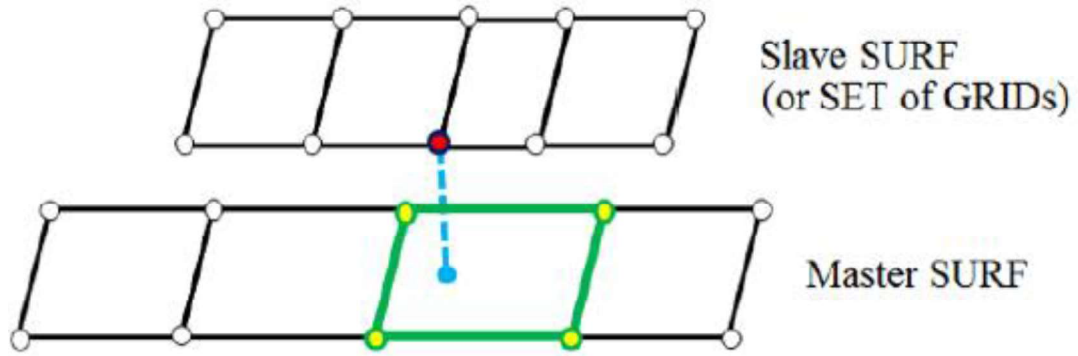


FIGURE 4-37 NODE-TO-SURFACE DISCRETIZATION [B2]

- *Surface-to-Surface Discretization*

The Surface-to-Surface Discretization approach involves the creation of contact elements linking the Master Surfaces to Slave Surfaces. The contact interface is constructed by searching, for each facet of the slave surface, respective facets of the master surface, which contains the normal projection of sample points on the slave facets and is within the Search Distance (SRCHDIS) distance from the sample points. For a slave node, a contact element is created with the surrounding slave facets and the master facets found by projection of the sample points on the slave facets [45].

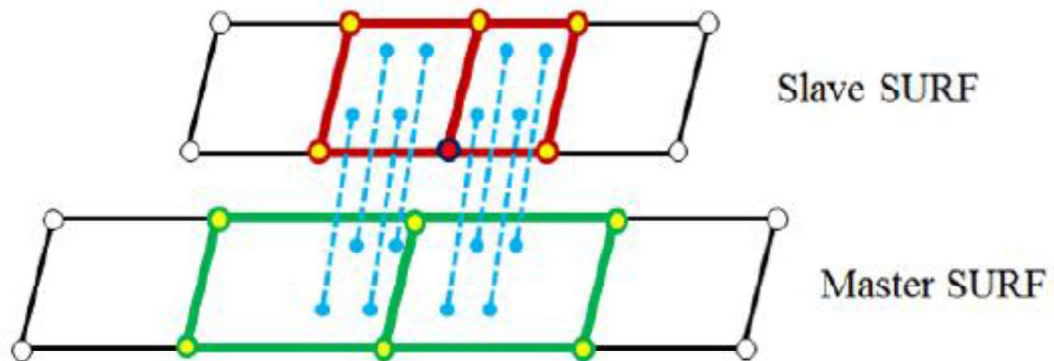


FIGURE 4-38 SURFACE-TO-SURFACE DISCRETIZATION [B2]

S2S is typically consumes higher computational time and memory resources compared to N2S. However, it typically can generate smoother contact, and give a better representation of the model. For this reasons, S2S contacts are used in this simulation.

The next step is the selection of the Contact Interface Type. This depends on the behavior being simulated at the contact interface

The three major type of contact interface available are:

- *Freeze Contact*

Freeze Contact enforces zero relative motion on the contact surface, the contact gap opening remains fixed at the original value and the sliding distance is forced to be zero. Additionally, rotations at the slave node are matched to the rotations of the master patch. The FREEZE condition applies to all respective contact elements, regardless of whether they are open or closed. Freeze Contact can be activated using TYPE=FREEZE on the CONTACT entry, or by using the Penalty-based Tied Contact. Penalty-based tied contact is activated by using the TIE entry for the contact interface (with CONTPRM,TIE,PENALTY, the default).

- *Sliding Contact*

Sliding Contact has only normal contact stiffness at the contact interface and no frictional effects. It is only valid for small sliding without friction and applies to both open and closed contacts. If convergence difficulties arise, adding a small value of friction may help, or the STICK condition can be used. Sliding Contact can be activated using TYPE=SLIDE on the CONTACT entry.

- *Stick Contact*

Stick contact is an enforced stick condition, wherein such contact interfaces will not enter the sliding phase. It only applies to contacts that are closed. Note that, in order to effectively enforce the stick condition, frictional offset may require to be turned off. Stick contact is activated using TYPE=STICK on the CONTACT. [45].

The model requires different types of contacts in different areas. The structure of the doors, as seen above, consists of two shells produced separately and then glued with a gluing thickness of about 20 mm. The manufacturing company uses an epoxy matrix compatible with the one used for pre-preg gluing, with consequent annealing in autoclave. This procedure, also used for the repair of carbon components, gives excellent results in terms of stiffness and uniformity of stress distribution along the two shells.

In view of this bonding method, TIE was adopted as type of contact interface between the two shells.


| | |
|---------------------------------------------------|-----------------------------------------------------------------------------------|
| Solver Keyword | TIE |
| Name | Schale_contact |
| ID | 2 |
| Color |  |
| Include File | [Master Model] |
| Card Image | TIE |
| User Comments | Hide In Menu/Export |
| SSID | slave_schale (30) |
| MSID | master_schale (31) |
| SRCHDIS | 5.0 |
| <input checked="" type="checkbox"/> Adjust Option | String Value |
| ADJUST | AUTO |
| DISCRET | S2S |

FIGURE 4-39 CONTACT CARD DEFINITION

Figure 4-40 shows the bonding area between the two shells.

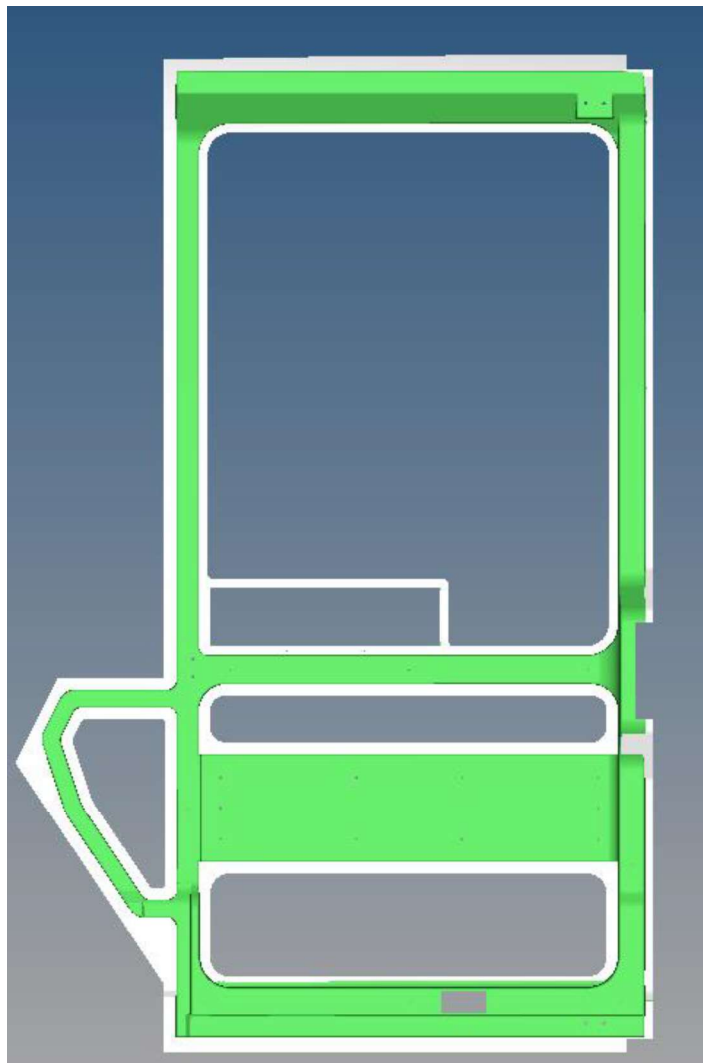


FIGURE 4-40 SURFACE WHERE TIE CONTACT IS DEFINED (WHITE)

To identify the interface between striker and innershell, a circular contact area with a radius of 25 mm is defined. This area is given by the pressure created by tightening the bolt.(Figure 4-41)

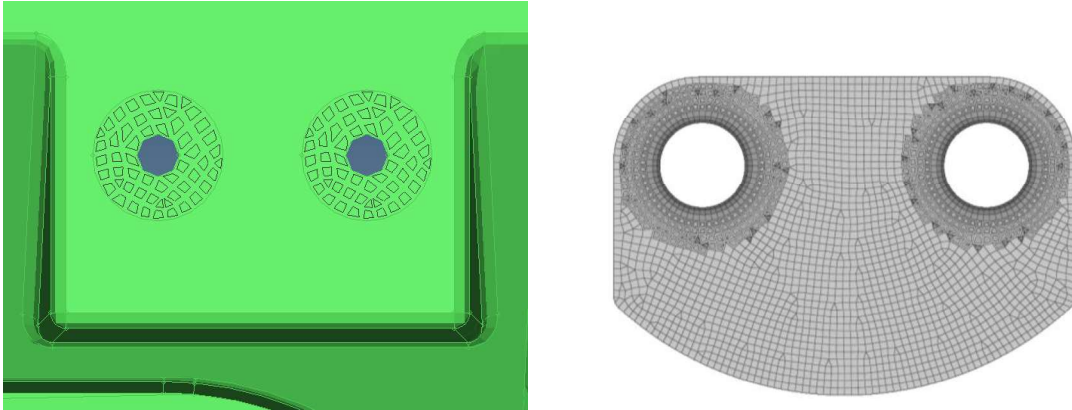


FIGURE 4-41 DETAIL OF THE CONTACT SURFACE DEFINITION OF A STRIKER

For the definition of the contacts for the strikers and the internal panels covering the door kinematics it was decided to use STICK as a type of contact interface. Both are connected to the door by screws.

4.6 Static Analysis

4.6.1 Sag test

The connection area between the hinges and the door plays an important role in the design of the door itself. During the opening and closing phases, it represents the only anchorage point between the car structure and the door itself. If not carefully examined, it can be damaged, causing the door to sag. Door sag causes misalignment and can prevent the door from shutting correctly and lead to safety issues. A load is applied to the door model on the side opposite the door hinges to imitate the weight of a person pushing the door down. Based on the stress results of the analysis, the deformation state of the components can be evaluated. The goal is to optimize the components for weight and stress in order to avoid excessive reinforcement while providing a safe design.

On the doors, UNICARagil decides to apply, to perform FEM simulations, a load of 950 N in the direction perpendicular to the latch case. This force corresponds to a person of 95 kg , that is the mass of a man belonging to the 95th percentile, hanging to the door while getting out of the vehicle, with an acceleration of $1g$ (Figure 4-42). The test must be performed following the worst-case scenario. Considering that the

hinges can slide along the door, the worst-case is identified with the doors opened for just the space needed to the person to exit.

This kind of test do not include maximum deformation because is carried out in open door configuration. The maximum composite stress allowed is 300MPa . This value come from the yielding point stress of the carbon fiber considering a safety factor of 2.

All the tests must be performed without the side window glass. In this way, more severe conditions are imposed, since the transparent panel increases the stiffness.

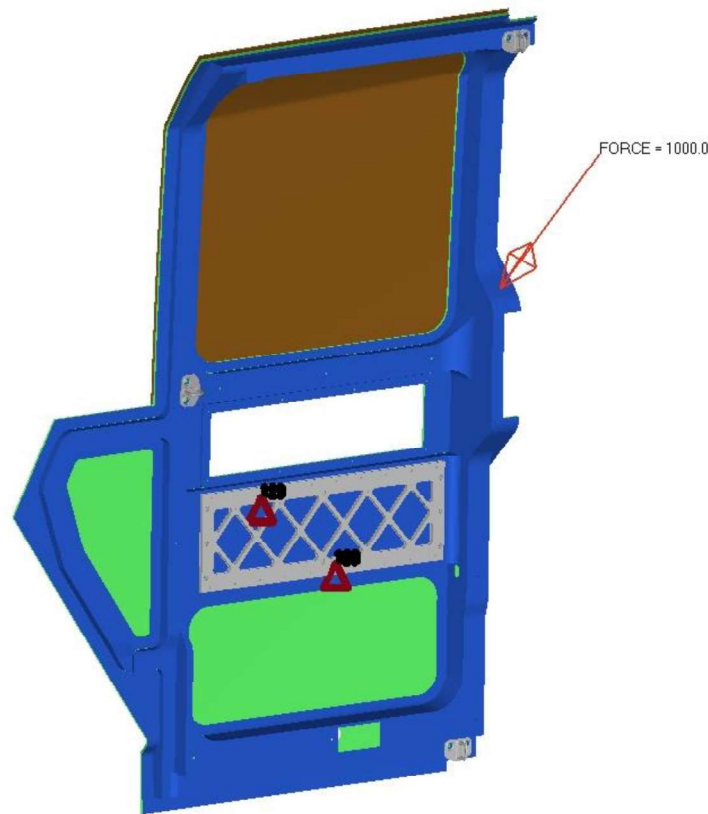


FIGURE 4-42 AUTOTAXI SAG TEST LOADSTEP

4.6.2 Strength in side internal impact against people

In situations such as driving tests or during vehicles driving exhibition shape cornering may arise. This test is going to analyse the behaviour of the door in case people onboard hit against the doors. The UNICARagil team decides to apply, to perform FEM simulations, a pressure of 0.15MPa and 0.095MPa which correspond to a load of 2500N or 1650N applied in an area of $350\text{mm} \times 50\text{mm}$ in the y direction for AUTOSHuttle and AUTOTaxi respectively. Also for this test is performed the worst case scenario. This force corresponds to 3 or 2 people of 95 kg, that is the mass of a

man belonging to the 95th percentile, falling against the door with an acceleration of $0.9g$. The consideration behind the adaptation of this acceleration come from an analysis of the lateral dynamics shown in Figure 4-43.

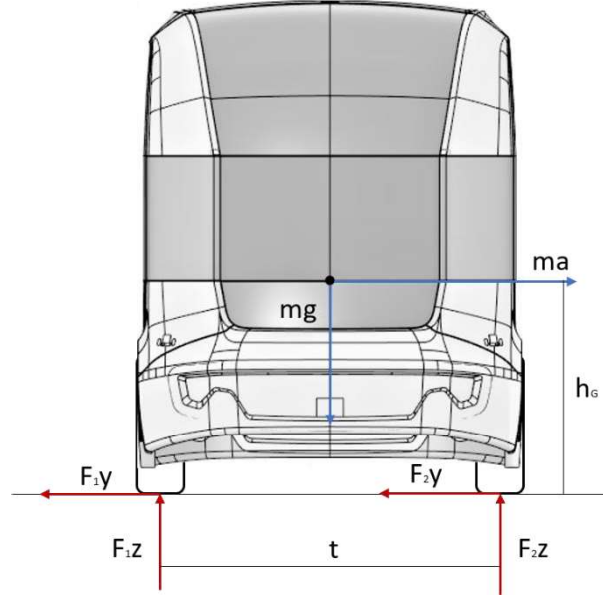


FIGURE 4-43 FREE BODY DIAGRAM OF THE VEHICLE

TABLE 4-8 VEHICLE DATA

| Vehicle | Mass [kg] | h_G [m] | t [m] |
|-------------|--------------|--------------|------------|
| AUTOtaxi | 2700 | 0.65 | 1.7 |
| AUTOshuttle | 2500 | 0.70 | 1.7 |

At this stage we are not aware of the type of tyres that the vehicles will mount, so we consider a reasonable value of $\mu_y = 0.9$

For maximum lateral grip:

$$F_{y1} + F_{y2} = ma$$

$$mg\mu_y = ma$$

$$a = \mu_y g$$

For roll over condition $F_{z1} = 0$, equilibrium equation around 2:

$$mgt/2 = mah_G$$

$$a = gt/(2h_G)$$

The acceleration that must be considered is the lower of the two because it is the lower for which one of the two situations occurs (lose of grip or roll over).

Through these equations the force to be applied on the door are the following:

TABLE 4-9 DATA FOR FORCE EVALUATION IN SIDE IMPACT TEST

| Vehicle | Mass of 95 th percentile [kg] | Number of people [-] | Acceleration [m/s ²] | Force [N] |
|-------------|------------------------------------------------|----------------------------|-------------------------------------|--------------|
| AUTOtaxi | 95 | 2 | 8.5 | 1650 |
| AUTOshuttle | 95 | 3 | 8.5 | 2500 |

The test must be performed with the doors closed and the load must be applied in correspondence with an area placed at arm height. The force is applied on the door structures at the door – to – door interface, as shown in Figure 4-44. The goal is to avoid plastic deformation or fracture in the doors structure under the load above-mentioned. The maximum deformation allowed is **10mm**, while the maximum composite stress is **300MPa**.

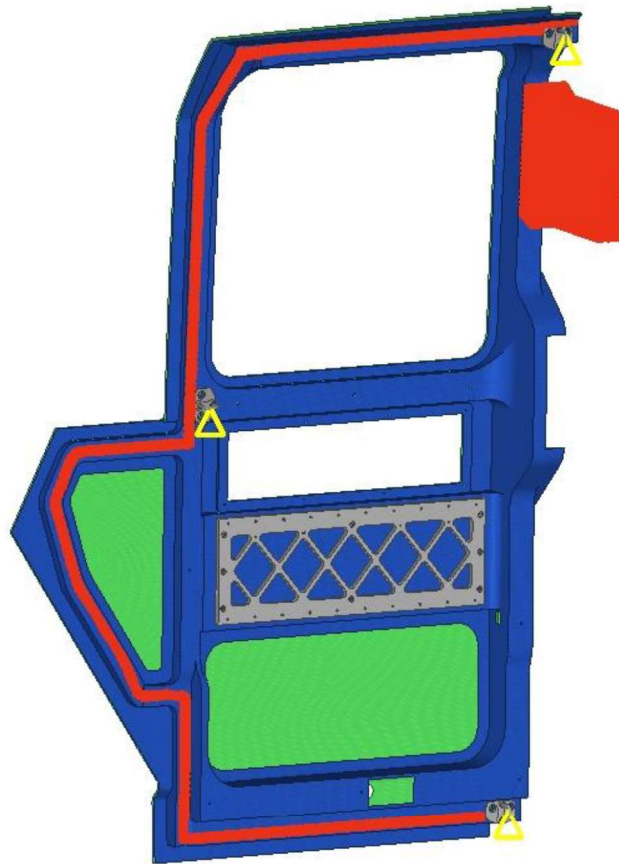


FIGURE 4-44 AUTOTAXI SIDE IMPACT LOADSTEP

The arm considered is that of a 95th percentile male, whose anthropometric data are reported in Figure 4-21. From these data, it is possible to obtain the dimensions and the height to which the surface where the load is placed. Since the height of the shoulder is 157 cm and of the elbow is 122 cm, the surface will have a height of 35 cm and will be placed at 157 cm with respect to the platform.

4.6.3 Door bending

Door stiffness is an ability of the resistance to deformation when the door is bearing load, which is represented by the relationship between the applied load and the deformation of the door with load.

The bending resistance must be tested in the event that the door is pushed in the opposite direction during the closing phase. This test gives an indication of the stiffness of the anchorage points between the door structure and the kinematics.

If the door stiffness is inadequate, it will have large deformation under load. When vehicle bears large load, the door of low stiffness will lead to increased deformation. Then it will appear a series of problems, such as, failure, noise, lax seal, closed too loose or tight, and so on.

For this load case, its constraint condition was that the door hinge parts are fully constrained except for rotation around z. A normal load of $340N$ for the AUTOshuttle and a load of $370N$ for the AUTOfaxi are applied on the central pillar of the door at the shoulder height. This test also wants to test the behavior of the door in case a passenger blocks the door while it is about to close. The load modulus come from consideration about the motor that moves the doors. The motor has a maximum torque of $350 Nm$. Behind this value the clutch of the motor start to slip. Then to consider the hinges as fully constrained, through an equilibrium equation is possible to get the corresponding force that must be applied on the door. Figure 4-45

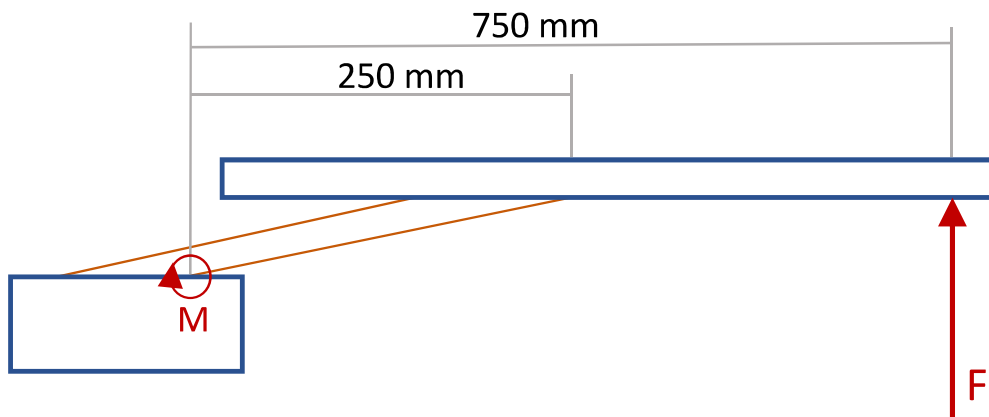


FIGURE 4-45 AUTOfaxi TOP VIEW OF THE DOOR KINEMATICS

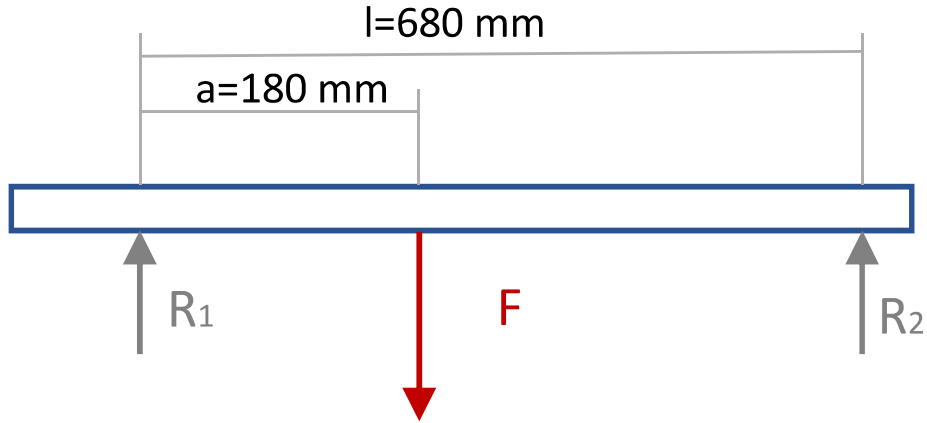


FIGURE 4-46 DOOR KINEMATICS SIMPLIFIED PROBLEM

Equilibrium equation about 1 with $F = M/0.25$:

$$Fa = R_2 l$$

$$R_2 = Fa/l$$

Moreover, under this load case it is analyzed the strength of the connection area between door and kinematics. As for the SAG test, the bending test is performed in open door configuration. For this reason, a maximum displacement is not included in the post-processing evaluation. Instead, the maximum composite stress allowed is 300 MPa.

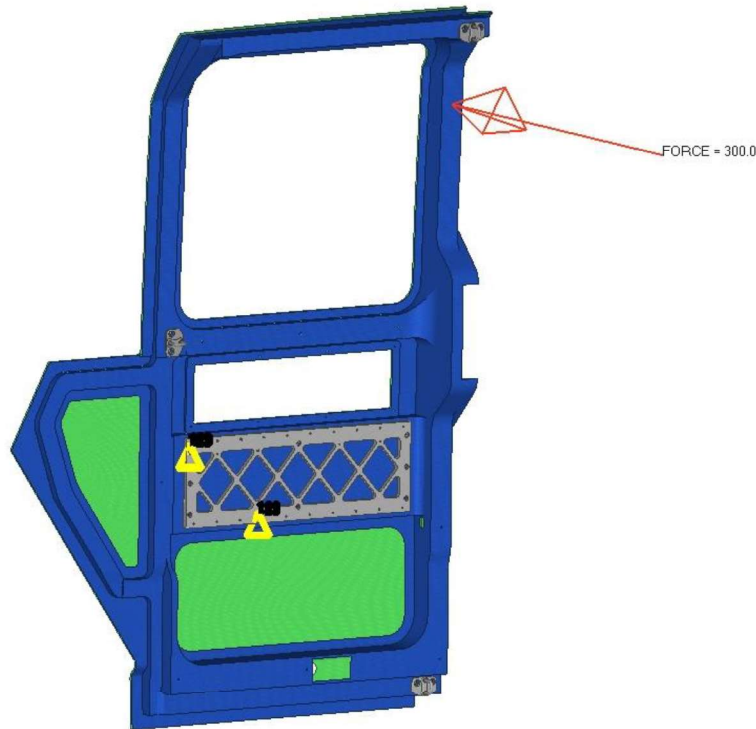


FIGURE 4-47 AUTOTAXI BENDING LOADSTEP

4.6.4 Strength of the interior panel against people

The doors of UNICARagil vehicles, as discussed in chapter 3, are of the swing and slide type. A mechanism of this type requires a cover that protects the mechanism from possible interference with other objects. At the same time, it acts as a structure on which the interiors will later be modeled.

The test involves a load being applied to the cover, simulating the weight of a person pushing the cover towards the door kinematics. To perform FEM simulations, a pressure of 0.03MPa corresponding to load of 950 N in an area of $150\text{mm} \times 215\text{mm}$ in y direction is applied. This force corresponds to a person of 95 kg, that is the mass of a man belonging to the 95th percentile, with an acceleration of 1g. (Figure 4-48)

The maximum deformation allowed in the z direction is 10 mm and the maximum stress allowed is 300 MPa . All the tests must be performed without the side window glass. In this way, more severe conditions are imposed, since the transparent panel increases the stiffness

The goal is to optimize the components for weight and stress in order to avoid excessive reinforcement while providing a safe design.

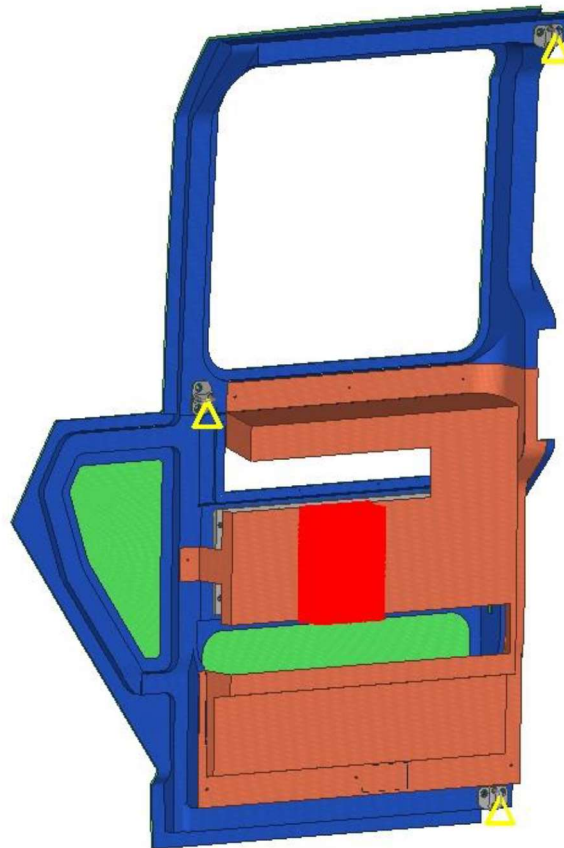


FIGURE 4-48 AUTOTAXI INTERIOR PANEL LOADSTEP

5 Post-processing and Results

For all the simulations carried out, a static linear approach was used and the required results are: displacements, stresses and constraining reactions in order to make a check on the analysed model.

As a first verification, the deformation of the structure is analysed, to check for any detached components or other problems. Subsequently, the Von Mises breakage criterion was used to examine whether the stresses are continuously spreading through the nodes.

5.1 AUTOshuttle

5.1.1 SAG test

Displacement

Figure 5-1 shows how the front door modify the own shape when subjected to a sag force. A deformation of this type was expected. This test together with the bending one are carried out without exploiting the constraints of the strikers. The connections present with the kinematics support the door.

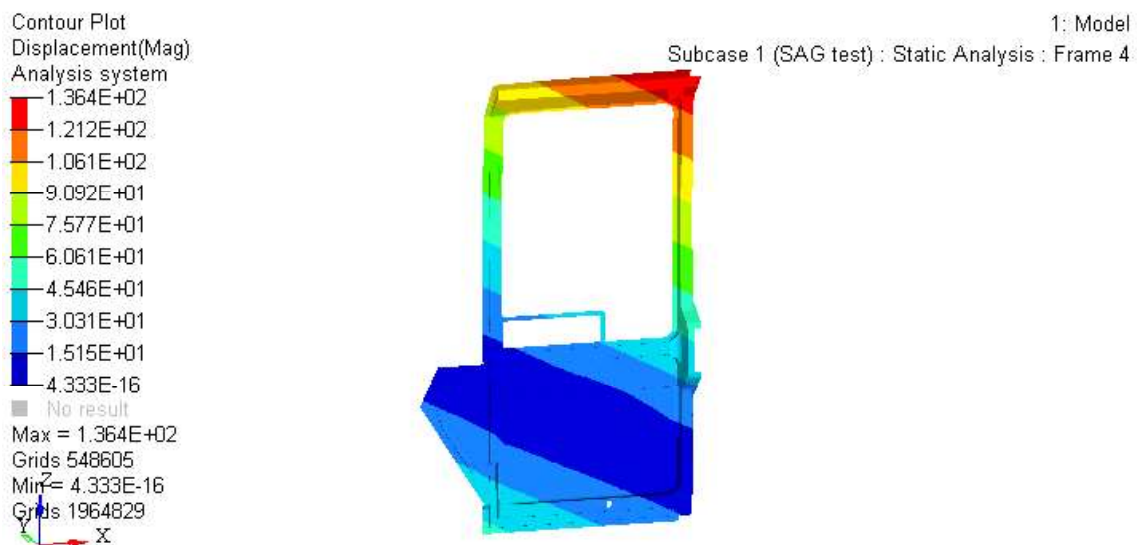


FIGURE 5-1 SAG TEST : DISPLACEMENT

As shown in Figure 5-1, the greatest deformation occurs in the farthest area from where the constraints are applied. In these areas, values of about 136 mm are reached.

Composite Stress

The composite stress evaluation allows to understand if, in some parts, the tensile strength is exceeded, reaching failure. From Figure 5-2, it is possible to notice that the stress values, in the area where door is connected to the kinematic, are higher than the tensile yield strength of the material.

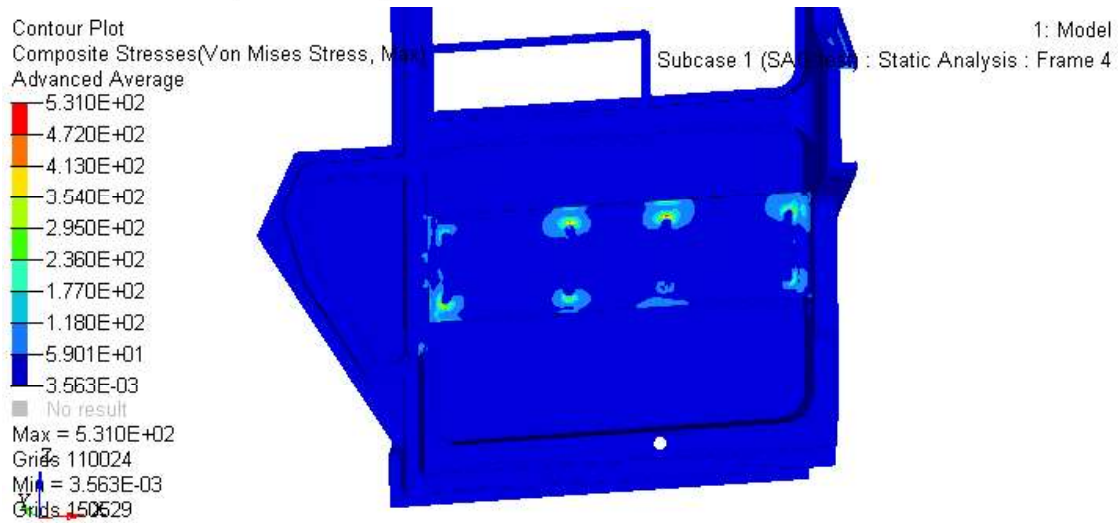


FIGURE 5-2 SAG TEST: COMPOSITE STRESS

5.1.2 Side Internal impact

Displacement

From the results of Figure 5-3, it is possible to understand which is the deformation of the door along the y-axis, i.e. the same axis of application of the force. As expected, a minor displacement is obtained. This is mainly due to a different configuration of the constraints because, the test is executed with the door in closed position. The front door can rely on three strikers that the structure stiff. During this test, it is also evaluated the displacements of the door along the perimeter due to the pressure exerted by the weather strips.

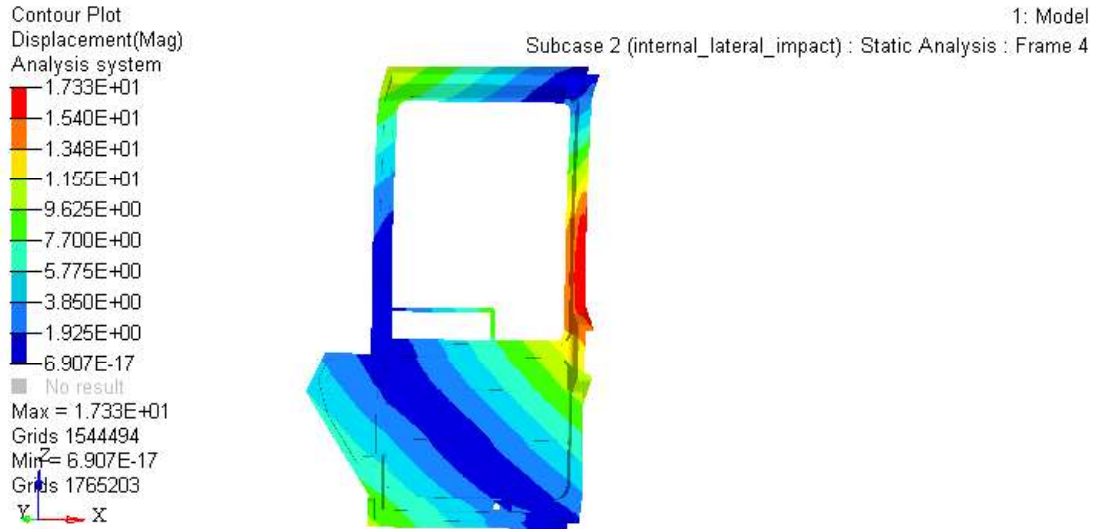


FIGURE 5-3 SIDE INTERNAL IMPACT: DISPLACEMENT

Composite Stress

Composite stress reaches value below the yielding strength but slightly higher than the threshold set in section 4.6.1. The areas with the higher composite stress are the ones in correspondence of the striker's connections

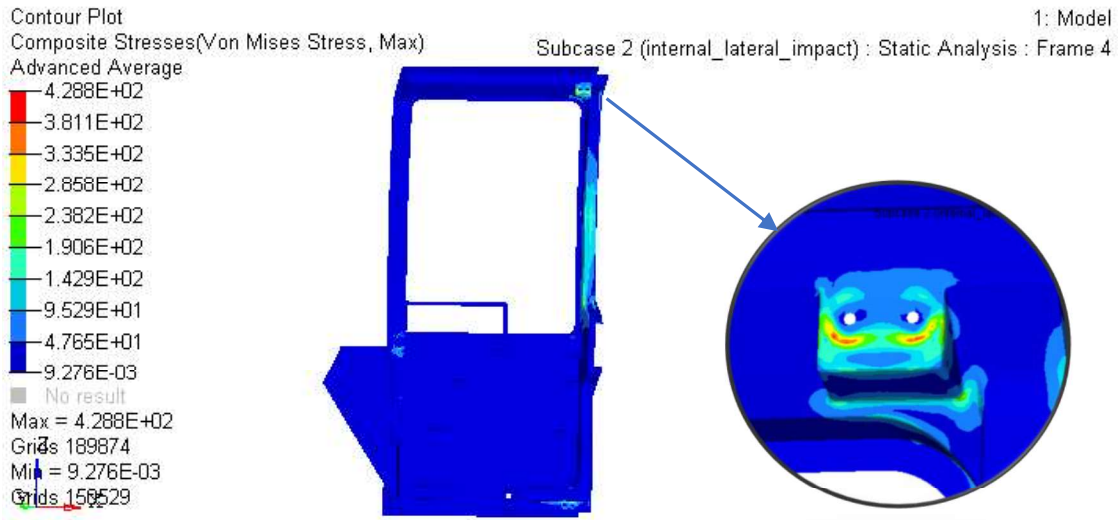


FIGURE 5-4 SIDE INTERNAL IMPACT: COMPOSITE STRESS

5.1.3 Door bending

Displacement

By observing the directional deformation along the y axis, it is possible to understand the problems associated with the compliance of the door-kinematic

connection. As shown in Figure 5-5, the deformation at the top of the structure is around 183 *mm*.

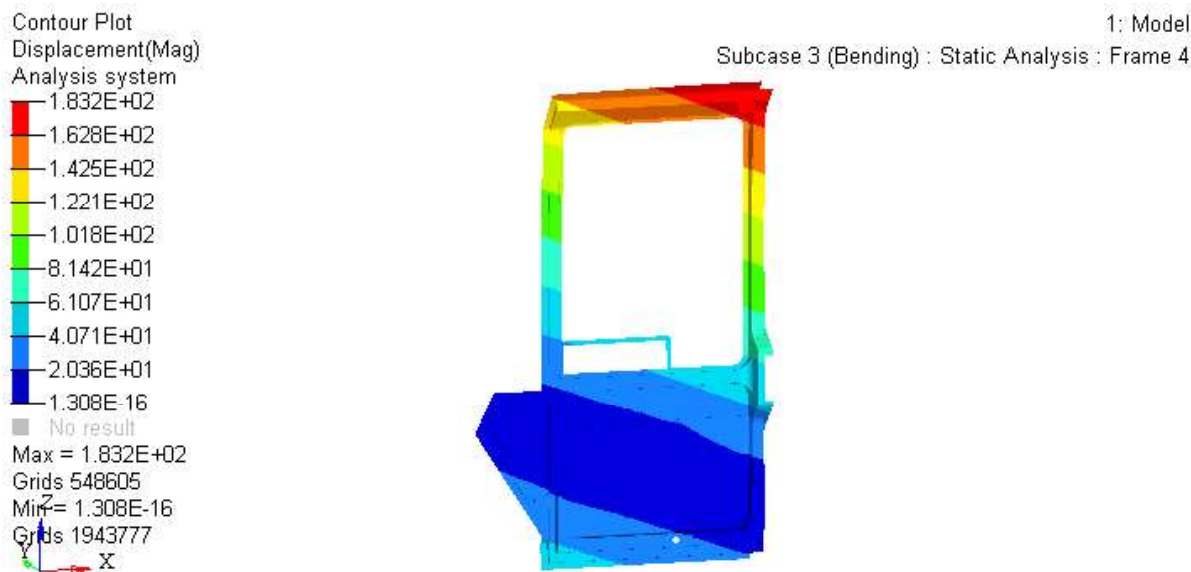


FIGURE 5-5 DOOR BENDING STIFFNESS: DISPLACEMENT

Composite Stress

As the analysis of the deformation suggests, along the fixing points of the kinematics with the door, the stress state reaches values even higher than the tensile yield strength. Around some holes the stress composite has peaks of 697MPa (Figure 5-6).

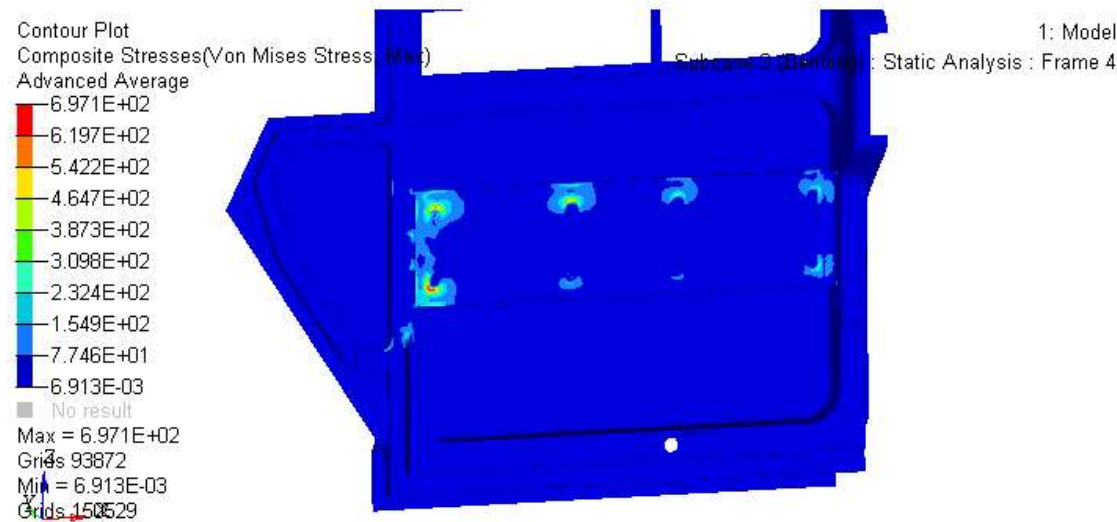


FIGURE 5-6 DOOR BENDING STIFFNESS: COMPOSITE STRESS

5.1.4 Interior panel

Displacement

Since the opening and closing mechanism does not allow for many supports, the component has a long and narrow body in the central part. This results in a deformation of 26.5 mm , well beyond the maximum permissible deformation of 10 mm . Moreover, the doors of the AUTOshuttle are wider, further accentuating this problem, compared to the case of the AUTOfaxi which will be analysed in the next chapter.

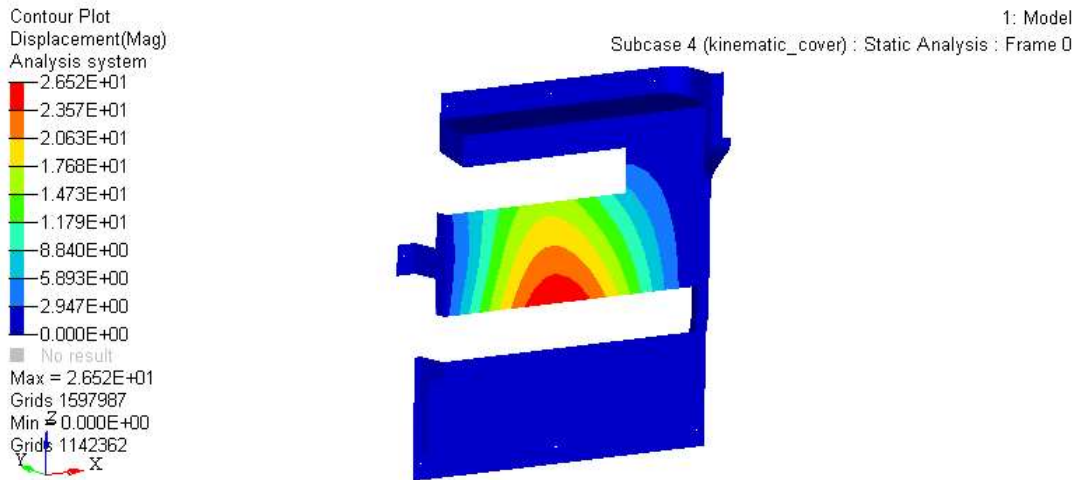


FIGURE 5-7 KINEMATIC INTERIOR COVER

Composite Stress

In Figure 5-8, it is possible to notice that the internal panel is subject to a wide deformation, the state of stress is lower than the maximum stress allowed. The slenderness of the structure allows the stress to be distributed over the whole surface, and thus preventing a concentration of the stress

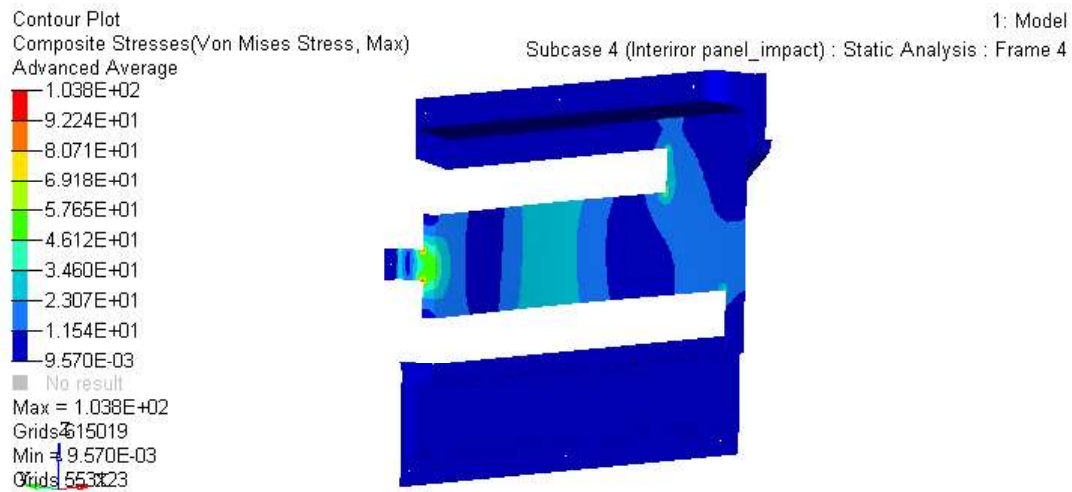


FIGURE 5-8 KINEMATIC INTERIOR COVER: DISPLACEMENT

5.2 AUTOfaxi

The doors of the AUTOfaxi have geometries similar to those of the AUTOfshuttle. moreover, since loads and constraints of the same nature are applied, even if with different magnitudes, you expect deformed and composite stress with trends similar to those found on AUTOfshuttle.

The differences that can be noticed derive from the fact that the AUTOfaxi front door has reduced dimensions and therefore overall the structure is more rigid.

5.2.1 SAG test

Displacement

As shown in Figure 5-9, the greatest deformation occurs in the farthest area from where the constraints are applied. In these areas, values of about 46 mm are reached.

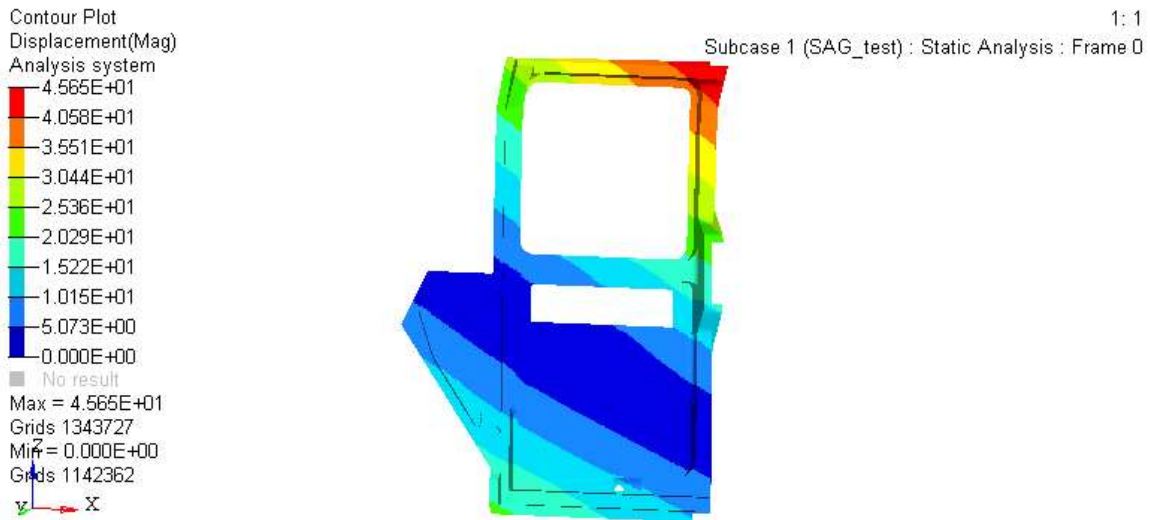


FIGURE 5-9 SAG TEST : DISPLACEMENT

Composite Stress

From Figure 5-10, it is possible to notice that the stress values, in the area where door is connected to the kinematic, are higher than the tensile yield strength of the material. Values that reach up to 1064 MPa in correspondence to the central upper joint of the adapter plate.

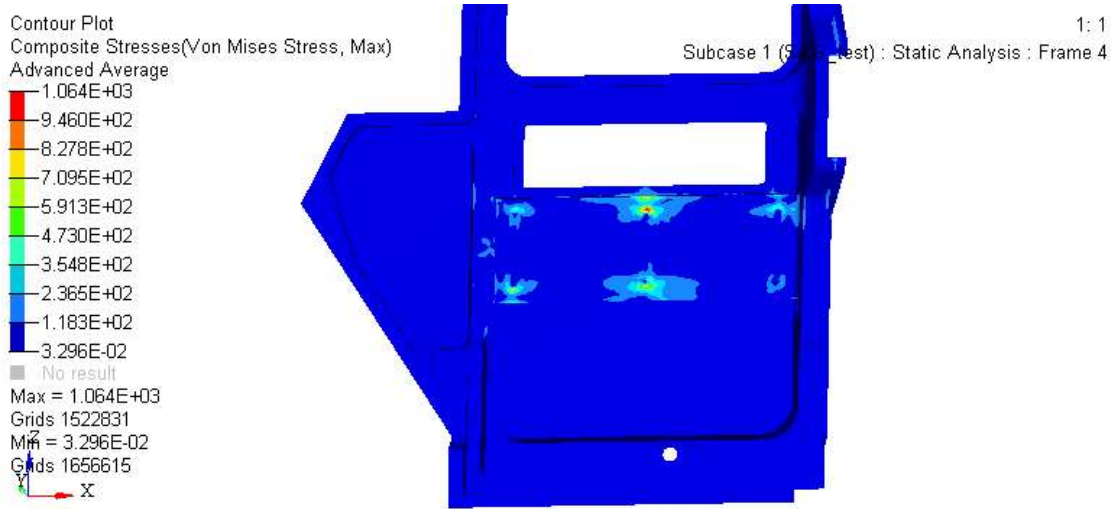


FIGURE 5-10 SAG TEST: COMPOSITE STRESS

5.2.2 Side Internal impact Displacement

As for the AUTOshuttle, from the results of Figure 5-11, it is possible to understand which is the deformation of the door along the y-axis, i.e. the same axis of application of the force. As expected, a minor displacement is obtained with respect to AUTOshuttle. The maximum deformation of 12.9 mm is just below the application of the force. During this test is also evaluated the displacements of the door along the perimeter due to the pressure exerted by the weather strips

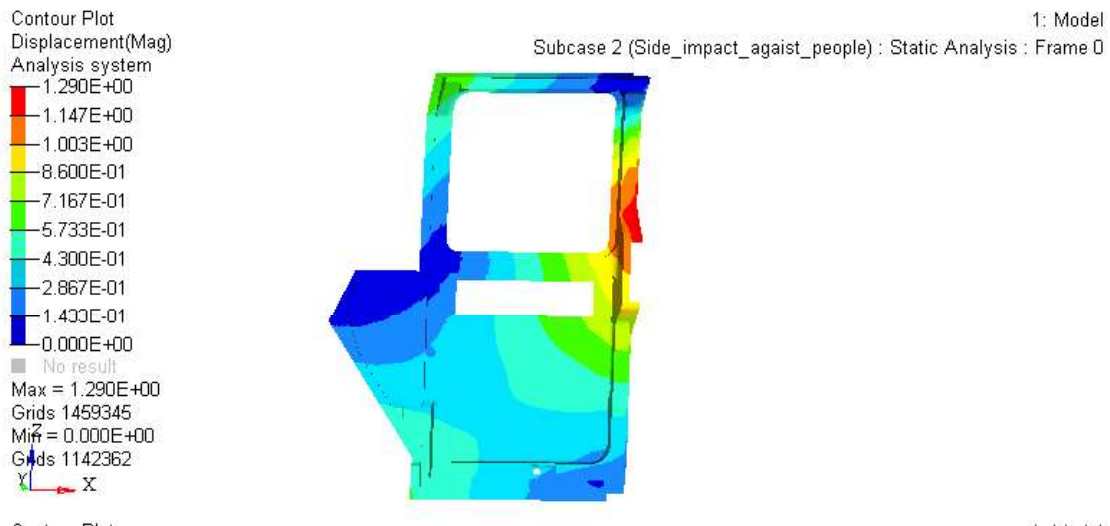


FIGURE 5-11 SIDE INTERNAL IMPACT: DISPLACEMENT

Composite Stress

Composite stress reaches value below the yielding strength but slightly higher than the threshold set in section 4.6.1. the areas with the higher composite stress are the ones in correspondence of central latch case.

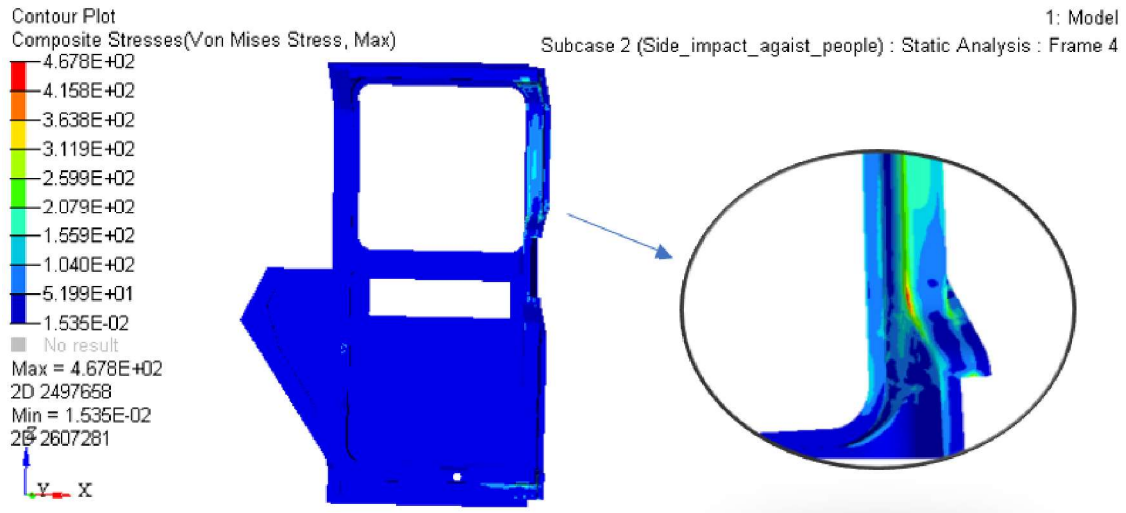


FIGURE 5-12 SIDE INTERNAL IMPACT: COMPOSITE STRESS

5.2.3 Door bending

Displacement

As shown in Figure 5-13, AUTOfaxi front door have a maximum displacement of 51mm, around 3 time smaller that in the case of AUTOshuttle. This is mainly due to the presence of a horizontal beam located in the upper part of the door. The horizontal beam substitutes the fix beam placed on the hut structure of the AUTOshuttle.

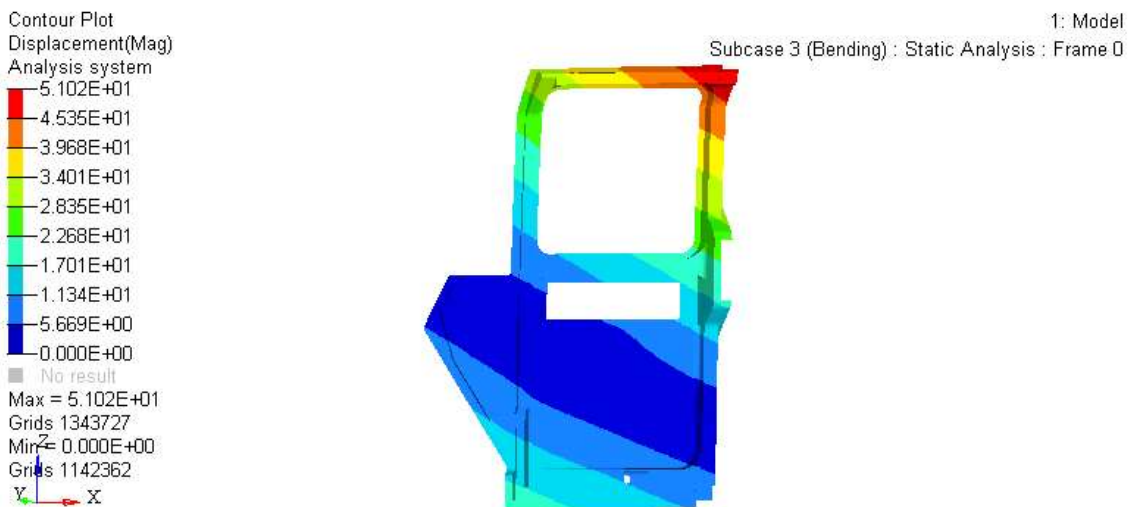


FIGURE 5-13 DOOR BENDING STIFFNESS: DISPLACEMENT

Composite Stress

As the analysis of the deformation suggests, along the fixing points of the kinematics with the door, the stress state reaches values even higher than the tensile yield strength. Around some holes the stress composite has peaks of 1292 MPa (Figure 5-14).

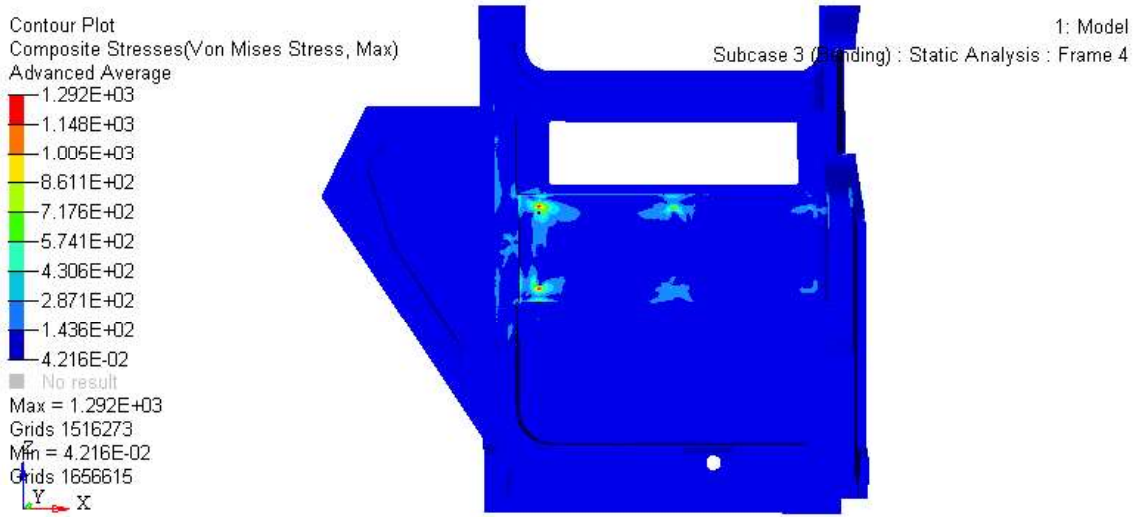


FIGURE 5-14 DOOR BENDING STIFFNESS: COMPOSITE STRESS

5.2.4 Interior panel

Displacement

As exposed during the analysis of the deformation in AUTOshuttle, in Figure 5-15 it is possible to see that in AUTOtaxi front door there is a minor deformation of 17 mm , even if it is still outside the imposed limits.

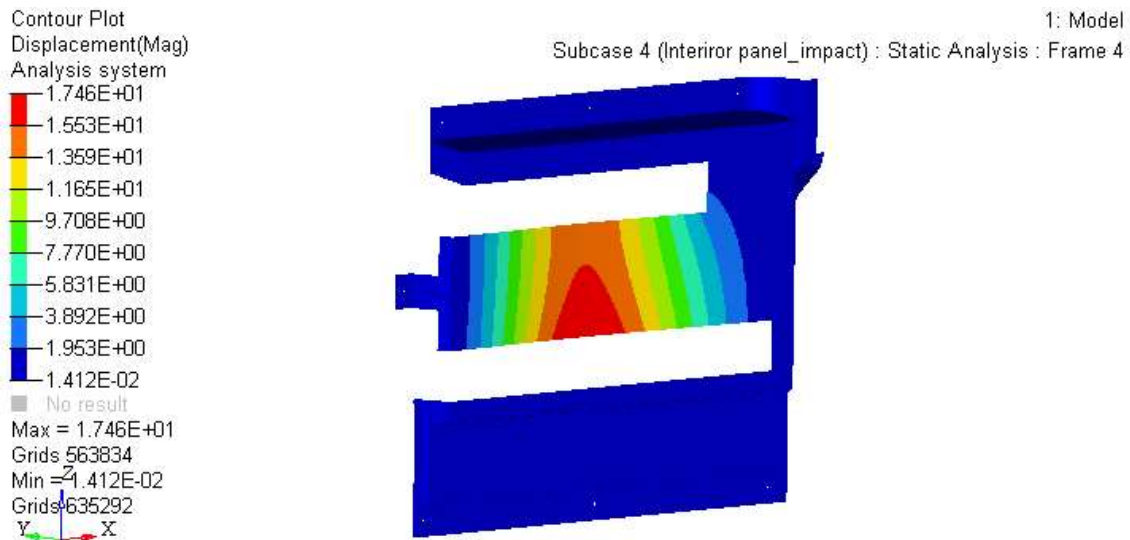


FIGURE 5-15 INTERIOR PANEL: DISPLACEMENT

Composite Stress

In Figure 5-16, it is possible to notice that the internal panel is subject to a wide deformation, the state of stress is lower than the maximum stress allowed. The slenderness of the structure allows the stress to be distributed over the whole surface, and thus preventing a concentration of the stress

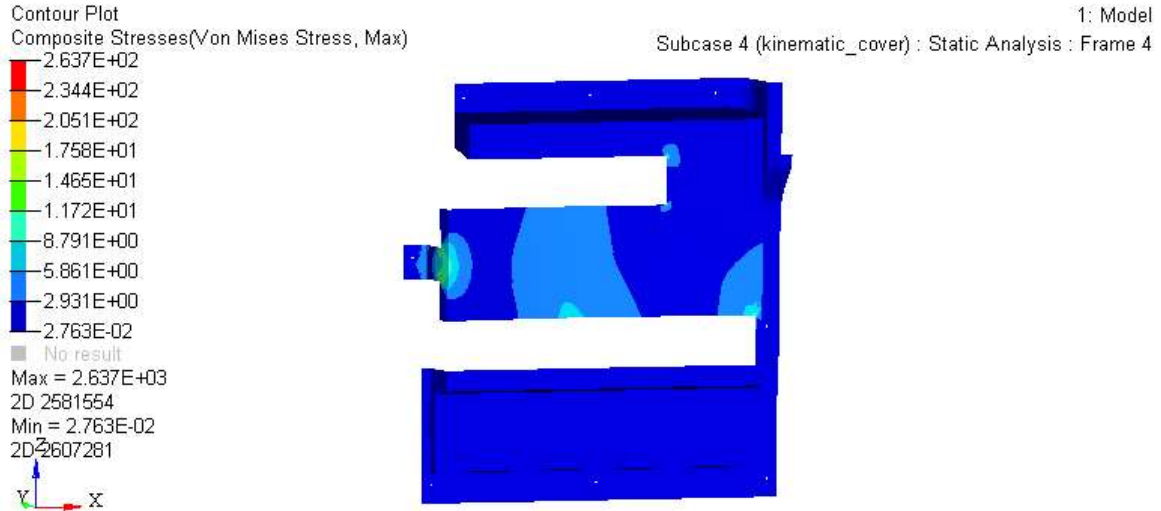


FIGURE 5-16 INTERIOR PANEL: COMPOSITE STRESS

These cases show the critical points of the current laminates adopted. In the next step, instead of adding reinforcement patches in some areas, a free-size optimization will be carried out. This type of analysis gives the possibility to obtain components that, in addition to respecting the constraints imposed by the delivery tests, have a higher stiffness/weight ratio.

6 Optimization

6.1 Structural Optimization

The structural optimization aims to improve the structure of a component in order to support loads and stresses in the best possible way. The optimization process aims to make a structure as light and resistant as possible, identifying the best arrangement of material, avoiding unnecessary use without sacrificing the required stress resistance [46].

The optimization process basically involves minimizing or maximizing a function within a predetermined value domain, e.g. minimizing mass or deformation, or maximizing the stiffness of the structure. In order to be able to optimize a structure, it is essential to define what loads the structure will have to withstand and the constraints to be taken into account, e.g. mass, dimensions, component materials.

The optimization is generally performed manually, with an iterative-intuitive approach of which we can generically distinguish the following steps:

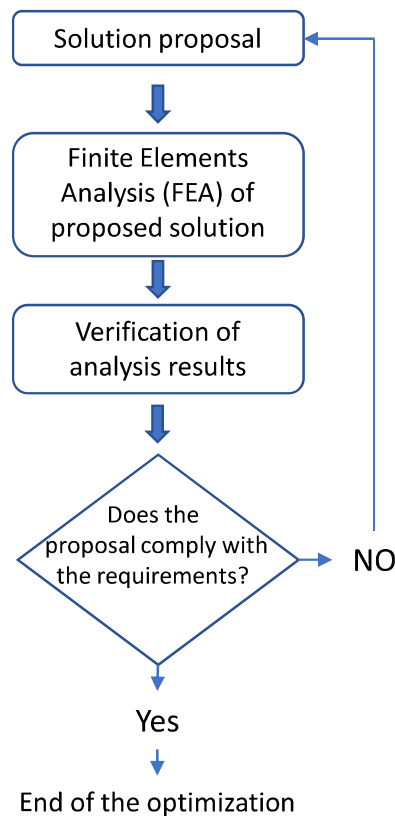


FIGURE 6-1 OPTIMIZATION LOGIC PATH

It can be easily understood, an optimization of this kind takes a long time to reach the final result and there is no certainty that the result obtained is in any case optimal.

In the last decades, programs dedicated to optimization have made considerable progress and it is now possible to approach the process of structural optimization in an increasingly easier and guided way and achieve acceptable results in most cases, significantly improving the results

Structural optimization problems can be distinguished in three different areas:

- size optimization
- shape optimization
- topology optimization

Size optimization will be used in this work. In this case the shape of the structure is known and the optimization is done by changing the size of the parts that compose it or the thickness if the model is made from surfaces as in the case of CFRP components. Therefore, the variables are the dimensions of the structural elements.

Given a spatial shell consisting of elements characterized by constant thickness, arranged according to a certain surface, an example of dimensional optimization could be to reduce the thickness of some areas without altering the arrangement or length of the elements [47].

The use of a size optimization presupposes that the design of the structure is already in a conclusive phase and is impossible to apply in the first design phases. It is particularly useful to further refine an existing design.

6.2 Composite Optimization

The process follows three phases. The first, Free-Size Optimization, has the task of creating a thickness distribution for each fiber angle. Discrete-Size Optimization calculates optimal number of each ply shape of each fiber angle. Finally, Shuffle Optimization finds optimal stacking order under consideration of ply book rules (Figure 6-2)

The cycle shall be executed with regard to the all already given load steps at the same time, because otherwise the component will fail most likely in later application at a not considered load step.

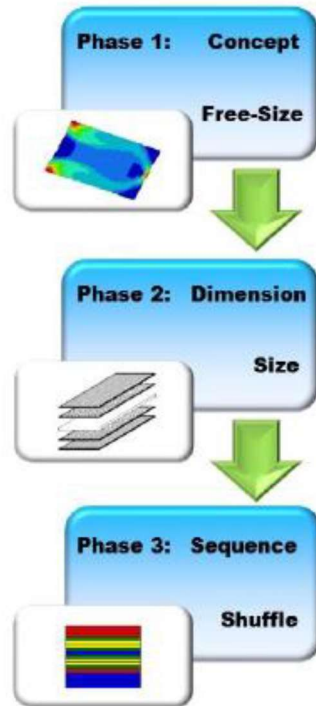


FIGURE 6-2 COMPOSITE OPTIMIZATION PHASES [B7]

6.2.1 Free-Size Optimization

Ply editing, Super-ply

Hence OptiStruct only can subtract material and cannot thicken it, the first step of setting up a composite Free-Size Optimization is the creation of so-called Super-ply, thus overthick layers as in Table 6-1

TABLE 6-1 PLY EDITING DESIGN SPACE

| | Material | Orientation [°] | Thickness [mm] |
|------------|----------|-----------------|----------------|
| Outershell | GG245TSE | 0 | 2 |
| | GG380T | 45 | 2 |
| | GG245TSE | -45 | 2 |
| | GG380T | 90 | 2 |
| | GG245TSE | 0 | 2 |

| | | | |
|--------------------------------|----------|-----|---|
| Innershell | GG380T | 45 | 2 |
| | GG245TSE | -45 | 2 |
| | GG380T | 90 | 2 |
| Kinematic interior cover | GG245TSE | 0 | 2 |
| | GG380T | 45 | 2 |
| | GG245TSE | -45 | 2 |
| | GG380T | 90 | 2 |

Freestyle design variable

For the freestyle -optimization initially a design variable is created. *Analysis > optimization > free size > create*. In this phase the laminates of design space are selected.

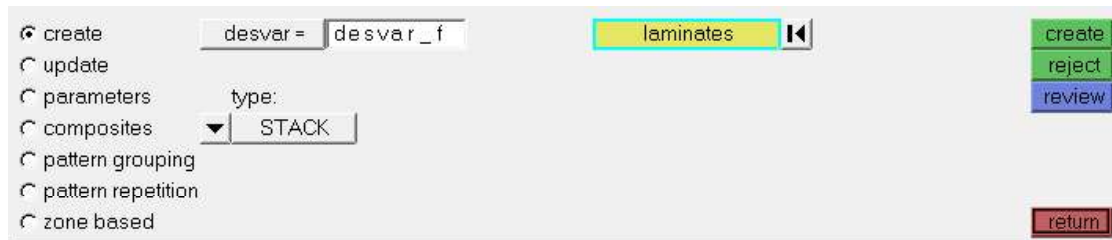


FIGURE 6-3 FREESTYLE DESIGN VARIABLE CREATION

Some necessary constraints have been defined to guide the optimization process towards an applicable result, a Manufacturing constraint of planar symmetry has been imposed. Furthermore, constraints have been defined on the minimum and maximum thickness of the laminate and on the minimum extension of the ply that can be obtained:

- Minimum laminate thickness: 0.52 mm
- Maximum laminate thickness: 5.0 mm
- Minimum ply size: 20 mm

The constraint on the minimum thickness has been placed different from zero, thus avoiding the creation of openings on the shell made. While the minimum size of the plies allows not to obtain patches to laminate with an extremely reduced surface extension.

Finally, the SMEAR option for the laminate has been defined, which allows to obtain results that are independent from the lamination sequence, this will be defined later in the last step of optimization on composite materials.

After editing all the specifications, the design variable for the laminate of the design space looks as follows.

| | | | |
|-----------|----------|----------|----------|
| ID | EID | EID | EID |
| 1 | 1 | 2 | 3 |
| DSIZE | 1STACK | | |
| | MINDIM | | |
| MEMBSIZ | 20.00000 | | |
| LTMIN | LTMAX | LTSET | LTEXC |
| 0.5200005 | 0.000000 | 0.000000 | 0.000000 |
| COMP | LAMTHK | | |
| 0.5200005 | 0.000000 | | |

FIGURE 6-4 FREESIZE DESIGN VARIABLE COMPOSITES

Responses for optimization

To carry on this optimization the responses “*mass*” and “*weighted compliance*” and “*stress*” are defined.

It has to be considered that the same weight at different single compliances (for example Sag test and bending) does not lead to a uniformly distributed weighted compliance. Rather the products (weight factor · single compliance) have to be compared to each other.

The following example explains that:

The results of the analytical calculation are

Loadstep a) creates a compliance of 1000 *mm/N*.

Loadstep b) creates a compliance of 10 *mm/N*.

The total compliance, which is used as a response, shall create a value of 2000 *mm/N* via the weight, for which it is defined that both loadsteps shall contract each with 50%.

$$\Sigma WCOMP = x \cdot COMP(a) + y \cdot COMP(b)$$

$$2000 \text{ mm/N} = 1 \cdot 1000 \text{ mm/N} + 100 \cdot 10 \text{ mm/N}$$

In the case of study, loadsteps have different single compliance, so the loadstep weight factors are calculated accordingly [48].

Constraints and objective of the optimization

Core of the optimization is the definition of constraints and objectives. Since the goal is to reduce the mass of the component while comply with the requirements previously defined. The response mass is defined as an optimization objective to minimize as shown in Figure 6-6 and the responses, while WCOMP and stress are defined as design constraint (*dconstraint*) with the design upper bound of **10 mm** for WCOMP and the design lower /upper bounds of **300 MPa**.(Figure 6-5)

The screenshot shows the 'DCONSTRAINTS DEFINITION' window. It contains two sections for defining constraints. The first section has 'constraint =' set to 'const_stre' and 'response =' set to 'comp_stres'. Below this, there are checkboxes for 'lower bound =' (set to -300.000) and 'upper bound =' (set to 300.000). The second section has 'constraint =' set to 'const_WCOMP' and 'response =' set to 'WCOMP'. Below this, there are checkboxes for 'lower bound =' (set to -10.000) and 'upper bound =' (set to 10.000). A 'loadsteps' button is located between the two sections.

FIGURE 6-5 DCONSTRAINTS DEFINITION

The screenshot shows the 'OBJECTIVE DEFINITION' window. It has a dropdown menu on the left set to 'min' and a 'response =' field on the right set to 'mass'.

FIGURE 6-6 OBJECTIVE DEFINITION

In order to take into account of the limitation on the stresses inside the carbon fiber shell, the Tsai-Wu failure criterion was used, a phenomenological criterion that considers both distortion and expansion energy. The laminate is expected to fail when its index value is greater than or equal to 1. The design constraint imposed foresees a maximum value of 0.5 so as to obtain a safety factor of 2 on the laminate. This made it possible to analyse what was the minimum mass obtainable on the component, comparing them with those obtained during the preliminary analysis.

Last setting before to run the optimization is the control card. In control cards section the OUTPUT-card with the keyword FSTOSZ (Freesize to Size) shall be defined to ensure the transition of design-information to the size- optimization.

Controlling the Out-files, information about responses constraints and objective can be extracted. While, by displaying the HyperView files, it is possible to check the element thicknesses as well as the orientation/ply thicknesses.

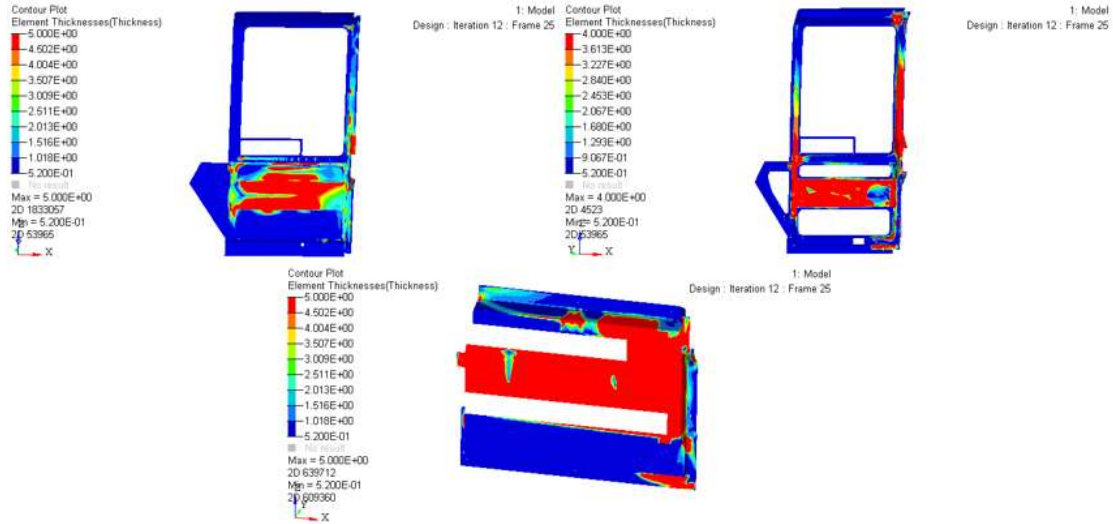


FIGURE 6-7 SUPER-PLY THICKNESS OF THE TWO SHELL AND THE INTERIOR PANEL

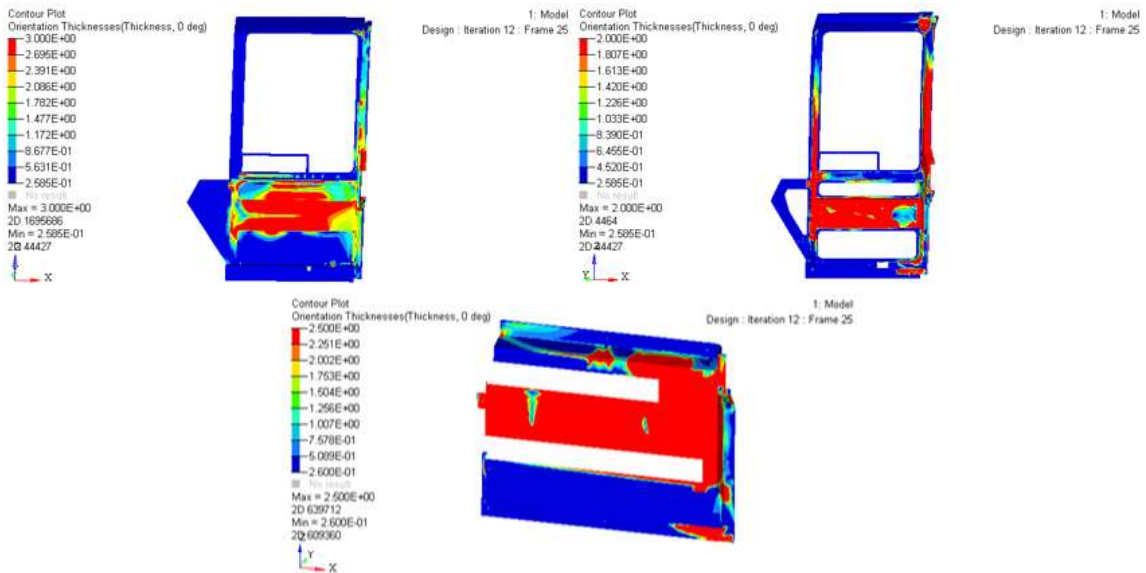


FIGURE 6-8 ORIENTATION THICKNESS OF THE COMPONENTS (0°)

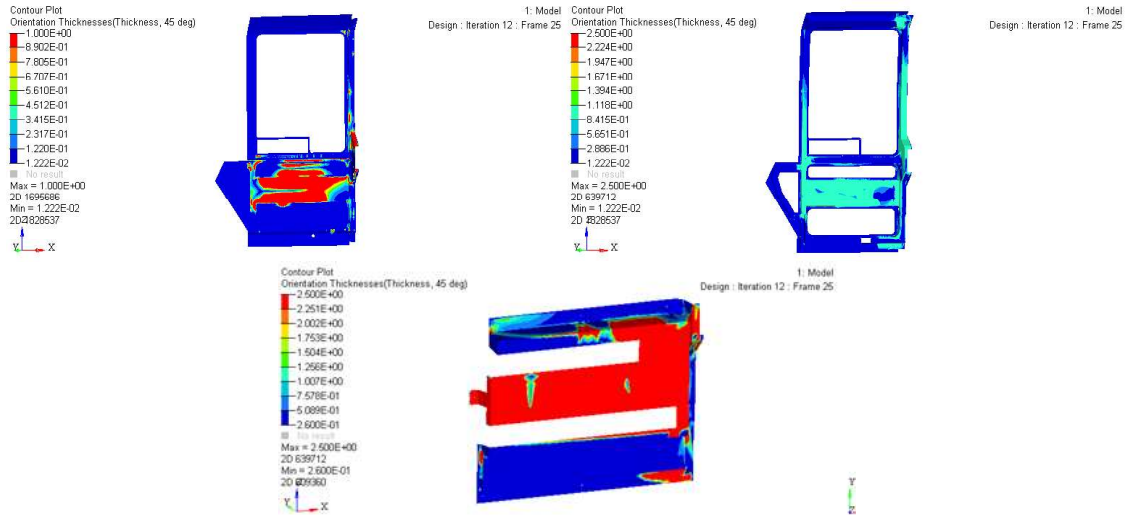


FIGURE 6-9 ORIENTATION THICKNESS OF THE COMPONENTS (45°)

Analyzing in detail the thickness obtained for each super-ply how the 0° - 90° arrangement is favored with respect to the 45° for outer shell and inner shell. Instead, the interior panel sees an equal division of the same between the two angles just mentioned. This result clarifies the type of stress to which the components are subjected.

The result of Free-Size optimization, however, produces a great variability of thickness within each super-ply and this would not be manageable from a production point of view considering that the real fabric thickness is constant. Through the optimization setting panel it is possible, to reduce this variability by dividing the super-ply into a maximum of four fabrics (Figure 6-10).

| Name | Id | Color | Material | Thickness | Orientation |
|-------------|--------|-------------|----------|-----------|-------------|
| PLYS_101100 | 101100 | Red | GG245TSE | 0.14290 | 0.0 |
| PLYS_101200 | 101200 | Green | GG245TSE | 0.28256 | 0.0 |
| PLYS_101300 | 101300 | Blue | GG245TSE | 0.46067 | 0.0 |
| PLYS_101400 | 101400 | Yellow | GG245TSE | 0.11387 | 0.0 |
| PLYS_102100 | 102100 | Cyan | GG380T | 0.09120 | 45.0 |
| PLYS_102200 | 102200 | Magenta | GG380T | 0.15846 | 45.0 |
| PLYS_102300 | 102300 | Grey | GG380T | 0.56415 | 45.0 |
| PLYS_102400 | 102400 | Dark Grey | GG380T | 0.18619 | 45.0 |
| PLYS_103100 | 103100 | Red | GG380T | 0.09120 | 0.0 |
| PLYS_103200 | 103200 | Dark Red | GG380T | 0.15846 | 0.0 |
| PLYS_103300 | 103300 | Blue | GG380T | 0.56415 | 0.0 |
| PLYS_103400 | 103400 | Dark Blue | GG380T | 0.18619 | 0.0 |
| PLYS_104100 | 104100 | Orange | GG380T | 0.08988 | -45.0 |
| PLYS_104200 | 104200 | Brown | GG380T | 0.15655 | -45.0 |
| PLYS_104300 | 104300 | Light Blue | GG380T | 0.56481 | -45.0 |
| PLYS_104400 | 104400 | Pink | GG380T | 0.18876 | -45.0 |
| PLYS_105100 | 105100 | Dark Red | GG245TSE | 0.13859 | 0.0 |
| PLYS_105200 | 105200 | Purple | GG245TSE | 0.27059 | 0.0 |
| PLYS_105300 | 105300 | Dark Purple | GG245TSE | 0.46531 | 0.0 |
| PLYS_105400 | 105400 | Light Pink | GG245TSE | 0.12551 | 0.0 |

FIGURE 6-10 52 PLY LAMINATION SEQUENCE, OBTAINED AS A RESULT OF THE FSTOSH OPTIMIZATION

6.2.2 Size Optimization

The second step consists in Size optimization, classified as fine tuning level optimization, necessary to optimize the thickness of the plies. This optimization also allows to take into account the real thickness of the fabric, in the case of GG245TSE and GG380T respectively equal to 0.26 mm and 0.44 mm , obtaining as a result for each ply-bundle a multiple thickness of the real one. A laminate made of ply of different shape and orientation will be obtained, thanks to the Free-Size optimization, and in such a number and thickness to meet the required target, thanks to the Size optimization.

Ply-shapes Edit

First, all the other components should be hidden. Editing the plies happens individually, that means that for every orientation the shapes 2 till 4 are edited because shape 1 includes all previous elements

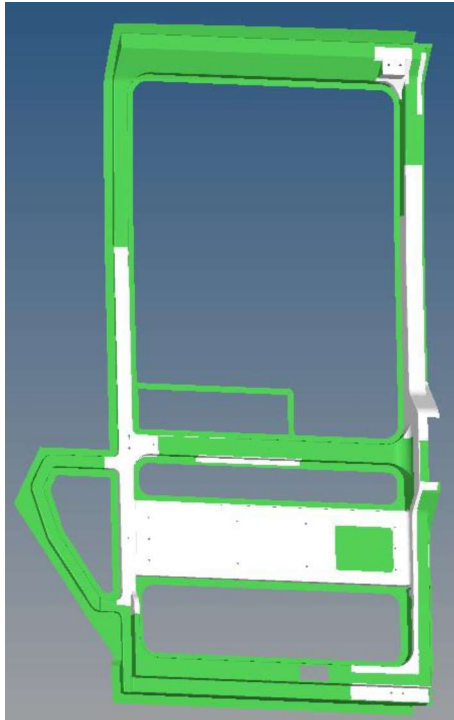


FIGURE 6-11 EDITED PLY-SHAPE (ID 207300)

After editing all the ply shapes for the three components of the door, the results in term of thickness distribution is shown in Figure 6-12

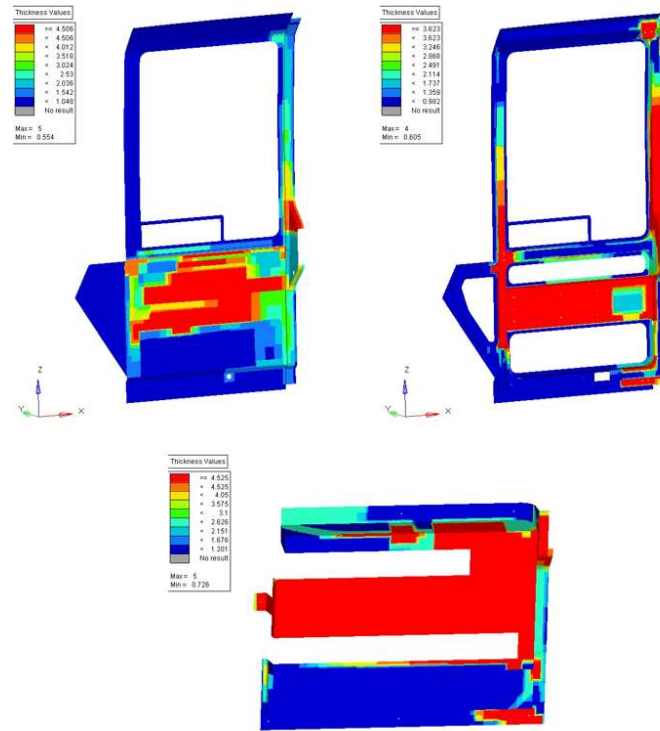


FIGURE 6-12 MANUFACTURABLE PLIES SHAPE RESULTS

Design Variables Edit

To perform this optimization, first of all, the thickness variability range for each ply-bundle shown in Figure 6-10 has been defined:

- Minimum ply thickness: 0 mm
- Maximum thickness ply: 5.0 mm
- Actual fabric thickness: 0.26 mm

The minimum value has been set to 0 mm to allow the optimizer to remove that ply-bundle if necessary.

Constraints on laminate thickness have also been included:

- Minimum laminate thickness: 0.52 mm
- Maximum laminate thickness: 5.0 mm

These were necessary to ensure that at least two layers were present and that the maximum thickness previously adopted as a constraint was not exceeded.

Before to run again the optimization the existing OUTPUT-card, entry FStoSZ shall be set to the output SZtoSH, that generate a Size to shuffle output.

Checking the Out-file as well as the Hgdata-file with HyperGraph shows that iteration 1 satisfied all constraints and is all in all the best iteration.

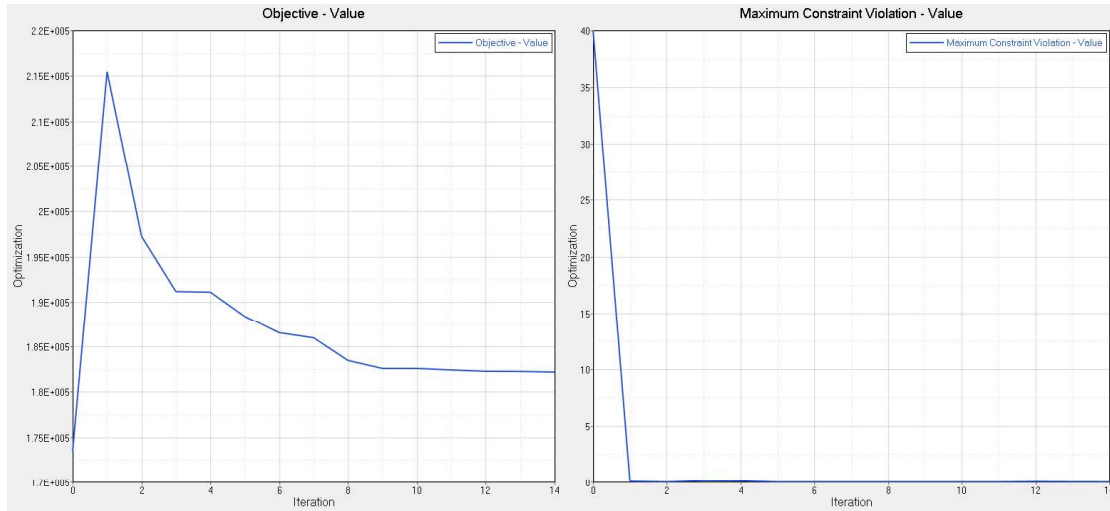


FIGURE 6-13 DISCRITE SIZE OPTIMIZATION RUN HYPERGRAPH RESULTS

The laminate obtained as a result of this optimization was considered acceptable to continue with the next step and is formed as follows (Figure 6-14)

| Name | Id | Color | Material | Thickness | Orientation |
|-------------|--------|-----------------------------------------|-----------------|-----------|-------------|
| PLYS_101101 | 101101 | ■ | 245_carbonfiber | 0.26000 | 0.0 |
| PLYS_101301 | 101301 | ■ | 245_carbonfiber | 0.26000 | 90.0 |
| PLYS_101401 | 101401 | ■ | 245_carbonfiber | 0.26000 | 0.0 |
| PLYS_101402 | 101402 | ■ | 245_carbonfiber | 0.26000 | 90.0 |
| PLYS_102401 | 102401 | ■ | 380 carbon | 0.44000 | 45.0 |
| PLYS_102402 | 102402 | ■ | 380 carbon | 0.44000 | -45.0 |
| PLYS_102403 | 102403 | ■ | 380 carbon | 0.44000 | 45.0 |
| PLYS_102404 | 102404 | ■ | 380 carbon | 0.44000 | -45.0 |
| PLYS_102405 | 102405 | ■ | 380 carbon | 0.44000 | 45.0 |
| PLYS_105401 | 105401 | ■ | 245_carbonfiber | 0.26000 | 0.0 |
| PLYS_105402 | 105402 | ■ | 245_carbonfiber | 0.26000 | 90.0 |

FIGURE 6-14 OUTER SHELL'S LAMINATION SEQUENCE, OBTAINED AFTER THE OPTIMIZATION OF SIZE

6.2.3 Shuffle Optimization

Shuffling optimization is specific for composite materials and serves to identify the optimal ply stacking sequence in order to maximize stiffness, starting from the result obtained from the Size optimization (Figure 6-14).

In this phase it is possible to insert constraints related to the manufacture of laminates, such as fixing a ply in a given position or indicating the maximum

number that can be laminated consecutively, for a given orientation. For aesthetic reasons, the outer ply of the outer shell and the inner ply of the inner shell will be a 0°/90° GG245TSE, because a thinner fiber weave will lead to a better surface finishing.

Table 6-2 shown the lamination sequence obtained. Can be recognized that beginning with iteration 3 all pretended shuffling manufacturing constraints are kept.

TABLE 6-2 AUTOSHUTTLE FRONT DOOR SHUFFLE OPTIMIZATION

Stacking sequence for STACK 1

| Iteration 0 | Iteration 1 | Iteration 2 | Iteration 3 | Iteration 4 | Iteration 5 | Legend |
|-------------|-------------|-------------|-------------|-------------|-------------|---------------|
| 101101 | 101101 | 101101 | 101101 | 101101 | 101101 | 90.0 degrees |
| 101301 | 101301 | 101301 | 101301 | 101301 | 101301 | 45.0 degrees |
| 101401 | 102401 | 105401 | 101402 | 105402 | 105402 | 0.0 degrees |
| 101402 | 102402 | 101402 | 102401 | 101402 | 101402 | -45.0 degrees |
| 102401 | 101401 | 102401 | 102402 | 102401 | 102401 | |
| 102402 | 101402 | 102402 | 102403 | 102402 | 102402 | |
| 102403 | 102403 | 102403 | 102404 | 102403 | 102403 | |
| 102404 | 102404 | 102404 | 102405 | 102404 | 102404 | |
| 102405 | 105401 | 102405 | 105402 | 102405 | 102405 | |
| 105401 | 105402 | 105402 | 105401 | 105401 | 105401 | |
| 105402 | 102405 | 101401 | 101401 | 101401 | 101401 | |

Stacking sequence for STACK 2

| Iteration 0 | Iteration 1 | Iteration 2 | Iteration 3 | Iteration 4 | Iteration 5 | Legend |
|-------------|-------------|-------------|-------------|-------------|-------------|---------------|
| 206301 | 209101 | 209101 | 209101 | 209101 | 209101 | 90.0 degrees |
| 206401 | 209401 | 209401 | 209401 | 209401 | 209401 | 45.0 degrees |
| 206402 | 207301 | 207301 | 207301 | 207301 | 207301 | 0.0 degrees |
| 207301 | 207401 | 207401 | 207401 | 207401 | 207401 | -45.0 degrees |
| 207401 | 206301 | 206301 | 206301 | 206301 | 206301 | |
| 207402 | 206402 | 206402 | 206402 | 206402 | 206402 | |
| 207403 | 207402 | 207402 | 207402 | 207402 | 207402 | |
| 207404 | 207403 | 207403 | 207403 | 207403 | 207403 | |
| 209101 | 209402 | 209402 | 209402 | 209402 | 209402 | |
| 209401 | 206401 | 206401 | 206401 | 206401 | 206401 | |
| 209402 | 207404 | 207404 | 207404 | 207404 | 207404 | |

Stacking sequence for STACK 3

| Iteration 0 | Iteration 1 | Iteration 2 | Iteration 3 | Iteration 4 | Iteration 5 | Legend |
|-------------|-------------|-------------|-------------|-------------|-------------|--------------|
| 310101 | 310101 | 310101 | 310101 | 310101 | 310101 | 90.0 degrees |
| 310301 | 310301 | 310301 | 310301 | 310301 | 310301 | 45.0 degrees |
| 310401 | 311401 | 311401 | 311401 | 311401 | 311401 | 0.0 degrees |
| 310402 | 310401 | 310401 | 310401 | 310401 | 310401 | |
| 311401 | 310402 | 310402 | 310402 | 310402 | 310402 | |

At the end, in order to have a better overview of the composite optimization's cycle, a bar diagram is shown in Figure 6-15

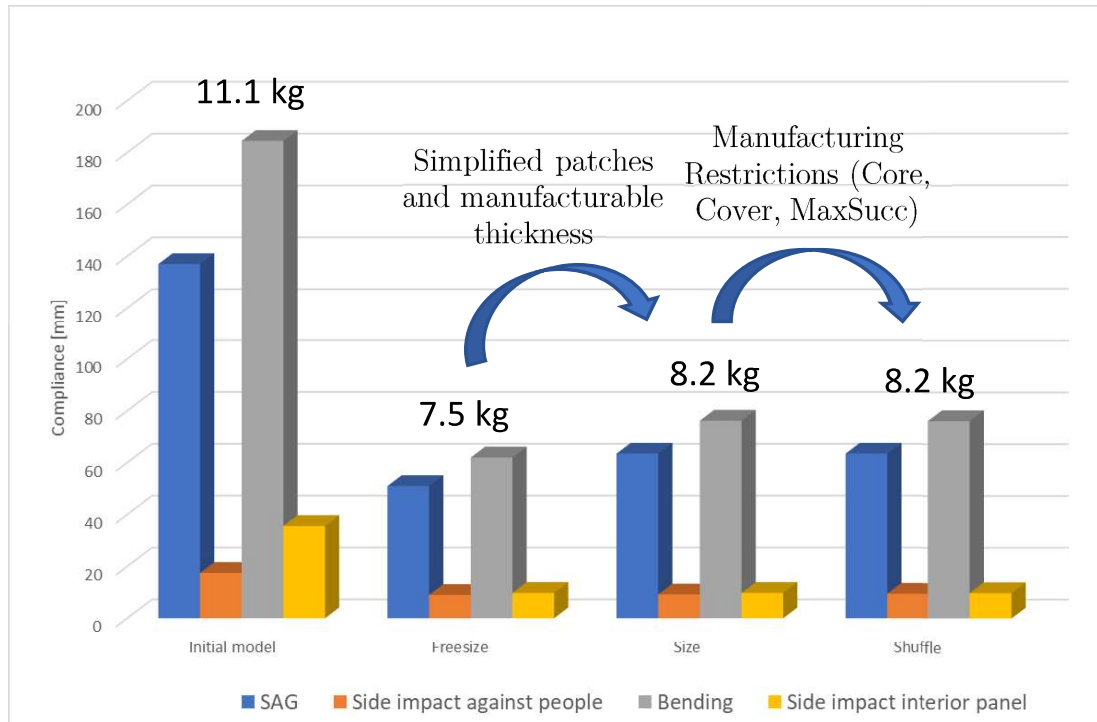


FIGURE 6-15 OVERVIEW OPTIMIZATION RESULTS

The graph shows the advantages of using an optimization.

In free size analysis, the material is no longer equally distributed over the entire component but rather is concentrated along the areas that are subject to the greatest stress. In addition, once the critical points are reinforced, it is possible to remove material on areas that do not contribute to the stiffness of the structure. This allows the desired stiffness to be achieved with the use of minimal material.

Since the distribution and shape of the plies in the free size phase is ideal in the second phase, where a shape is given considering the limits of manufacturability, a small increase in mass and greater compliance can be noted.

The third phase, on the other hand, does not affect the structural characteristics of the compound. In this phase the solver identifies the best arrangement of the plies to be adopted during the production phases.

6.3 Comparison between Optimization and Patch Adding

As a final verification, the comparison between preliminary analysis, analysis with preliminary laminate modified and optimization in Table 6-3 is presented below.

By analysing the preliminary analyses, the critical areas for action were identified. Reinforcement patches were added near the strikers and in the connection interface with the kinematics and, finally, on the load application zone along the central beam.

The comparison is in terms of displacement stress and weight.

TABLE 6-3 COMPARISON OF THE ANALYSIS'S RESULTS OF AUTO SHUTTLE FRONT DOOR

| | | Preliminary analysis | Preliminary laminates modification | Optimization |
|----------------|------------------------|----------------------|------------------------------------|--------------|
| SAG test | Displacement [mm] | 137 | 90.5 | 63.5 |
| | Composite Stress [MPa] | 661.5 | 269 | 275 |
| Side Impact | Displacement [mm] | 17.5 | 10.2 | 9.5 |
| | Composite Stress [MPa] | 543.8 | 285 | 293 |
| Bending | Displacement [mm] | 184.5 | 96.7 | 76.2 |
| | Composite Stress [MPa] | 869 | 297 | 295 |
| Interior panel | Displacement [mm] | 35.6 | 9.8 | 9.7 |
| | Composite Stress [MPa] | 187 | 91 | 151 |
| Door mass [kg] | | 11.1 | 12.9 | 8.2 |

7 Conclusions

The study carried out in this thesis is part of a larger project, the UNICARagil project. This project believes in research and development and wants to bring the technology of electric and autonomous cars into public and private mobility.

The aim of this thesis was to complete the CAD realization of the various components and to verify the structural resistance of the doors of AUTOshuttle and AUTOtaxi vehicles. Then, the last step was to perform an optimization of the structures that would allow to limit the weight and guarantee the structural integrity.

Before starting with the structural analyses on the components, changes were made at the functional level:

- passenger safety geometries
- position of the latches
- seal path of the doors.

By analysing the movements of the doors during the opening and closing phases, it was possible to identify some areas where an unwanted collision with the passengers' limbs could have led to their crushing. By simplifying the geometries in these areas, it is hoped that anti-crushing devices will be more reliable for passengers.

It was necessary to position the latches to facilitate the manual opening of one of the two doors in case of emergency. Considering that the opening sequence of the doors requires the rear door to open first, it was therefore decided to position the upper and lower latches not on the rear door but on the front door, in order to deal just with the opening of two latches during an emergency phase.

Sealing was one of the critical aspects of UNICARagil project, especially in AUTOtaxi and AUTOelf that have two doors and a lifting roof. It has been decided to install the seal on the vehicle structure and not on the doors, as this solution allows to have a single continuous seal ring along the vehicle structure. This is the solution commonly used in twin rear doors of commercial vehicles. Between the two doors, a bulb weather strip located.

Once the necessary CAD modifications have been completed, delivery tests have been carried out on the components in order to verify and improve their structural characteristics.

The following load cases have been identified:

- Sag test
- Strength in side internal impact against people
- Bending stiffness
- Strength of the internal panel against people

The cases analysed showed the critical points of the preliminary laminates adopted. Therefore, instead of adding reinforcement patches in some areas, a free-size optimization has carried out. This type of analysis gives the possibility to obtain components that, in addition to respect the constraints imposed by the delivery tests, have a higher stiffness/weight ratio

The free size optimization process has resulted in lighter and better performing components. The optimized AUTOshuttle front door has a mass reduction of 36.4% compared to the one made with the modified laminate, guaranteeing performances that allow its correct functioning.

Bibliography

- [1] E. Commission, "EU Road Safety Policy Framework 2021-2030 - Next steps towards "Vision Zero," Jun. 2019.
- [2] F. Biechl, "Dokumentation Heckklappenschloss BMW für UNICARagil," 2019. [Online].
- [3] A. Z. J. W. T. L. a. S. P. Siyuan Gong, "Cooperative Adaptive Cruise Control for a Platoon of Connected and Autonomous Vehicles Considering Dynamic Information Flow Topology".
- [4] M. G. J. C. L. B. a. W. H. Maurer, "Autonomous Driving. Berlin, Heidelberg: Springer Berlin Heidelberg," 2016.
- [5] K. LLP, "Connected and Autonomous Vehicles – The UK Economic Opportunity," 2015.
- [6] UNICARagil, " UNICARagil - Disruptive Modular Architectures for Agile, Automated Vehicle Concepts,, " in *27th Aachen Colloquium Automobile and Engine Technology*, 2018.
- [7] UNICARagil, "UNICARagil in neuem Design," 2019.
- [8] N. S. M. R. M. W. T. a. E. L. Herzberger, " Mobilitätskonzepte der Zukunft - Ergebnisse einer Befragung von 619 Personen in Deutschland im Rahmen des Projekts UNICARagil," 2019.
- [9] N. Bringmann, " Entwicklung einer Methodik zur anwendungsspezifischen Auswahl von Türkonzepten und Anwendung auf ein autonomes Fahrzeugkonzept," 2018.
- [10] A. H. H. a. M. D. R. Kuztalan, "Recent Patents in Automotive Gull-Wing door Hinge Mechanisms," *London: Faculty of Engineering, Kingston University*, 2009.
- [11] V. G. Communication, "Sedric in Shanghai: Self-Driving Car without a cockpit celebrates premiere in China," *Auto Shanghai*, 2017.
- [12] V. G. Communications, " "The Volkswagen Group provides an insight into the SEDRIC model family," *Wolfsburg*, 2017.
- [13] L. Reiche, "Fahrerloses Auto zu teuer und komplex wie eine Mars-Mission," *manager magazin*, [Online]. Available: <https://www.manager-magazin.de/>.
- [14] T. M. Corporation, "TOYOTA LAUNCHES NEW MOBILITY ECOSYSTEM AND CONCEPT VEHICLE AT 2018 CES®," *Las Vegas*, 2018.
- [15] T. M. Corporation, " Toyota announces EV service "e-Palette Concept" at CES," [Online]. Available: " <https://www.toyota.co.kr/>. [Accessed 13 04 2020].
- [16] M. Karkafiris, "Toyota Is Bringing A Solid State Battery-Powered Electric Vehicle At The 2020 Olympics," 2019. [Online]. Available: <https://www.carscoops.com>. [Accessed 20 04 2020].

- [17 W. POD, "Westfield POD," 2020. [Online]. Available: www.westfieldpod.com..
]
- [18 ITCILO, "The future of wheels," [Online]. Available: <https://www.itcilo.org/it/node/1739>.
] [Accessed 14 04 2020].
- [19 UNICARagil, "CAD data, Platform and Hut. file," 2020.
]
- [20 UNICARagil, "UNICARagil -Annahmen Ergonomie," 2018.
]
- [21 S. Guske, "Konzepte zur Schließung der Aufbaustruktur automatischer Dachöffnungen,"
] 2019.
- [22 J. Horstmann, "Analysis of existing technologies of door components and design for an
] automatic door in an autonomous vehicle," 2019.
- [23 L. N. a. V. D. Palma, ", "UNICARagil – Development of doors and roof structures for a
] multi-use platform based vehicle concept," 2019.
- [24 C. d. P. a. H. f. 2. UNICARagil, " CAD data, Roof kinematic. file," 2020.
]
- [25 UNICARagil, "CAD data, Aussenhaut. file," 2020.
]
- [26 UNICARagil, "CAD data, AUTOshuttle doors, file," 2020.
]
- [27 UNICARagil, "CAD data, AUTOfaxi door, file," 2020.
]
- [28 B. Rexroth., " Roller rail systems," [Online]. Available: <https://www.boschrexroth.com>.
] [Accessed 14 06 2020].
- [29 A. Gmeinwieser, "Konstruktion einer Kinematik für ein Einstiegsystem," 2019.
]
- [30 Bosch., " Power tailgate drive NSA-H.," [Online]. Available: <https://www.bosch-mobility-solutions.com> . [Accessed 13 06 2020].
]
- [31 Mädler., " Schnecken-Kleingetriebe mit Gleichstrommotor SFS," [Online]. Available:
] <https://www.maedler.de>. [Accessed 13 06 2020].
- [32 A. K. F. S. A. Koch, "Türauslegung Entscheidungsgrundlge," 2018.
]
- [33 E. C. K.-H. T. J. C. K. K. G. I. a. Y. X. Hardee, A CAD-based design parameterization for shape
] optimization of elastic solids, 1999.

- [34 L. R. L. R. P. G. a. T. A. Morello, The Automotive Body, Springer Netherlands, 2011.
]
- [35 3M, "Door Rubber Seal Strip Weatherstrip Sealing D-shape," [Online]. Available:
] www.3mdeutschland.de. [Accessed 20 04 2020].
- [36 C. Zweben, Composite Materials, Mechanical Engineers' Handbook, 2015.
]
- [37 M. R. Gazzette, "Global Carbon Fiber Reinforced Plastic Market 2019-2025," [Online].
] Available: <https://amarketresearchgazette.com> . [Accessed 14 06 2020].
- [38 A. M. i. T. A. S. (AMTAS), "Summary of methods used to Manufacture PMCs," [Online].
] Available: <https://depts.washington.edu>.. [Accessed 15 05 2020].
- [39 Hexcel, "HexPly® Prepreg Technology," 2013. [Online]. Available:
] <https://www.hexcel.com>.
- [40 J. D. Rehkopf, "Automotive Carbon Fiber Composites: from Evolution to Implementation,"
] 2012.
- [41 A. E. Society, "Using Design and Build Guidelines to Reduce Ergonomic Risk," [Online].
] Available: <https://www.iise.org>.. [Accessed 14 06 2020].
- [42 A. Bacchetto, "Introduzione al metodo degli elementi finiti e alla modellazione FEM".
]
- [43 T. L. E. Y. M. Desai, Finite Element Method with Applications in Engineering, Pearson
] India, 2011.
- [44 A. University, "Practical-Aspects-of-Finite-Element-Simulation.
]
- [45 A. University, "Concact," [Online]. Available: Altair University, "Contact,"
] https://altairhyperworks.com/hwhelp/Altair/hw14.0/help/hwsolvers/contact_ug.htm?to c=0&printWindow..
- [46 R. T. H. Sobieszczanski-Sobieski, Structural Optimizazion: History.
]
- [47 A. University, "Size optimization".
]
- [48 A. W. Markus Kriesch, "Composite Optimization with Optistruct 11.0 on the example of a
] Formula-Student-Monocoque," Altair University.
- [49 X. L. X. a. W. Y. Ge, "'Methodologies for Evaluating and Optimizing Multimodal Human-
] Machine-Interface of Autonomous Vehicles," SAE Technical Paper Series, 2018.

List of Figure

| | |
|--------------------------------------------------------------------------------------------------------------------------|----|
| Figure 1-1 Levels of driving automation [2] | 1 |
| Figure 1-2 UNICARagil project partners [7] | 3 |
| Figure 1-3 Schematic overview of the overall UNICARagil concept [6] | 4 |
| Figure 1-4 UNICARagil prototypes [8] | 7 |
| Figure 1-5 Structure of the thesis | 8 |
| Figure 2-1 Single-leaf swing door - construction principle and FIAT 500 [9] | 10 |
| Figure 2-2 Double leaf swing door - construction principle and Volkswagen UP [9] | 11 |
| Figure 2-3 co-rotating double-leaf swing door with B-pillar - construction principle and Opel Meriva [9] | 11 |
| Figure 2-4 co-rotating double-leaf swing door without B-pillar - construction principle and bmw i3 [9] | 12 |
| Figure 2-5 Sliding door - construction principle and ford b-max | 12 |
| Figure 2-6 Folding door - construction principle and scania citywide | 13 |
| Figure 2-7 Swing- arm door – construction principle and DB bus | 14 |
| Figure 2-8 Gull-wing - construction principle and tesla model x | 14 |
| Figure 2-9. Volkswagen Sedric [13] | 15 |
| Figure 2-10. Possible uses of e-Palette concept [15] | 16 |
| Figure 2-11. Toyota e-Palette for 2020 Tokyo Olympics [16]. | 17 |
| Figure 2-12. Westfield POD – opening of the doors [17] | 18 |
| Figure 2-13. Westfield POD inside view [17] | 19 |
| Figure 2-14 Olli-3D printed model [18] | 20 |
| Figure 3-1. Platform and vehicle structure: larger vehicles vs. smaller vehicles [19] | 21 |
| Figure 3-2 Height in AUTOtaxi and AUTOelf [20] | 22 |
| Figure 3-3 Dimensional requirements for the roof hatch due to ergonomics [20] | 23 |
| Figure 3-4. Swing arm roof [22] | 24 |
| Figure 3-5. 3-link mechanism [24] | 24 |
| Figure 3-6. Blocking - Striker fixed to the roof bar and support with a rotating hook fixed to the upper body [24] | 25 |
| Figure 3-7 support with a rotating hook fixed to the upper body [24] | 25 |

| | |
|---------------------------------------------------------------------------------------------------------------|----|
| Figure 3-8. Exploded view of the AUTOfaxi and AUTOfelf door [26]..... | 30 |
| Figure 3-9. CFRP doors - view from the inside and the outside [26] | 30 |
| Figure 3-10. Inner shell of the roof hatch [23] | 31 |
| Figure 3-11. Roof solution without transparent parts [23] | 32 |
| Figure 3-12. Roof solution with transparent parts [B6]..... | 32 |
| Figure 3-13 Roof solution with transparent total coverage [23]..... | 33 |
| Figure 3-14. Roof and doors assembly – view from the outside [27]..... | 33 |
| Figure 3-15. Roof hatch installed on the roof kinematics [24]..... | 34 |
| Figure 3-16. Details of the 3-link mechanism [24]..... | 34 |
| Figure 3-17. AUTOfshuttle and AUTOfcargo vs. AUTOftaxi and AUTOfelf doors (inside- outside) [26][B6] | 35 |
| Figure 3-18, AUTOftaxi and AUTOfelf door with trapezoidal panel and HMI matrix [27] . | 36 |
| Figure 3-19. AUTOftaxi and AUTOfelf doors assembled on the vehicle structure [19] | 37 |
| Figure 3-20. Possible door opening concept of the AUTOftaxi [25]..... | 37 |
| Figure 3-21. Space available for the installation of the arms on the vehicle structure..... | 38 |
| Figure 3-22.Rails and runner blocks used for doors automation [28]..... | 38 |
| Figure 3-23. AUTOfshuttle and AUTOfcargo door kinematics [29] | 39 |
| Figure 3-24.Bosch motor mounted in the Audi Q7 4M [30]..... | 40 |
| Figure 3-25. Bosch motor with gearbox [30] | 40 |
| Figure 3-26.Maedler motor used for the sliding mechanism automation [31] | 41 |
| Figure 3-27. New kinematics, used in the final solution [29]..... | 41 |
| Figure 3-28. Lock positions in VW Sedric, right door closes first [22]..... | 42 |
| Figure 3-29. Locks position in UNICARagil vehicles [32]..... | 43 |
| Figure 3-30. Soft-close mechanism | 44 |
| Figure 3-31. Latch of the soft-close mechanism [2] | 44 |
| Figure 4-1 lateral beam before(left) and after(right) editing..... | 47 |
| Figure 4-2 latches in AUTOftaxi and AUTOfelf [19] | 48 |
| Figure 4-3 detail of the latch case before(left)and after (right) editing..... | 49 |
| Figure 4-4 roof soft-closing motor case | 49 |
| Figure 4-5 Second latch of the roof fixed to the upper body [24] | 50 |

| | |
|-------------------------------------------------------------------------------------|----|
| Figure 4-6. Design radius to avoid buckling (BU) [34] | 51 |
| Figure 4-7. Bulb seal used for UNICARagil vehicles [35] | 52 |
| Figure 4-8. Seal between door structure and platform | 52 |
| Figure 4-9. Seal ring of AUTOtaxi and AUTOelf [19] | 53 |
| Figure 4-10 roof-Door sealing | 54 |
| Figure 4-11. Seal placed along the front door flange | 54 |
| Figure 4-12. Seal ring on AUTOshuttle and AUTOcargo [19] | 55 |
| Figure 4-13. CFRP [37] | 58 |
| Figure 4-14. Production volume and performance of composite technologies [39] | 59 |
| Figure 4-15. Different production techniques for prepreg [39][B5] | 59 |
| Figure 4-16. Different weave styles [39] | 60 |
| Figure 4-17. Properties of Fabric and Unidirectional composites [39] | 60 |
| Figure 4-18. Different ways to arrange the fibre directions [39] | 61 |
| Figure 4-19. Steps of the vacuum bag processing [39][B5] | 62 |
| Figure 4-20. Difference between vacuum bag/oven and autoclave process [39] | 63 |
| Figure 4-21 Anthropometric data of 95th percentile male [41] | 64 |
| Figure 4-22 mesh definition | 65 |
| Figure 4-23 Conjunction lines of surfaces not matched | 67 |
| Figure 4-24 Conjunction lines of surfaces matched | 67 |
| Figure 4-25 mesh creation panel | 70 |
| Figure 4-26 Critical area meshing [44] | 71 |
| Figure 4-27 Damaged elements control | 71 |
| Figure 4-28 Elements normals check | 72 |
| Figure 4-29 Material orientation | 73 |
| Figure 4-30 TS245 (up) - TS380 (down) | 74 |
| Figure 4-31 GG245TSE pre-preg | 75 |
| Figure 4-32 TDS-GG380T pre-preg | 76 |
| Figure 4-33 Ply-sets; Element-sets | 77 |
| Figure 4-34 Laminate outer shell | 78 |

| | |
|-------------------------------------------------------------------------|----|
| Figure 4-35 Laminate inner shell | 78 |
| Figure 4-36 laminate kinematic interior cover | 78 |
| Figure 4-37 Node-to-surface discretization [B2] | 80 |
| Figure 4-38 Surface-to-surface discretization [B2]..... | 80 |
| Figure 4-39 contact card definition..... | 82 |
| Figure 4-40 Surface where tie contact is defined (white) | 82 |
| Figure 4-41 Detail of the contact surface definition of a striker | 83 |
| Figure 4-42 AUTOfaxi SAG test loadstep | 84 |
| Figure 4-43 Free body diagram of the vehicle..... | 85 |
| Figure 4-44 AUTOfaxi Side impact loadstep..... | 86 |
| Figure 4-45 AUTOfaxi Top view of the door kinematics | 87 |
| Figure 4-46 Door kinematics simplified problem..... | 88 |
| Figure 4-47 AUTOfaxi Bending loadstep..... | 88 |
| Figure 4-48 AUTOfaxi interior panel loadstep | 89 |
| Figure 5-1 SAG test : displacement | 90 |
| Figure 5-2 SAG test: composite stress..... | 91 |
| Figure 5-3 Side internal impact: displacement | 92 |
| Figure 5-4 side internal impact: composite stress | 92 |
| Figure 5-5 Door bending stiffness: displacement..... | 93 |
| Figure 5-6 Door bending stiffness: composite stress..... | 93 |
| Figure 5-7 Kinematic interior cover | 94 |
| Figure 5-8 Kinematic interior cover: displacement | 94 |
| Figure 5-9 SAG test : displacement | 95 |
| Figure 5-10 SAG test: composite stress..... | 96 |
| Figure 5-11 Side internal impact: displacement | 96 |
| Figure 5-12 side internal impact: composite stress | 97 |
| Figure 5-13 Door bending stiffness: displacement..... | 97 |
| Figure 5-14 Door bending stiffness: composite stress..... | 98 |
| Figure 5-15 interior panel: displacement | 98 |

| | |
|--------------------------------------------------------------------------------------------------|------------|
| Figure 5-16 interior panel: composite stress | 99 |
| Figure 6-1 Optimization logic path..... | 100 |
| Figure 6-2 Composite optimization phases [B7]..... | 102 |
| Figure 6-3 Freesize design variable creation..... | 103 |
| Figure 6-4 Freesize design variable composites..... | 104 |
| Figure 6-5 Dconstraints definition | 105 |
| Figure 6-6 objective definition..... | 105 |
| Figure 6-7 Super-ply thickness of the two shell and the interior panel..... | 106 |
| Figure 6-8 orientation thickness of the components (0°)..... | 106 |
| Figure 6-9 Orientation thickness of the components (45°) | 107 |
| Figure 6-10 52 ply lamination sequence, obtained as a result of the FStoSH optimization | 107 |
| Figure 6-11 Edited ply-shape (ID 207300) | 108 |
| Figure 6-12 Manufacturable plies shape results..... | 109 |
| Figure 6-13 Discrete size optimization run HyperGraph results..... | 110 |
| Figure 6-14 outer shell's lamination sequence, obtained after the optimization of Size | 110 |
| Figure 6-16 Overview optimization results..... | 112 |

List of Tables

| | |
|-----------------------------------------------------------------------------------------|------------|
| Table 3-1 Transparent panel: comparison between glass and PC [23] | 29 |
| Table 3-2 Dimensions of larger and smaller doors | 35 |
| Table 4-1 Front and rear door masses for the three door solutions [23]..... | 56 |
| Table 4-2 Percentage variation of the door masse with respect to CFRP door mass [23] .. | 57 |
| Table 4-3 comparison among different composites processing methods [39]..... | 61 |
| Table 4-4 1d type of mesh..... | 68 |
| Table 4-5 2D type of mesh..... | 68 |
| Table 4-6 3D type of mesh..... | 69 |
| Table 4-7 Woven laminate properties..... | 76 |
| Table 4-8 Vehicle data..... | 85 |
| Table 4-9 Data for force evaluation in side impact test | 86 |
| Table 6-1 Ply editing design space | 102 |
| Table 6-2 SHUTTLE FRONT DOOR SHUFFLE OPTIMIZATION..... | 111 |
| Table 6-3 comparison of the analysis's results of AUTOshuttle front door..... | 113 |